AWARD NUMBER: W81XWH-12-1-0370

TITLE: Targeting N-RAS as a Therapeutic Approach for Melanoma

PRINCIPAL INVESTIGATOR: Douglas V. Faller, PhD, MD

CONTRACTING ORGANIZATION: Trustees of Boston University
Boston, MA 02118

REPORT DATE: December 2014

TYPE OF REPORT: Final

PREPARED FOR: U.S. Army Medical Research and Materiel Command
Fort Detrick, Maryland 21702-5012

DISTRIBUTION STATEMENT: Approved for Public Release;
Distribution Unlimited

The views, opinions and/or findings contained in this report are those of the author(s) and should not be construed as an official Department of the Army position, policy or decision unless so designated by other documentation.

REPORT DOCUMENTATION PAGE

Form Approved
OMB No. 0704-0188

1. REPORT DATE	2. REPORT TYPE	3. DATES COVERED

1. REPORT DATE
Ö^&^{ à^¦Á€14

2. REPORT TYPE Ô↔^´á→

3. DATES COVERED
H€Â´Ù^]Á€FGÆÁGÁÙ^]Á€FI

4. TITLE AND SUBTITLE
Targeting N-RAS as a Therapeutic Approach for Melanoma

5a. CONTRACT NUMBER

5b. GRANT NUMBER
Y Ì FÝY PÈ€GÊ€HÌ €

5c. PROGRAM ELEMENT NUMBER

6. AUTHOR(S)
Douglas V. Faller, PhD, MD

E-Mail: dfaller@bu.edu

5d. PROJECT NUMBER

5e. TASK NUMBER

5f. WORK UNIT NUMBER

7. PERFORMING ORGANIZATION NAME(S) AND ADDRESS(ES)
Trustees of Boston University, Medical Campus;
72 East Concord St.
Boston, MA 02118

8. PERFORMING ORGANIZATION REPORT NUMBER

9. SPONSORING / MONITORING AGENCY NAME(S) AND ADDRESS(ES)
U.S. Army Medical Research and Materiel Command
Fort Detrick, Maryland 21702-5012

10. SPONSOR/MONITOR'S ACRONYM(S)

11. SPONSOR/MONITOR'S REPORT NUMBER(S)

12. DISTRIBUTION / AVAILABILITY STATEMENT
Approved for Public Release; Distribution Unlimited

13. SUPPLEMENTARY NOTES

14. ABSTRACT   Activating mutations in N-RAS are found in 33% of primary melanomas, and are correlated with sun exposure and nodular lesions. Potential therapeutic strategies have been devised in the past to "directly" target RAS. Unfortunately, these have shown minimal if any activity in melanoma in clinical trials, because wild-type Ras and its downstream effectors are required for many critical cellular functions in normal cells, the therapeutic window for inhibiting Ras directly may be too narrow to exploit. Our novel alternative strategy has the potential to circumvent this limitation. Aberrantly activated, K-RAS or Ha-RAS are lethal to a tumor cell unless a survival pathway requiring PKCd is also active. Inhibition of PKCd in human and murine cells containing an activated K- or Ha-RAS protein initiates rapid and profound apoptosis. The dependency of tumor cells upon the activity of a non-oncogenic protein is sometimes termed "non-oncogene addiction." Hypothesis: inhibition or down-regulation of PKCd in human and murine models of melanoma with aberrant activation of N-RAS signaling will cause targeted cytotoxicity in these tumors. The Specific Aims/Study Design of this Discovery Proposal are: Test the hypothesis that inhibition or down-regulation of PKCd in human melanoma cell lines with NRAS mutations selectively induces apoptosis; 2) Determine whether aberrant activation of pathways downstream of RAS (in the setting of wild-type RAS alleles) will similarly sensitize human melanoma cells to PKCd inhibition; 3) Test this targeted approach in in vivo models of human melanoma. Impact: A novel therapeutic modality selectively targeting melanomas with activation of N-RAS would make a significant impact on the way melanoma is treated.

15. SUBJECT TERMS
Prostate cancer; Ras; small molecule inhibitors; drug development

16. SECURITY CLASSIFICATION OF:			17. LIMITATION OF ABSTRACT	18. NUMBER OF PAGES	19a. NAME OF RESPONSIBLE PERSON USAMRMC
a. REPORT U	**b. ABSTRACT** U	**c. THIS PAGE** U	UU	JÌ	**19b. TELEPHONE NUMBER** (include area code)

Table of Contents

1. INTRODUCTION:

In the US, the risk of invasive melanoma has increased almost tenfold in the last 50 years. Patient survival from metastatic disease is only 15%, and the prognosis is extremely poor. (The excitement generated by the initial unprecedented clinical activity of BRAF inhibitors in melanoma has now been tempered by the realization that the tumor responses are unfortunately temporary, with a median time to progression of approximately seven months.) The RAS family members (which are proto-oncogene GTPases serving as critical signal transducers) are frequently mutated in melanomas. Activating mutations in N-RAS are found in 33% of primary melanoma tumors, and are correlated with sun exposure and nodular lesions. Because aberrant activation of N-RAS is so common in melanoma, RAS is an attractive target for a melanoma therapeutic. Indeed, strategies have been devised to target RAS "directly," but, unfortunately, these approaches have shown minimal if any activity in melanoma -- because wild-type RAS and its downstream effectors are required for many critical cellular functions in normal cells, the therapeutic window for inhibiting RAS activity "directly" may be too narrow to exploit effectively.

-    Our novel, alternative strategy has the potential to circumvent this limitation. We have demonstrated that aberrant activation of K-RAS or Ha-RAS is lethal to a tumor cell unless a specific survival pathway (also initiated by RAS) is also active.[1-5] This survival pathway specifically requires PKCδ.[1-3] Unlike the classical PKC isozymes, PKCδ is not required for survival of normal cells, and its inhibition or down-regulation in normal cells, tissues, and mice has no significant adverse effects *in vitro* or *in vivo*.[1-3] (PKCδ -null mice are healthy.) Inhibition of PKCδ in human and murine tumor cells with mutated K-RAS or H-RAS, however, initiates rapid and profound apoptosis. This molecular approach, targeting tumor cells containing a mutated oncogenic protein (and sparing normal cells) by modulating a second protein or its activity, is sometimes termed "synthetic lethality." Analogously, the dependency of tumor cells upon the activity of a non-oncogenic protein, in this case PKCδ, is sometimes termed "non-oncogene addiction." ***First Hypothesis***: Inhibition or down-regulation of PKCδ in human and murine models of melanoma with mutational activation of N-RAS will cause targeted cytotoxicity in these tumors. (We have previously demonstrated the sensitivity of human tumor cells with mutational activation of K- or HRAS proteins to PKCδ inhibition. NRAS, however, has some significant differences compared to K- and HRAS, and whether mutated N-RAS would efficiently sensitize melanoma cells to apoptosis after PKCδ inhibition is unknown.)

-    Importantly, our prior work has also suggested that aberrant activation of downstream RAS-effector pathways, even in the setting of normal RAS proteins, can sensitize cells to PKCδ inhibition.[1] BRAF (a downstream effector of RAS comprising an early component of the RAS/RAF/MEK/ERK signaling pathway) is activated by mutation (BRAFV600E) in 50–70% of melanomas. We predict that this activation of a RAS effector pathway by BRAF would make this subset of melanoma cells dependent upon PKCδ activity. Another major effector pathway leading from RAS is the RAS/PI$_3$K/AKT signaling pathway. The tumor suppressor PTEN negatively-regulates the PI$_3$K pathway. Loss PTEN activity, leading to aberrant PI$_3$K/AKT activation, occurs in up to 40% of melanomas. ***Second Hypothesis***: Aberrant activation of RAS downstream effector pathways, by the [V600E]BRAF mutation or PTEN loss, will sensitize melanoma cells to PKCδ inhibitors, even in the setting of wild-type N-RAS proteins.

Resistance to the new highly-active BRAF-inhibitor drugs for melanoma unfortunately invariably arises in treated patients, generally through alternative routes leading to aberrant activation of RAS/RAF/MEK signaling. Resistance most commonly results from the new development of

activating mutations of NRAS, or activation of receptor tyrosine kinases (RTKs), like the PDGF-Rβ which then cause aberrant activation of (normal) RAS proteins. Interestingly, our published studies have indicated that cell survival during pathological, chronic activation of even normal cellular RAS proteins requires PKCδ-dependent survival pathways.[1] Chronic activation of the PDGF-Rβ should cause chronic aberrant activation of the normal cellular Ras proteins, mimicking a mutated RAS state. Our targeted approach may therefore have <u>anti-tumor activity in melanomas that have relapsed</u> after an initial response to the new BRAF inhibitors. ***Third Hypothesis***: Melanomas which have become resistant to BRAF-inhibitor drugs [by virtue of new mutations in NRAS or chronic activation of upstream RAS activators (PDGF-Rβ)] will be sensitive to PKCδ inhibition.

Innovation: N-Ras signaling is an attractive target for therapy of melanoma, but approaches aimed at Ras itself, or its critical signaling pathways, which are required in normal tissues, have had limited success. This "non-oncogene addiction" approach, however, exploits a weakness of tumor cells with aberrant activation of N-Ras or N-Ras effectors – their absolute requirement for a survival pathway mediated by PKCδ. In contrast, normal cells and tissues do not require PKCδ.

Impact: Current therapies for advanced melanoma are inadequate, and aberrant activation of N-Ras or Ras pathways is common in melanoma. A novel therapeutic modality selectively targeting melanomas with activation of Ras or Ras pathways would make a significant impact on the way melanoma is treated.

2. Keywords

Protein kinase; RAS; melanoma; synthetic lethality; non-oncogene addiction; kinase inhibitor

3. Overall Project Summary:

General Materials and Methods

Reagents

BJE6-106 and BJE6-154 were synthesized, the details of which will be reported elsewhere. Rottlerin, PLX4032 (vemurafenib), propidium iodide, and RNase A were purchased from Axxora (San Diego, CA), LC Labs (Woburn, MA), Sigma-Aldrich (St. Louis, MO) and Fisher Scientific (Pittsburgh, PA), respectively. Z-VAD-FMK was purchased from R&D Systems (Minneapolis, MN) and Enzo Life Sciences (Farmingdale, NY). Antibodies against phospho-SAPK/JNK (Thr183/Tyr185) (#4668), SAPK/JNK (#9252), phospho-Histone H2A.X (Ser 139) (#2577), Histone H2A (#2578), phospho-SEK1/MKK4 (#4514), SEK1/MKK4 (#9152), phospho-MKK7 (Ser271/Thr275) (#4171), MKK7 (#4172), phospho-c-Jun (Ser63) (#9261), c-Jun (#9165), phospho- ERK1/2 (Thr202/Tyr204) (#4370), phospho-p38 (Thr180/Tyr182) (#4511) and p38 (#9212) were purchased from Cell Signaling Technologies (Danvers, MA). Antibodies against ERK1 (K-23) and PKCδ (#610398) were purchased from Santa Cruz Biotechnology (Dallas, TX) and BD Biosciences (San Jose, CA), respectively. Antibodies against ±-Tubulin (#T6074), ²-Actin (#A1978) and GAPDH (#G8795) were purchased from Sigma-Aldrich. ON-TARGETplus SMART pool siRNA against JNK1 (L-003514), JNK2 (L-003505), H2AX (L-011682) and Non-targeting siRNA #1 (D-001810-01) were purchased from Dharmacon (Lafayette, CO). Silencer Select siRNA against PKCδ (PRKCD) was purchased from Life Technologies (Carlsbad, CA).

Cell culture, siRNA transfection, plasmid stable transfection & PLX4032-resistant sub cell lines

SBcl2 was generously provided by the Department of Dermatology, Boston University School of Medicine (Boston, MA). A375 and SKMEL5 were generously provided by Dr. Remco Spanjaard (Boston University School of Medicine, Boston, MA). WM1366, WM1361A, WM852, FM28, FM6, SKMEL2 and SKMEL28 were generously provided by Dr. Anurag Singh (Boston University School of Medicine, Boston, MA). RAS or BRAF mutations were verified by sequencing. SBcl2 and A375 and its derivative lines were maintained in Dulbecco's modified Eagle's medium (DMEM) supplemented with 10% fetal bovine serum. SKMEL5 was maintained in minimum essential medium (MEM) supplemented with 10% fetal bovine serum. All media were additionally supplemented with L-glutamine 2mM, penicillin 100 units/ml and streptomycin 100µg/ml. siRNA transfection was performed by reverse transcription using Lipofectamine RNAiMax (Invitrogen [Carlsbad, CA]) according to the product protocol, and media was changed the following day of transfection. PLX4032-resistant cell sublines were established according to the method described.[1] Briefly, A375 and SKMEL5 cells were plated at low cell density and treated with PLX4032 at 1µM or 0.5µM, respectively. The concentration of PLX4032 was gradually increased up to 4µM (A375) or 2µM (SKMEL5) over the course of a 3-4 week period, and clonal colonies were picked. Derived sublines of A375 and SKMEL5 were maintained in PLX4032-containing medium at 1-2µM (A375) or 0.5µM (SKMEL5).

Cell proliferation & Caspase assays

Cell proliferation assays (MTS assay) and caspase assays were performed with CellTiter 96 AQueous Non-Radioactive Cell Proliferation Assay kit and Caspase-Glo 3/7 Assay Systems (Promega [Madison, WI]) according to the manufacturers' protocols. Briefly, for the assays employing inhibitors, cells were plated in a 96-well plate (500-4000 cells per well depending on the cell lines and duration of the experiment), exposed to inhibitors 24 hours later and cultured for the durations indicated in the individual figure legends. For the assays employing siRNA, cells were plated the day of siRNA transfection, cultured for the duration indicated in the figure legends, and if indicated, treated with inhibitors. After the indicated treatment times, assay reagent was added and cell plates were incubated for 1 hour at 37°C (MTS assay) or 30 minutes at RT (caspase assay). Absorbance at 490nm (MTS assay) or luminescence (caspase assay) were measured using microplate readers for quantification.

Clonogenic colony assay

Cells were treated with drugs for the time indicated in the figure, and then the same number of viable cells from each treatment was replated at low cell density and cultured in medium without inhibitors for 8 days, at which time colony formation was quantitated. Cell colonies were stained with ethidium bromide for visualization on an ImageQuant LAS 4000 (GE Healthcare [Little Chalfont, United Kingdom]) and colonies enumerated.

DNA fragmentation assays

Cells were harvested and fixed in 1 ml of a 35% ethanol/DMEM solution at 4°C for 30 min. Cells were then stained with a solution containing 25 µg/ml of propidium iodide/ml and 50 µg/ml of RNase A in PBS and incubated in the dark at 37°C for 30 min for flow cytometric analysis. The proportion of cells in the sub-G1 population, which contain a DNA content of less than 2N (fragmented DNA), was measured as an indicator of apoptosis.

Immunoblotting

Whole cell lysates were prepared in a buffer containing 20mM Hepes (pH 7.4), 10% glycerol, 2mM EDTA, 2mM EGTA, 50mM ²-glycerophosphate and 1% Triton-X100, 1mM dithiothreitol

(DTT) and 1mM sodium vanadate, supplemented with Halt Protease and Phosphatase Inhibitor Cocktail (100X) (Thermo Scientific [Waltham, MA]). Lysates were subjected to SDS-PAGE and transferred to nitrocellulose membranes. Membranes were blocked at RT for 1-1.5h with 5% BSA or 5% non-fat dry milk in TBS-T (10mM Tris [pH 7.5], 100mM NaCl, 0.1% Tween 20) and probed with the appropriate primary antibodies (1:500-1:10,000) overnight. After washing, the blots were incubated with horseradish peroxidase-conjugated secondary antibodies (1:2000-1:10,000) and visualized using the ECL system (GE Healthcare) on an ImageQuant LAS 4000.

Quantitative real-time PCR

RNA was extracted with RNeasy Mini kit purchased (Qiagen [Venlo, Netherlands]) according to the manufacturer's protocol. 1µg of RNA was used to synthesize cDNA in a 20 µl reaction volume employing SuperScript III First-Strand Synthesis System (Invitrogen) or QuaniTect Reverse Transcription Kit (Qiagen) according to the product protocol. Quantitative real-time PCR was performed with SYBR Green PCR Master Mix (Applied Biosystems (now under Life Technologies)) according to the manufacturer's protocol. Briefly, cDNA was diluted to a final concentration of 25ng per reaction, added to a primer set (5 µM) and SYBR Green PCR Master Mix to a final volume of reaction mixture of 20 µl, and run on an Applied Biosystems 7500 Fast Real-Time PCR system using the following thermal cycling protocol: 50°C for 2 min, 95°C for 10 min, and 40 cycles of 95°C for 15 sec and 60°C for 1 min. The relative amount of an mRNA of interest was calculated by normalizing the Ct value of the mRNA to the Ct of the internal control (β-actin). Primer sequences were: H2AX Forward: 5'-CAACAAGAAGACGCGAATCA-3', H2AX Reverse: 5'- CGGGCCCTCTTAGTACTCCT-3•, β-actin Forward: 5'-GCTCGTCGTCGACAACGGCTC-3•, β-actin Reverse: 5'-CAAACATGATCTGGGTCATCTTCTC-3'

TASK 1: Testing N-RAS-mutant human melanoma cells for apoptosis after inhibition or down-regulation of PKCδ:

Status: Completed. ***Please see the attached publication Takashima, et al, 2014, and supplementary data, also attached, for complete details.***

Takashima, A., Chen, Z., English, B., Williams, R.A., Faller, D.V. Protein kinase C ´ is a therapeutic target in malignant melanoma with NRas mutation or BRaf inhibitor-resistance. 2014. ACS Chemical Biology, 2014 9(4):1003-14. PMC4160068

Methods: *Methods*: Inhibition of PKC □ by siRNA, of PKCδ protein levels, and assay of relative cell numbers at 48 or 72 hrs, compared to control siRNA. MTS (3-(4,5-dimethylthiazol-2-yl)-5-(3-carboxymethoxyphenyl)-2-(4-sulfophenyl)-2H-tetrazolium) assay for enumeration of cells after treatment. PI staining with flow cytometry or LDH (Lactate Dehydrogenase) release assay will be used to document apoptosis in at least one responsive cell line from each group.
Cell lines to be tested include (depending upon their susceptibility to siRNA transfection):
- at least 3 of the following mutant N-RAS cell lines: SKMEL2, SBCl2, FM-28, SKMEL30, IPC-298
- at least 2 of the following wild-type N-RAS melanoma cell lines: A375, A2058, and SKMEL5

Assays: MTS assay for enumeration of cells at 48 and 72 hrs after treatment. LDH release assays or flow cytometry assays to assess cytotoxicity
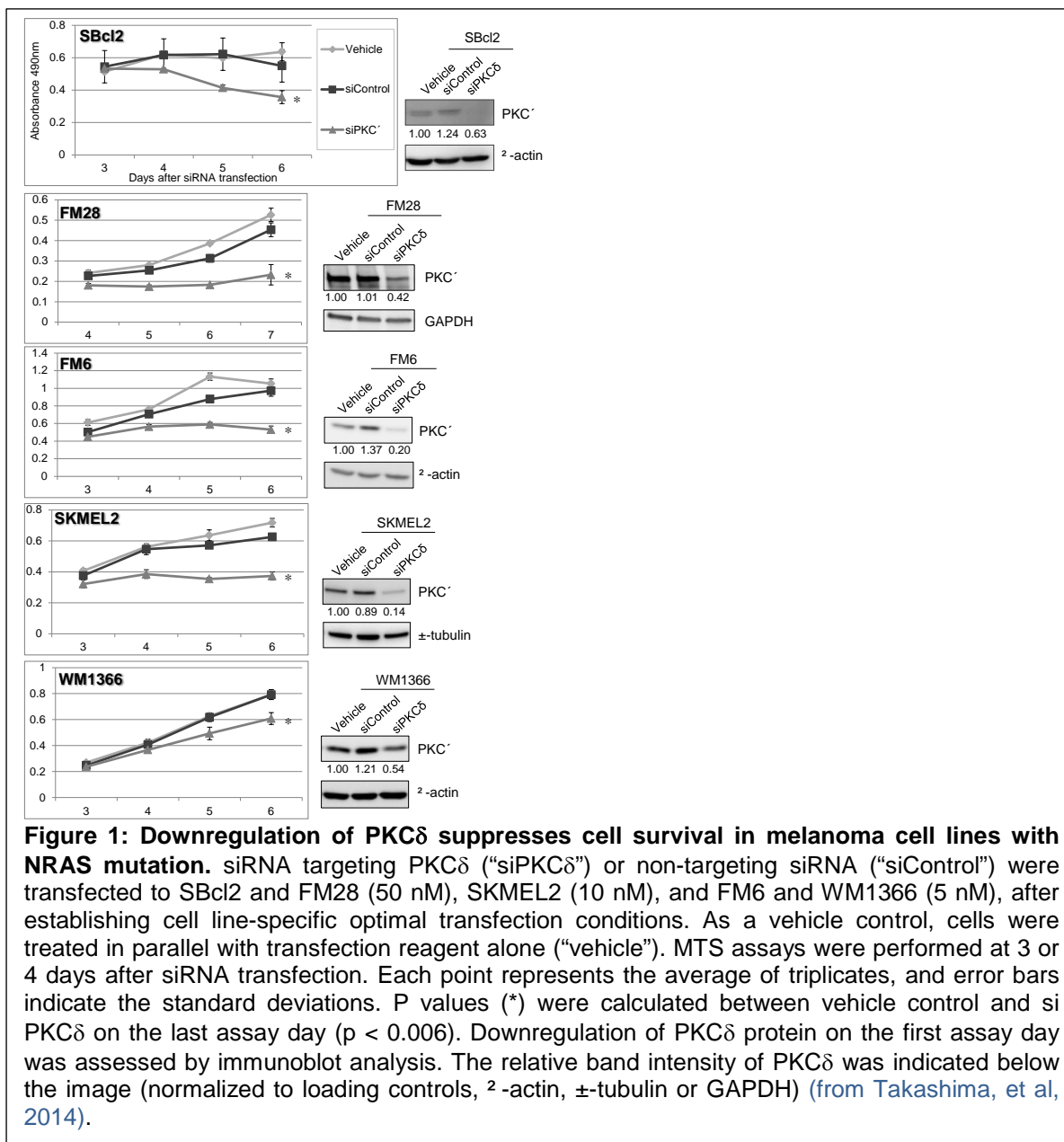
Results:
siRNA – The rationale for PKCδ as a target for a NRAS-specific therapy is supported by prior reports: 1) PKCδ inhibition preferentially inhibits the growth of pancreatic cancer cells with KRAS mutations (which are also prominent in many types of cancers with particularly high prevalence and mortality rates), and similarly inhibits cells into which activated KRAS or HRAS have been ectopically introduced, as well as a variety of other tumor cell lines with RAS mutations.[2-5] PKCδ is not required for the proliferation or survival of normal cells or organisms.[3-5]

To validate the potential of this synthetic lethal approach targeting PKCδ in melanomas with NRAS mutations, we first examined the effect of PKCδ-selective inhibition on cell growth by knocking down PKCδ protein expression in multiple melanoma cell lines harboring NRAS mutations, using siRNA. MTS assays were conducted daily starting 3 or 4 days after siRNA transfection to quantitate the number of viable cells. Transfection reagent alone (without siRNA) served as a vehicle control. Even partial knockdown of PKCδ protein significantly inhibited proliferation of multiple melanoma cell types with NRAS mutations, including SBcl2, FM28, FM6 and SKMEL2 cells (**Figure 1**). Although transfection with negative-control siRNA produced slight cytotoxicity in some cell lines, the resulting proliferation curves did not differ significantly from those of vehicle control in these cell lines. Interestingly, the degree of protein knockdown, quantified by densitometric analysis, did not appear to be the sole factor in determining the degree of growth inhibitory effect by siRNA transfection, as these parameters did not always correlate among the cell lines. It is likely that some cell lines are more susceptible than others to cell growth inhibition resulting from PKCδ downregulation.

Figure 1: Downregulation of PKCδ suppresses cell survival in melanoma cell lines with NRAS mutation. siRNA targeting PKCδ ("siPKCδ") or non-targeting siRNA ("siControl") were transfected to SBcl2 and FM28 (50 nM), SKMEL2 (10 nM), and FM6 and WM1366 (5 nM), after establishing cell line-specific optimal transfection conditions. As a vehicle control, cells were treated in parallel with transfection reagent alone ("vehicle"). MTS assays were performed at 3 or 4 days after siRNA transfection. Each point represents the average of triplicates, and error bars indicate the standard deviations. P values (*) were calculated between vehicle control and si PKCδ on the last assay day (p < 0.006). Downregulation of PKCδ protein on the first assay day was assessed by immunoblot analysis. The relative band intensity of PKCδ was indicated below the image (normalized to loading controls, β-actin, α-tubulin or GAPDH) (from Takashima, et al, 2014).

These cell survival assays verified that PKCδ can be a potential therapeutic target for melanomas with NRAS mutations.

Small Molecule inhibitors. We describe the development of new specific PKCδ inhibitory molecules, and then show the results of the testing of these compounds on prostate cancer cell lines.

Pharmacophore Modeling and Development of new PKCδ *Inhibitors:* Highly isotype-specific PKCδ-inhibitory small molecules had not been identified by others to date. With our discovery and genetic validation that PKCδ is the specific target molecule for this Ras-targeted approach, we generated a pharmacophore model based on molecular interactions with "novel" class PKC isozymes. We established an initial pharmacophore model for PKCδminhibitors, using mallotoxin/rottlerin [Lead Compound 1 (**LC-1**)] as a prototype structure for a moderately PKCδ - specific inhibitor (IC$_{50}$=5μM), and incorporated protein structural data for PKCθ, another member

of the "novel" group of PKC enzymes, which is also inhibited by mallotoxin. LC-1 is a naturally-occurring product, with moderate aqueous solubility, and oral bioavailability. It inhibits purified PKCδ at an IC$_{50}$ of 3-5 μM *in vitro,* and inhibits PKCδ in cultured cells with an IC$_{50}$ of 5 μM *in vivo* (but at 0.5 μM with exposure for >24 hrs, because of down-regulation of the PKCδ protein)*.* It is relatively selective for PKCδ over PKCα (PKCα IC$_{50}$:PKCδ IC$_{50}$ is approximately 30:1). Furthermore, as we have published, this compound not only directly inhibits purified PKCδ, but also, over longer periods of exposure, significantly down-regulates PKCδ protein specifically, while having no effect on the levels of other PKC isozymes.[5] Thus, this compound inhibits PKCδ at two levels. We have demonstrated "Ras-specific" activity of this compound in a number of publications and assays (see above). Daily *i.p.* doses of up to 40 mg/kg (800 μg/20 g) in mice do not produce any overt toxicity in our xenograft studies or others. Stability: Informal stability testing demonstrates >95% stability as a powder at room temp for >6 months. Toxicology: Pilot and published toxicity data indicate that the compound has a low toxicity profile (lowest lethal dose = 750 mg/kg, rat oral); 120 mg/kg (oral 6-day rat study) is the lowest toxic dose.[6,7] This relative safety, combined with its *in vivo* efficacy, makes Lead Compound I attractive as a starting point for modification and drug development. We have demonstrated that better therapeutic candidates can be developed from it. The rationale for the development of new inhibitors was to improve the PKCδ -selectivity and potency. [Potential limitations on LC-1 itself as a therapeutic agent (despite its *in vivo* safety and activity) include its lack of high specificity for PKCδ, its off-target effects, including inhibition of Cam Kinase III, MAPKAP-K2, and PRAK1 at IC$_{50}$s of <10 μM; its non-PKC-mediated effects on mitochondrial uncoupling and modulation of death receptor pathways; and the lack of composition-of-matter IP around it, which would preclude eventual clinical development by big pharma.]

We designed and synthesized a 2nd generation set of analogs. In Analogs 1 and 2, the "head" group (A) was been made to resemble that of staurosporine, a potent general PKC inhibitor and other bisindoyl maleimide kinase inhibitors, with domains B and C conserved to preserve isozyme specificity. Ease of synthesis was a major factor in the design of this head group. Analogs 3 to 5 have "head groups" from other known kinase inhibitors: 1) Analog 3 from the crystal structure of an inhibitor bound to CDK2 (pdb code: 1FVT); 2) Analog 4 based on purine, found in a number of different potent kinase inhibitors; and 3) Analog 5 from a potent inhibitor of aurora kinase (pdb code 2F4J). The first 2nd generation chimeric molecule, KAM1, was indeed active, and more PKCδ -specific (see **Table 2,** below), and showed activity against cancer cells with activation of Ras or Ras signaling. Another 2nd generation compound we generated (CGX, with a very different composition but which fit the pharmacophore model) has demonstrated activity against multiple human cancer cell lines with activated K- or H-Ras alleles *in vitro* and *in vivo* in animal models. On the basis of SAR analysis of KAM1, we generated 36 new 3rd generation compounds (**Table 3**).

The PKCδ inhibitory activity and isozyme-specificity of the 36 3rd generation analogs was assayed *in vitro,* using recombinant PKC isozymes, prior to comparative testing on prostate cancer cell lines.

Method: These assays utilize fluorogenic FRET detection (Z-lyte, R&D Systems) technology and peptide substrates, are robust and validated, and have been used to screen the 2nd and 3rd generation PKCδ inhibitors we have synthesized.

Results:

1. PKCδ Activity Assays of 3rd Generation Compounds

Compound	IC$_{50}$ (in vitro)[1]			IC$_{50}$ (in culture)[3]
	PKCδ IC$_{50}$ (μM)	PKCα IC$_{50}$ (μM)	PKCδ/PKCα (IC$_{50}$ ratio)[2]	
Rottlerin	4.4	75	28	10
KAM-1	3.6	177	56	5
B058	5.8	NA[4]	-	>50
B071	3	NA	-	>100
B095	8	NA	-	>100
B097	9.5	NA	-	>100
B106	0.08	15	200	1
B108	3	NA	-	>100
B109	0.09	75	800	>100
B111	2.5	25	100	40
B112	6	NA	-	>50
B117	4.5	NA	-	>100
B118	10	NA	-	>100
B121	4	NA	-	>100
B125	0.25	20	800	>100
B128	6.5	NA	-	>100
B129	6.5	NA	-	>50
B130	4	NA	-	40
B131	10	NA	-	>100
B136	14	NA	-	>100
B137	3	NA	-	>100
B141	4.8	NA	-	>50
B142	3.5	NA	-	>100
B143	6	NA	-	>100
B146	5	NA	-	>100
B147	5.8	NA	-	20
B148	4	NA	-	>100
B149	0.31	>300	>1000	20
B150	0.625	500	800	30
B151	< 0.05	50	>1000	>100
B152	< 0.05	50	>1000	>100
B153	3	NA	-	>100
B154	23	NA	-	>100
B155	3	NA	-	>100
B156	7.5	NA	-	>100
B157	5	NA	-	>100
B158	4.5	NA	-	>100
B159	7	NA	-	40

[1] IC$_{50}$ measured using recombinant PKCδ or PKCα

[2] Ratio of PKCδ IC$_{50}$ to PKCα IC$_{50}$

[3] IC$_{50}$ for cytotoxicity on a KRAS-mutant cell line H460.

[4] NA = not assayed (PKCα inhibitory activity was only assayed on compounds with an IC$_{50}$ for PKCδ of <2.5 μM).

Table 1: Summary PKCδ and PKCα inhibitory activity of 36 3rd generation compounds, expressed as IC$_{50}$. Summary of relative cytotoxicity on multiple cancer cell lines, relative to rottlerin (from Takashima, et al, 2014).

Compounds were tested at 0.01, 0.05, 0.1, 0.5, 1.0, 5, 10 and 50 μM. and results were shown in prior progress report. The selectivity of the inhibitors for PKCδ were assessed by comparison with PKCδ inhibitory activity, using recombinant PKCδ enzyme and FRET substrate.
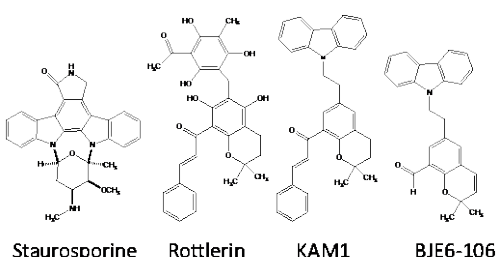
The information from the enzymatic activity/inhibitor assays above were compiled into a summary table (**Table 1**) for purposes of comparison.

Interpretation: Certain of the 3rd generation compounds show substantially greater PKCδ inhibitory activity and specificity than LC-1 or 2nd generation compounds. For example, one such novel compound ("B106") is <u>much more potent</u> than LC-1 (**Table 1**), producing substantial cytotoxicity against Ras-mutant tumor lines at concentrations ~40 times lower than LC-1. This compound is <u>also active *in vivo*</u>, in a Ras-mutant cell xenograft assay. Both LC-1 and B106 dramatically inhibited clonogenic capacity of Ras-mutant tumor cell lines after as little as 12 h exposure. A newer derivative of this particular compound (CGD63), not yet optimized with respect to drug-like properties, has a PKCδ IC$_{50}$ in the range of <u>0.05 μM</u> (compared to 3 μM for LC-1), is <u>1000-fold more inhibitory</u> against PKCδ than PKCα *in vitro,* and produces cytotoxic activity against Ras-mutant cells at nM concentrations. (Specificity for PKCδ over classical PKC isozymes, like PKCα, is important: inhibition of PKCα is generally toxic to <u>all</u> cells, normal and malignant, and would make our agent non-"tumor-targeted.") We are therefore seeking to maximize PKCδ <u>-isozyme-specificity</u> for the inhibitors to retain the tumor-targeted cytotoxic properties. We will eventually test selected inhibitors against an entire panel of recombinant PKC isozymes, including the classical, novel and atypical classes.

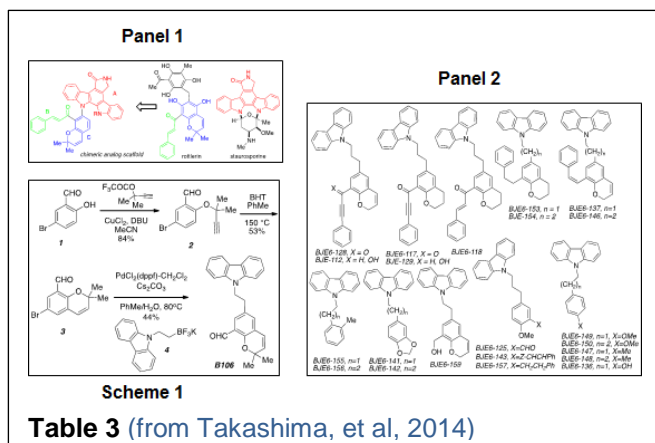**Table 2** compares the 3 generations of PKCδ - inhibitory compounds tested to date.

PKCd inhibitors

Staurosporine   Rottlerin   KAM1   BJE6-106

Generation	PKCδ IC$_{50}$	PKCα IC$_{50}$	PKCδ/PKCα Selectivity Ratio
1	3 μM	75 μM	28-fold
2	2 μM	157 μM	56-fold
3	0.05 μM	50 μM	1000-fold

Table 2

3. Testing of 3rd Generation PKCδ Inhibitor Compounds in Melanoma Cell lines

Table 3 (from Takashima, et al, 2014)

Materials and Methods:
- Cells were grown on 60 mm tissue culture dishes, seeded to 1 x 10^5 cells per well:
- Cells were allowed to grow 24 hrs at 37°C and 5% CO2.
- On treatment day, media was removed from each plate and replaced with either vehicle or test compound in growth media
  - DMSO (vehicle for compounds)
  - Compounds tested at various concentrations
- At 48 or 72 hrs, cells were harvested, and viable cell mass quantitated via MTT or MTS assay.

We initially tested the entire panel of 36 3rd generation compounds against human cancer cell lines with an activating Ras mutation. The compounds were prepared in stock solutions. We found that certain 3rd generation compounds (106, 147, 149, 112 and 159) showed toxicity against this cell line comparable to LC-1 or greater than LC-1. Compound 106 ("B106") consistently showed the most consistent and highest activity and was chosen as the lead compound for the subsequent studies.

B106 was tested at multiple concentrations against a panel of human melanoma cell lines with activation of Ras signaling pathways, and compared to LC1 (rottlerin) or vehicle.

Approach:

MTS Assay: SBcl2. FM6, WM1366, SKMEL2, WM1361A, and WM852 + vehicle (DMSO), or 2 or 5uM Rottlerin or 0.2 or 0.5 uM B106 or 5 uM B154 (negative control compound) x 96hrs. Treated on 3rd day after plated cells.

Objective:
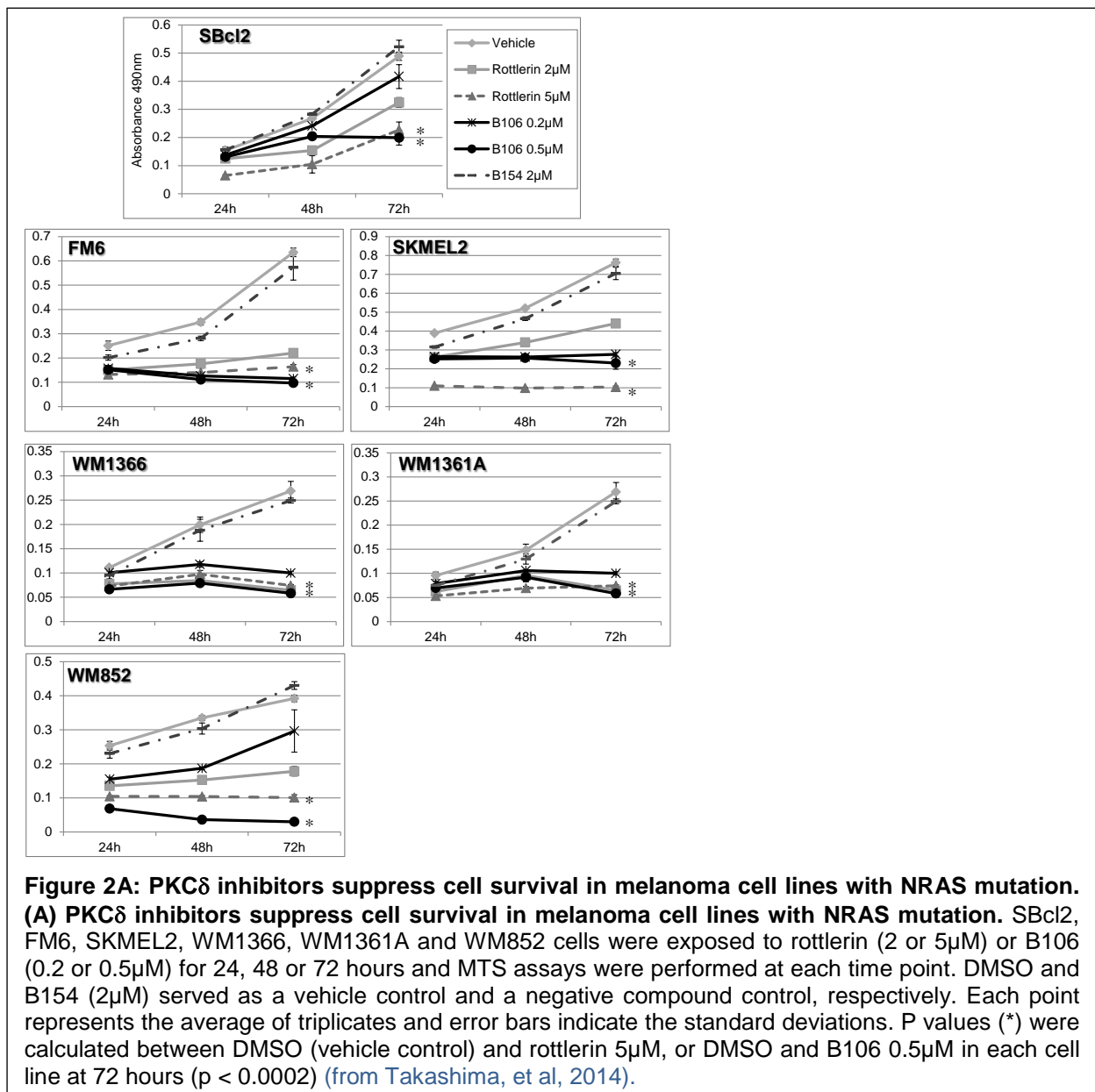- To quantitate effects of small molecule PKC inhibitors on melanoma cell lines

Materials and Methods
- Day 0: Cell plating day
  - Cells were plated at 2000 cells per well in 96 well plates. Quadruplicate samples were plated and grown at 37oC in 5% CO$_2$. Cells were allowed to grow for three days.
  - melanoma cells: 10%FBS (Invitrogen); Dulbecco's Modification of Earle's Media (MediaTech); 2mM L-Glutamine (Invitrogen); 200 U Penicillin/ml; 200ug Streptomycin/ml (Invitrogen); 0.015M HEPES; Passage 10.
- Day 3: Treatment day
  - Media was removed from each well and replaced with 0.1ml of treatment prepared in fresh growth media and filter sterilized:
    - DMSO (Fisherbrand), vehicle.
    - Rottlerin (EMD Chemical), 40 mM stock in DMSO, aliquoted, not re-frozen.
    - B106, 40 mM stock in DMSO, aliquoted, not re-frozen.

- B154, 40 mM stock in DMSO, aliquoted, not re-frozen.

- Day 4 (24 hr tmt), Day 5 (48 hr tmt), Day 6 (72 hr tmt), Day 7 (96 hr tmt):
  - Observations were made on the confluency of treated cells compared with vehicle treatment.

- MTS Assay was performed at each time point (CellTiter 96 Aqueous One Solution Cell Proliferation Assay (Promega)) as described by manufacturer.
  - 20 ul of the assay buffer was added to each well. Cells were incubated for one hour at 37oC in 5% CO_2 humidified atmosphere.
  - The absorbance at 490 nm was read on the Molecular Devices, SpectraMax 190 plate reader.

Results and Interpretation: Inhibition of PKCδ activity induces cell growth inhibition in melanoma cell lines with NRAS mutations

To investigate the effect of PKCδ inhibition by small molecule compounds on tumor cell growth, tumor cell survival was assessed in the presence of rottlerin or B106 using multiple melanoma cell lines with NRAS mutations, including SBcl2, FM6, SKMEL2, WM1366, WM1361A and WM852 (**Figure 2A**). Cells were exposed to rottlerin (2 or 5µM) or B106 (0.2 or 0.5µM) and viable cells were quantitated at 24, 48 and 72 hours after treatment. Rottlerin consistently inhibited proliferation of all cell lines at 5µM, and intermediate inhibitory effects were observed at 2µM. The 3rd generation PKCδ inhibitor B106 effectively inhibited growth of all cell lines tested at 0.5µM, and at 0.2µM in some cell lines, which is at least ten times lower than the concentration of rottlerin required to exert the same magnitude of cytotoxic effect. Exposure to B154 at 2µM produced a proliferation curve similar to vehicle (DMSO) treatment in all cell lines, consistent with our hypothesis that the cell growth inhibition induced by B106 resulted from the inhibition of PKCδ activity. These assays demonstrated the greater potency of B106 on tumor cell growth inhibition in comparison to rottlerin, with activity at nanomolar concentrations. A clonogenic colony assay was performed using SBcl2 cells to determine the kinetics of the action of PKCδ inhibitors on the growth and proliferative characteristics of the cells. In contrast to a proliferation assay, which examines potentially temporary and reversible effects on proliferation and survival of cells while being exposed to a compound, clonogenic assays assess irreversible effects on cell viability and proliferative capacity, which are likely more relevant to potential clinical application. Cells were exposed to rottlerin or B106 for 12, 24 or 48 hours and then re-plated in medium without inhibitors, and the difference in colony-forming ability of cultures was assessed. Both rottlerin and B106 treatment significantly decreased the number of colonies formed in SBcl2 cells after as little as 12 hours of treatment, and approximately 40-fold reduction in the number of colonies was observed with 48 hours of drug treatment (**Figure 2B**). These results demonstrate an irreversible cytotoxic effect of these PKCδ inhibitors on tumor cell growth, and dose-dependency (**Figure 2C**).

Figure 2A: PKCδ inhibitors suppress cell survival in melanoma cell lines with NRAS mutation. (A) PKCδ inhibitors suppress cell survival in melanoma cell lines with NRAS mutation. SBcl2, FM6, SKMEL2, WM1366, WM1361A and WM852 cells were exposed to rottlerin (2 or 5μM) or B106 (0.2 or 0.5μM) for 24, 48 or 72 hours and MTS assays were performed at each time point. DMSO and B154 (2μM) served as a vehicle control and a negative compound control, respectively. Each point represents the average of triplicates and error bars indicate the standard deviations. P values (*) were calculated between DMSO (vehicle control) and rottlerin 5μM, or DMSO and B106 0.5μM in each cell line at 72 hours (p < 0.0002) (from Takashima, et al, 2014).

Cytotoxicity Assays

Inhibition of PKCδ activity triggers caspase-dependent apoptosis

We next determined how PKCδ inhibition results in suppression of tumor cell growth in melanoma. Apoptosis, which can be initiated by various stimuli, intrinsic or extrinsic inducers, is mediated in many cases by a proteolytic cascade of caspases, a family of cysteine proteases. Activated caspase 3 and caspase 7, the ultimate executioners of apoptosis, trigger proteolytic cleavage of crucial key apoptotic proteins, which in turn leads to late apoptotic events, including DNA fragmentation. To explore the possible involvement of apoptosis in the cell growth inhibition induced by PKCδ inhibition, the activity of effector caspases 3 and 7 was assessed in cells treated with PKCδ inhibitors. Twenty-four hours of exposure to rottlerin (5μM) or B106 (0.2 and 0.5 μM) significantly increased the activity of caspase 3/7 in SBcl2 cells compared to

Figure 2B: PKCδ inhibitors suppress cell survival in melanoma cell lines with NRAS mutation. (B) PKCδ inhibitors induce irreversible effect on cell growth. SBcl2 cells were treated with rottlerin or B106 at 5μM for 0, 12, 24 or 48 hours. After these exposure times, the same number of viable cells from each treatment condition was replated at low cell density and cells were cultured in medium without inhibitors for 8 days. Cell colonies were stained with ethidium bromide for visualization and counted. Each point represents the average of triplicates and error bars indicate the standard deviations. P values: ** p<0.01, * p<0.001 compared to time 0 h (from Takashima, et al, 2014).
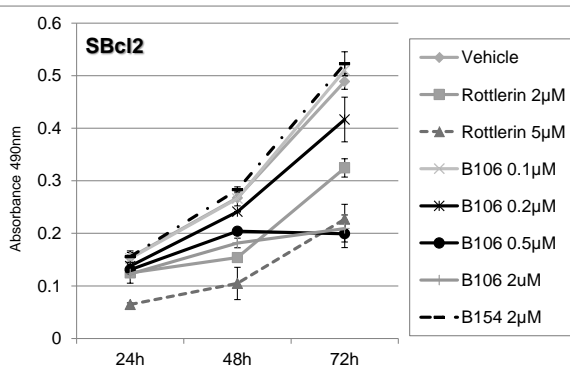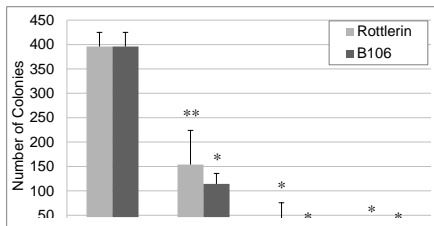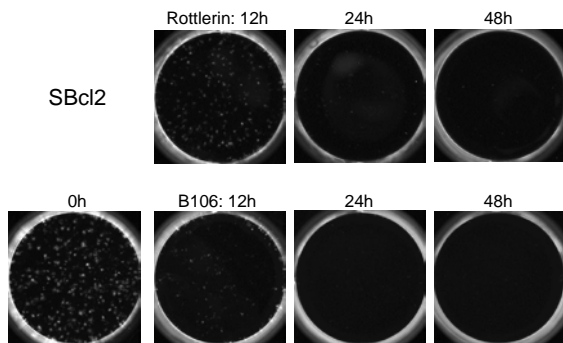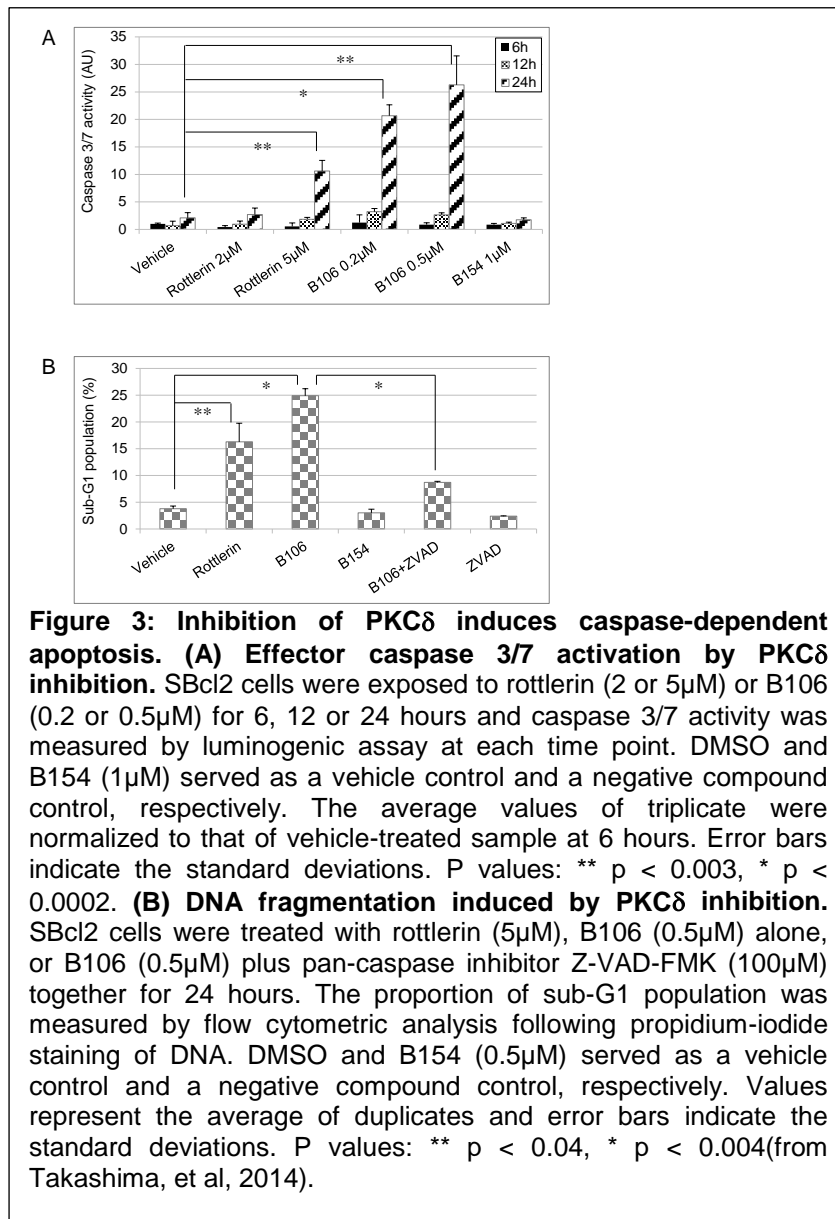

Figure 2C: Titration of PKCˊ inhibitor treatment. The expanded doses of B106 (0.1 μM and 2 μM) in the MTS assay in SBcl2. ** indicates a p value less than 0.5 between treatment of 2 μM of rottlerin and B106 (from Takashima, et al, 2014).

apoptosis in NRAS-mutant melanoma cells.

vehicle (DMSO) (**Figure 3A**). The effect of B106 on caspase 3/7 activation was greater than that of rottlerin: a 10-fold increase at 0.2μM and a 12.5-fold increase at 0.5μM of B106, in contrast to a 5-fold increase by rottlerin at 5μM. The negative-control compound B154 did not induce the activity of caspase 3/7. These findings indicated the potential involvement of caspase 3/7-mediated apoptosis in response to PKCδ inhibition.

As evidence of apoptosis, induction of DNA fragmentation, a hallmark of late events in the sequence of the apoptotic process, in the presence or absence of PKCδ inhibitors was assessed by flow cytometric analysis following propidium iodide staining of DNA. The proportion of cells containing a DNA content of less than 2n (fragmented DNA), categorized as the "sub-G1" population and considered in the late apoptotic phase, was significantly higher after treatment with rottlerin at 5μM and even higher after treatment with B106 at 0.5μM, whereas B154, a negative-control compound for B106, lacking PKCδ-inhibitory activity, produced no more fragmented DNA than did vehicle control (DMSO), suggesting the effect of B106 on DNA fragmentation was related to inhibition of PKCδ activity (**Figure 3B**). To determine whether activation of caspases by PKCδ inhibitors was necessary for the observed apoptosis, the pan-caspase inhibitor Z-VAD-FMK (carbobenzoxy-valyl-alanyl-aspartyl-[Omethyl]-fluoromethylketone) was employed. Z-VAD-FMK irreversibly binds to the catalytic site of caspase proteases and prevents caspases from being cleaved and activated. Pre-treatment of cells with Z-VAD-FMK (50μM) prevented B106-induced caspase 3 cleavage in immunoblot analysis (data not shown). B106-induced DNA fragmentation was significantly abrogated when SBcl2 cells were pretreated with Z-VAD-FMK (100μM) (**Figure 3B**). Exposure to Z-VAD-FMK alone produced only a similar fraction of sub-G1 cells as did vehicle or B154 treatment. Taken together, these data suggest that PKCδ inhibition attenuates tumor cell growth by inducing caspase-dependent

Figure 3: Inhibition of PKCδ induces caspase-dependent apoptosis. (A) Effector caspase 3/7 activation by PKCδ inhibition. SBcl2 cells were exposed to rottlerin (2 or 5μM) or B106 (0.2 or 0.5μM) for 6, 12 or 24 hours and caspase 3/7 activity was measured by luminogenic assay at each time point. DMSO and B154 (1μM) served as a vehicle control and a negative compound control, respectively. The average values of triplicate were normalized to that of vehicle-treated sample at 6 hours. Error bars indicate the standard deviations. P values: ** p < 0.003, * p < 0.0002. **(B) DNA fragmentation induced by PKCδ inhibition.** SBcl2 cells were treated with rottlerin (5μM), B106 (0.5μM) alone, or B106 (0.5μM) plus pan-caspase inhibitor Z-VAD-FMK (100μM) together for 24 hours. The proportion of sub-G1 population was measured by flow cytometric analysis following propidium-iodide staining of DNA. DMSO and B154 (0.5μM) served as a vehicle control and a negative compound control, respectively. Values represent the average of duplicates and error bars indicate the standard deviations. P values: ** p < 0.04, * p < 0.004(from Takashima, et al, 2014).

PKCδ inhibition triggers apoptotic response via the stress-responsive JNK pathway

To identify which intracellular signaling pathway PKCδ inhibition employs to induce cytotoxicity, the activation status of known downstream targets of PKCδ was examined after PKCδ inhibition, including MAPKs (ERK, p38 and JNK), AKT, NFᵒB pathway, cyclin-dependent kinase inhibitors, p53, IAPs, GSK3² or c-Abl. Inhibition of PKCδ activity in SBcl2 cells by B106 induced phosphorylation (activation) of JNK1/2 (T183/Y185) most strongly after two hours of exposure, with phosphorylation diminishing subsequently (**Figure 4A**). In contrast, phosphorylation of the closely-related MAPKs p38 and ERK was not affected by PKCδ inhibitors (**Figure 4A**). Consistent with these observations generated using chemical inhibitors, selective downregulation of PKCδ by transfection of PKCδ-specific siRNA induced phosphorylation of JNK1/2 at 24 hours (when effects of siRNA on PKCδ levels were first observed), whereas transfection of negative-control non-targeting siRNA did not affect JNK1/2 phosphorylation (**Figure 4B**). Transfection of PKCδ-specific or negative control siRNA did not affect phosphorylation levels of ERK or p38.
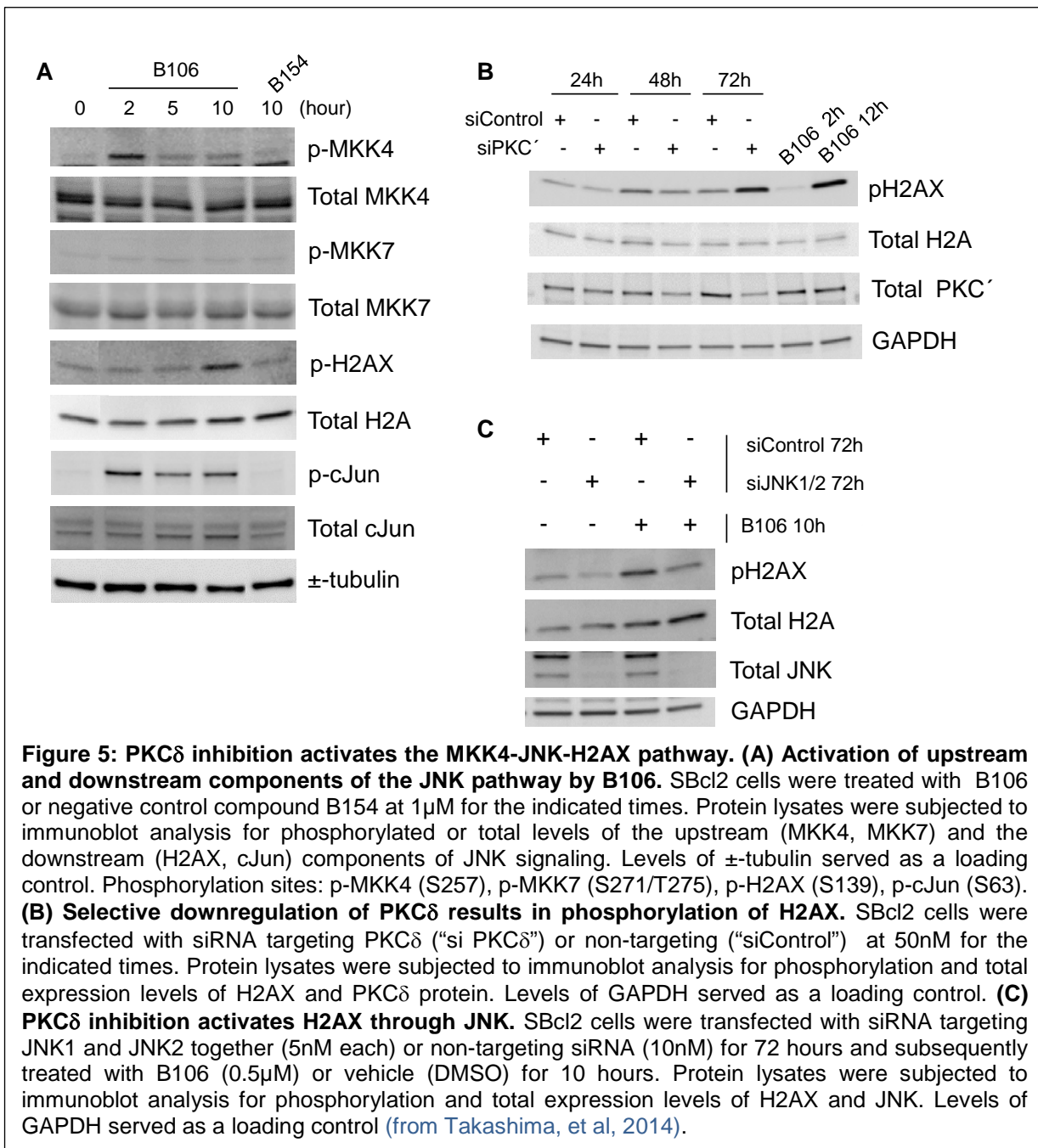
Among its pleiotropic cellular activities, JNK is an effector in certain apoptotic responses, and some chemotherapeutic agents, including paclitaxel, cisplatin and doxorubicin, employ the JNK pathway for their cytotoxic activity. Because of the data demonstrating that PKCδ inhibition causes caspase-dependent apoptosis (**Figure 3**) and JNK activation (**Figures 4A and 4B**), the effect of inhibition of the JNK pathway during B106 treatment was explored to determine if there is a functional relationship. SBcl2 cells were transfected with non-specific siRNA or siRNA specific for JNK1 or JNK2 alone, or co-transfected with JNK1- plus JNK2-specific siRNA for 72 hours, and then exposed to B106 or DMSO (vehicle) for 6, 12 or 24 hours, followed by measurement of caspase activity (**Figure 4C**). Analysis at 24 hours after B106 treatment showed that knockdown of JNK2 alone, and co-knockdown of JNK1 and 2, mitigated B106-induced caspase 3/7 activation in rough proportion to the knockdown efficiency of JNK1/2 proteins, as determined by immunoblot analysis. These data indicated that JNK is a necessary mediator of the apoptotic response induced by PKCδ inhibition.

Figure 4: PKCδ inhibition triggers an apoptotic response through activation of JNK. (A, B) PKCδ inhibition activates JNK. SBcl2 cells were exposed to B106 (1μM) or negative control compound B154 (1μM) for indicated times (A) or transfected with siRNA targeting PKCδ ("siPKCδ") or non-targeting siRNA ("siControl") at 5nM for the indicated times (B). Protein lysates were subjected to immunoblot analysis for levels of phosphorylated or total MAPK proteins. Phosphorylation sites: p-JNK1/2 (T183/Y185), p-ERK1/2 (T202/T204), p-p38 (T180/Y182). **(C) Activation of caspase 3/7 is mitigated by knockdown of JNK prior to B106 treatment.** SBcl2 cells were transfected with siRNA targeting JNK1 or JNK2 alone (5nM), or the combination of JNK1 and JNK2 siRNA (5nM each), or non-targeting siRNA (10nM) for 72 hours, and subsequently treated with B106 (0.5μM) or vehicle (DMSO) for 6, 12 and 24 hours. Caspase 3/7 activity was measured by luminogenic assay at each time point. The average values of triplicates were normalized to that of the vehicle-treated sample at 6 hours between the pairs of the same siRNA. Error bars indicate the standard deviations. P values: * p < 0.005. Downregulation of JNK1/2 proteins were confirmed by immunoblot analysis. Cells were lysed after 72 hours of siRNA transfection. Each of the two bands detected in immunoblotting with JNK1/2 antibodies represent assembly of different splicing variants from both JNK1 and 2 isoforms. Levels of GAPDH served as a loading control (from Takashima, et al, 2014).

PKCδ inhibition activates the MKK4-JNK-H2AX pathway

We tested for involvement of known upstream and downstream effectors of the JNK pathway following PKCδ inhibition. The MAPKK kinases MKK4 and MKK7 lie one tier above JNK. MKK4 was activated by B106 (as assessed by activating phosphorylation) whereas MKK7 was not (**Figure 5A**). Activation of the canonical JNK substrate, c-Jun, was also observed in response to B106 exposure, confirming the activation of the JNK pathway by PKCδ inhibitors (**Figure 5A**). Furthermore, activation of H2AX (histone H2A variant X), another downstream effector of JNK associated with its apoptotic actions, was noted at later time points in response to B106 treatment (**Figure 5A**). B106 consistently induced H2AX phosphorylation as early as 10 hours (times later than 24 hours were not studied because significant cytotoxicity is occurring after this time). The effect of PKCδ inhibition on H2AX activation was further confirmed by selective downregulation of PKCδ with siRNA. Phosphorylation of H2AX was observed at 72 hours after

Figure 5: PKCδ inhibition activates the MKK4-JNK-H2AX pathway. (A) Activation of upstream and downstream components of the JNK pathway by B106. SBcl2 cells were treated with B106 or negative control compound B154 at 1µM for the indicated times. Protein lysates were subjected to immunoblot analysis for phosphorylated or total levels of the upstream (MKK4, MKK7) and the downstream (H2AX, cJun) components of JNK signaling. Levels of ±-tubulin served as a loading control. Phosphorylation sites: p-MKK4 (S257), p-MKK7 (S271/T275), p-H2AX (S139), p-cJun (S63). **(B) Selective downregulation of PKCδ results in phosphorylation of H2AX.** SBcl2 cells were transfected with siRNA targeting PKCδ ("si PKCδ") or non-targeting ("siControl") at 50nM for the indicated times. Protein lysates were subjected to immunoblot analysis for phosphorylation and total expression levels of H2AX and PKCδ protein. Levels of GAPDH served as a loading control. **(C) PKCδ inhibition activates H2AX through JNK.** SBcl2 cells were transfected with siRNA targeting JNK1 and JNK2 together (5nM each) or non-targeting siRNA (10nM) for 72 hours and subsequently treated with B106 (0.5µM) or vehicle (DMSO) for 10 hours. Protein lysates were subjected to immunoblot analysis for phosphorylation and total expression levels of H2AX and JNK. Levels of GAPDH served as a loading control (from Takashima, et al, 2014).

PKCδ siRNA transfection, but not in the cells transfected with negative-control siRNA (**Figure 5B**). This temporal course was consistent with the observation above of H2AX phosphorylation subsequent to the initiation of the MKK4/JNK cascade activation seen with PKCδ inhibitor treatment (**Figure 5A**). To ensure that activation of JNK pathway by B106 is not a cell-type-specific response, these pathway effectors were examined in another NRAS mutant melanoma cell lines WM1366. PKCδ inhibition by B106 treatment similarly induced phosphorylation of MKK4, JNK and H2AX in WM1366 cells (data not shown).

Because JNK affects diverse downstream effectors, we next determined whether JNK activation caused by PKCδ inhibition is directly linked to B106-induced H2AX activation. Cells were transfected with either negative-control siRNA or JNK1/2-specific siRNA for 72 hours and then exposed to vehicle or B106 for another 24 hours. Knockdown of JNK1/2 itself slightly reduced basal phospho-H2AX (pH2AX) expression, indicating that basal phosphorylation of H2AX is regulated by JNK (Lane 2, **Figure 5C**). B106 exposure robustly induced phosphorylation of H2AX in control siRNA-treated cells (Lane 3, **Figure 5C)** as expected; in comparison, prior downregulation of JNK1/2 protein by siRNA attenuated B106-induced H2AX phosphorylation (Lane 4, **Figure 5C**). These findings confirmed that JNK lies upstream of H2AX, because H2AX is not activated in response to PKCδ inhibitors in the absence of JNK, supporting a model in which inhibition of PKCδ by B106 causes JNK/H2AX pathway signaling.

Collectively, these data suggest that PKCδ inhibition in cells containing mutated NRAS activates MKK4, directly or indirectly, which in turn activates JNK1/2 and subsequently H2AX.

H2AX is a critical regulator of caspase-dependent apoptosis induced in response to PKCδ inhibition

Although phosphorylation of H2AX is best known as a consequence of DNA double-strand breaks in the DNA damage response, recent studies have demonstrated that phosphorylation of H2AX resulting from JNK activation actively mediates the induction of apoptosis.[6] Our findings of PKCδ inhibition-induced activation of the JNK/H2AX pathway and caspase-dependent apoptosis raised the possibility that inhibition of PKCδ activity caused caspase-dependent apoptosis through activation of the JNK/H2AX pathway. Accordingly, the direct involvement of H2AX in apoptotic response to PKCδ inhibition was examined. SBcl2 cells were transfected with siRNA targeting H2AX, or non-targeting siRNA, for 72 hours and then exposed to B106 for 6, 12 or 24 hours, with subsequent assay of caspase 3/7 activation. Downregulation of H2AX prior to B106 treatment greatly decreased the level of caspase 3/7 activation at 24 hours of B106 exposure compared to the cells pre-treated with control siRNA (**Figure 6A**).

Subsequently, in order to explore a direct link between H2AX and the execution of apoptosis, PKCδ inhibition-induced DNA fragmentation was examined in the presence or absence of H2AX. Similar to the experiment in Figure 6A, SBcl2 cells were transfected with either negative-control siRNA or siRNA targeting H2AX for 72 hours, and then subjected to PKCδ inhibition by B106 treatment for the next 24 hours. DNA fragmentation was assessed by flow cytometric analysis following propidium iodide staining of DNA. PKCδ inhibition by B106 treatment increased DNA fragmentation 8.5-fold in the cells transfected with negative control siRNA (**Figure 6B**). In contrast, PKCδ inhibition by B106 treatment failed to induce DNA fragmentation in the absence of H2AX, induced by transfection of siRNA targeting H2AX (**Figure 6B**). B106-induced DNA fragmentation in the cells with H2AX downregulation was significantly reduced compared to that in the cells with H2AX expression, indicating that H2AX is necessary for B106-induced apoptosis (**Figure 6B**). Collectively, these results suggest that inhibition of PKCδ by B106 treatment triggers caspase-dependent apoptosis through activation of the JNK-H2AX stress-responsive signaling pathway.

Figure 6: H2AX is a critical apoptotic regulator in apoptosis induced by PKCδ inhibition. (A) Activation of caspases 3/7 is mitigated by knockdown of H2AX prior to B106 treatment. SBcl2 cells were transfected with siRNA targeting H2AX or non-targeting siRNA at 5nM for 72 hours, and subsequently treated with B106 (0.5µM) or vehicle for 6, 12 or 24 hours. Caspase 3/7 activity was measured by luminogenic assay at each time point. The average values of triplicates were normalized to that of the vehicle-treated sample at 6 hours between the pairs of the same siRNA. Error bars indicate the standard deviations. P values: * $p < 0.005$. Downregulation of H2AX was confirmed by quantitative PCR. mRNA was extracted 72 hours after siRNA transfection. **(B) Induction of DNA fragmentation is mitigated by knockdown of H2AX prior to B106 treatment.** SBcl2 cells were transfected with siRNA targeting H2AX, or non-targeting siRNA, at 5nM for 72 hours, and subsequently exposed to B106 (0.5µM) or vehicle for 24 hours. The proportion of sub-G1 population was measured by flow cytometric analysis following propidium-iodide staining of DNA. The average values of duplicate were normalized to that of the vehicle-treated sample between the pairs of the same siRNA. Error bars indicate the standard deviations. P value: * $p < 0.0004$. Downregulation of H2AX was confirmed by quantitative PCR. mRNA was extracted after 96 hours of siRNA transfection (from Takashima, et al, 2014).

Task: Testing the activities of next generation PKCδ inhibitors on non-transformed human cells, including primary human melanocytes and endothelial cells and other non-tumor cells.

B106 produced no statistically-significant effects on the proliferation of primary human melanocytes at concentrations of 0.5 and 1.0 μM, indicating the tumor-specific effect of B106 (**Figure 7**).
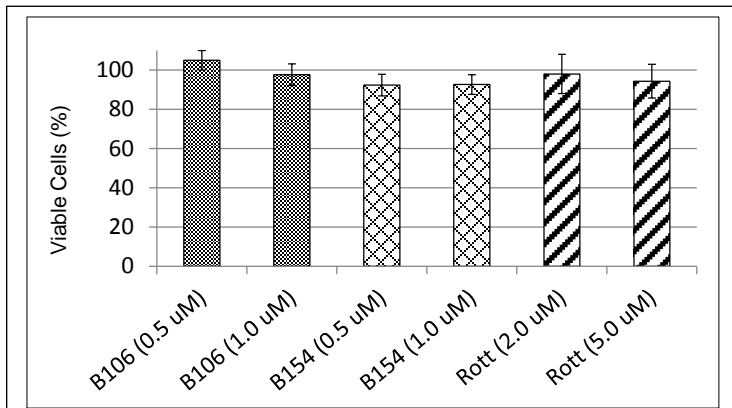
Figure 7: Effects of PKCδ inhibitors on primary human melanocytes. Cell survival of human primary melanocytes exposed to the indicated concentrations of the compounds for 72 h (relative to DMSO-treated controls; mean ± SD, n = 3) (from Takashima, et al. 2014).

The effects of the 3rd generation PKCδ inhibitors on other non-tumor cells was examined. The pZ-HPV-7 cell line was derived from primary human prostate epithelial cells by transformation with human papilloma virus. While not tumorigenic, they do exhibit some properties of transformed cells.

Approach: MTS Assay: pZ-HPV-7 cells (Immortalized Prostate Epithelial Cells) were treated with Rottlerin or B106 at the indicated concentrations for 96 hrs. MTS assay was then carried to quantitate cell growth.

Results: The pZ-HPV-7 cells were sensitive to PKCδ inhibition to some extent (**Fig. 8**). Whether this was caused by the transformation with HPV is not clear.
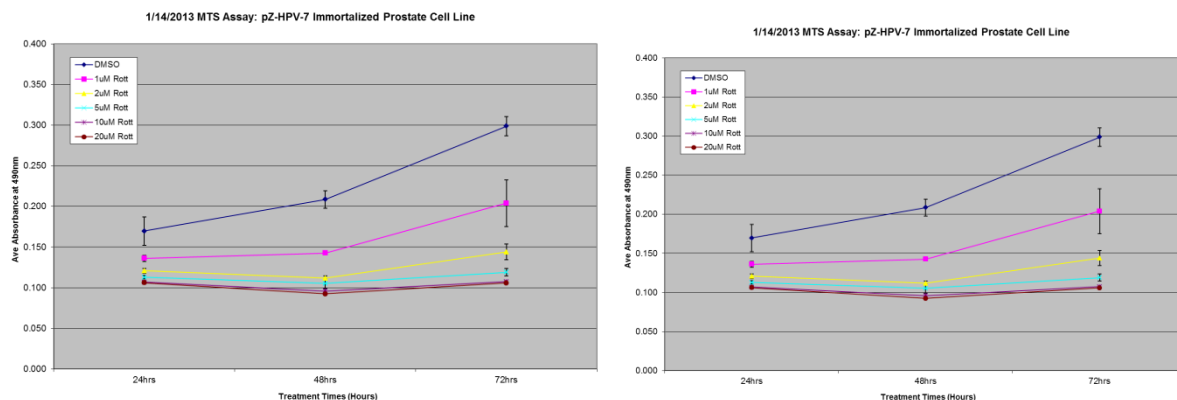
Figure 8

We decided therefore to examine the sensitivity of another epithelial cell line derived from a hormone responsive tissue, the breast epithelial cell line MCF 10A.

Approach:

MCF 10A cells were treated with Rottlerin or B106 at the indicated concentrations. MTS assay was then carried out at 24, 48 and 72 h to quantitate cell growth.
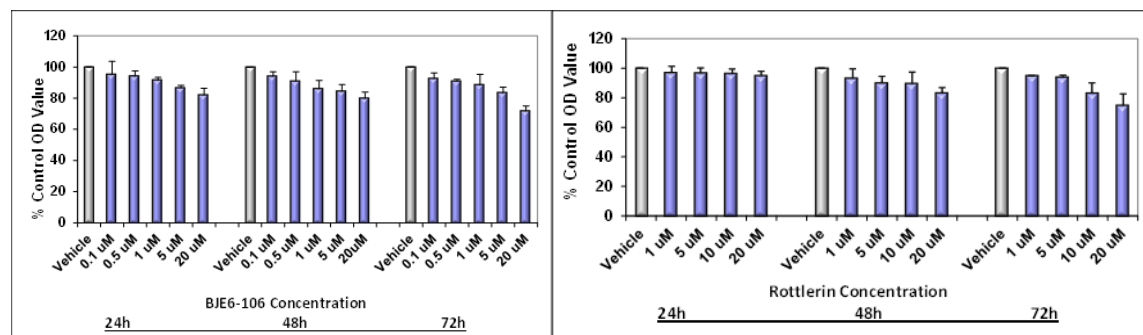
Figure 9

Results: The "normal" human epithelial cell line MCF 10A was insensitive to 1st and 3rd generation PKCδ inhibitors (**Fig. 9**). For MCF 10A, IC_{50} for B106 was consistently >> 20 uM, and IC_{50} for rottlerin was also >> 20 uM at all timepoints.

As an even more stringent assessment of the effects of 3rd gen PKCδ inhibitors on normal tissue, primary human microvascular endothelial cells were exposed to the compound in culture.

Approach:
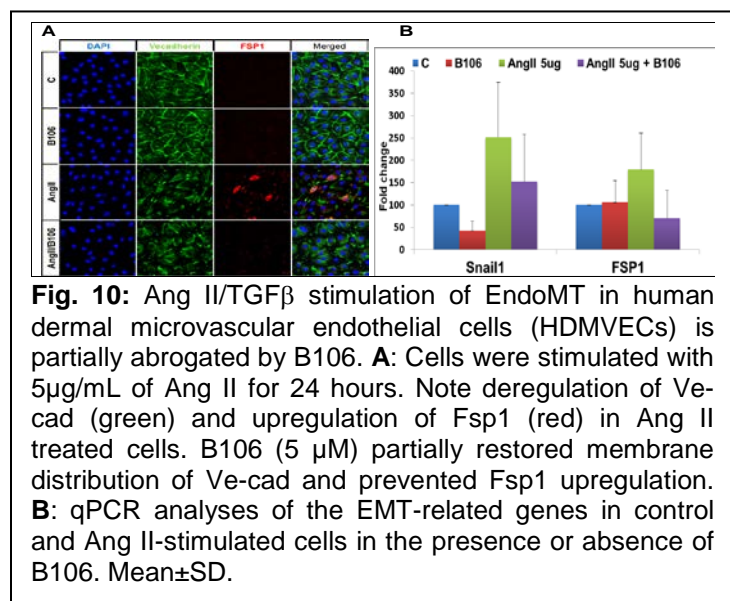
Fig. 10: Ang II/TGFβ stimulation of EndoMT in human dermal microvascular endothelial cells (HDMVECs) is partially abrogated by B106. **A**: Cells were stimulated with 5μg/mL of Ang II for 24 hours. Note deregulation of Ve-cad (green) and upregulation of Fsp1 (red) in Ang II treated cells. B106 (5 μM) partially restored membrane distribution of Ve-cad and prevented Fsp1 upregulation. **B**: qPCR analyses of the EMT-related genes in control and Ang II-stimulated cells in the presence or absence of B106. Mean±SD.

In this particular experiment, primary human microvascular endothelial cells were exposed to vehicle, B106, angiotensin (and inducer of endo to mesenchumal transition), or angiotensin + B106. Effects on morphology and gene induction were analyzed.

Results: Normal human endothelial cells were insensitive to this 3rd generation PKCδ inhibitor at a concentration of 5 uM, as assessed by morphology (**Fig. 10A)** and induction of mesenchymal genes (**Fig. 10B)**.

As the most stringent assessment of the effects of 3rd gen PKCδ inhibitors on normal tissue, B106 was infused into the dermis of mice over 4 days.

***Approach*:**

In this particular experiment, B106 (5 µM/day/mouse) was administered alone or together with the Ang II (an inducer of skin fibrosis) via the Alzet osmotic pump.

Fig. 11. B106 inhibits collagen deposition and myofibroblast accumulation in the Ang II treated mice. Top panels, representative histochemical staining with picrosirius red in the indicated conditions. Polarized images were obtained using the Olympus Bx41 microscope equipped with a digital camera. Bottom panels, αSMA-positive cells are indicated by arrows.

***Results*:** Treatment with B106 alone had a minimal effect on skin collagen content as assessed by picrosirius red staining (**Fig. 11**). Collagen deposition was markedly increased in the skin of Ang II treated mice as illustrated by the yellow and red birefringenence characteristic of the thicker, more densely packed collagen fibers and was visibly reduced by the addition of B106 with weaker greenish birefringenece representing thinner, more loosely packed fibers 80. Treatment with Ang II + B106 showed reduced number of CD163+ macrophages (not shown) as well as myofibroblasts, when compared to Ang II treatment alone (**Fig. 11**).

Importantly, systemic administration of B106 in this model <u>did not result in clinically apparent toxicity</u> in these mice (as would be expected from the finding that PKCδ null mice grow and develop normally, and are fertile), indicating there is a therapeutic window for PKCδ inhibition.

***Interpretation*:** B106, a potent and selective 3rd generation PKCδ inhibitor, is not toxic to normal cells either in culture or and *in vivo* at therapeutic concentrations.

Task: Testing the activities of 3rd generation PKCδ inhibitors on melanoma cancer stem cells (CSCs).

These data are presented in the attached publication: Chen, Z., Forman, L.W., Williams, R.M. Faller, D.V. Protein Kinase C-delta Inactivation Inhibits the Proliferation and survival of Cancer Stem Cells in culture and in vivo. 2014. BMC Cancer, 14: 90-98. PMC3927586.

A **Summary** of these data is as follows:

A subpopulation of tumor cells with distinct stem-like properties (cancer stem-like cells, CSCs) may be responsible for tumor initiation, invasive growth, and possibly dissemination to distant organ sites. CSCs exhibit a spectrum of biological, biochemical, and molecular features that are consistent with a stem-like phenotype, including growth as non-adherent spheres (clonogenic potential), ability to form a new tumor in xenograft assays, unlimited self-renewal, and the capacity for multipotency and lineage-specific differentiation. PKCδ is a novel class serine/threonine kinase of the PKC family, and functions in a number of cellular activities including cell proliferation, survival or apoptosis. PKCδ has been validated as a synthetic lethal target in cancer cells of multiple types with aberrant activation of Ras signaling, using both

genetic (shRNA, dominant-negative PKCδ) and small molecule inhibitors. PKCδ is not required for the proliferation of normal cells, suggesting the potential tumor-specificity of a PKCδ-targeted approach. In this report, we demonstrate that CSC-like populations derived from multiple types of human primary tumors, including melanoma, from human cancer cell lines, and from transformed human cells require PKCδ activity and are susceptible to agents which deplete PKCδ protein or activity. Inhibition of PKCδ by genetic strategies or by novel small molecule inhibitors is growth inhibitory and cytotoxic to multiple types of human CSCs, including melanoma, in culture. PKCδ inhibition also efficiently prevents the selection of tumor sphere outgrowth from tumor cell cultures, with exposure times as short as six hours. Small-molecule PKCδ inhibitors also inhibit human CSC growth *in vivo* in a mouse xenograft model. These findings suggest that PKCδ may represent a new molecular target for cancer stem cell populations.

Interpretation of TASK 1 results:

Collectively, these results supported PKCδ as a potential therapeutic target in melanomas with NRAS mutation, including melanoma cancer stem cells. The new PKCδ inhibitor B106 demonstrated activity at nanomolar concentrations, and will serve as a lead compound for future modifications. The compound also appears to be selective in its activity, sparing normal human epithelial cells, melanocytes and endothelial cells and is non-toxic *in vivo*.

TASK 2: Determine whether aberrant activation of <u>pathways downstream of Ras</u> (in the setting of wild-type Ras alleles) will similarly sensitize human melanoma cells to PKCδ inhibition.

Status: *Completed. **Please see the attached publication Takashima, et al, 2014, and supplementary data, also attached, for complete details.***

   2a) BRAF V600E melanoma cells which have developed resistance to BRAF inhibitors
   Cell lines tested include:
   - A375 cell line and derivative lines selected for resistance to BRAF inhibitor
   - SKMEL5 cell line and derivative lines selected for resistance to BRAF inhibitor

Methods: These lines were tested for susceptibility to PKCδ inhibition by at least 2 small
   molecule inhibitors of PKCδ (*e.g.*, "B106" and "B154") with assay of cell numbers at 24, 48, and 72 hrs by MTS assay. PI staining with flow cytometry <u>or</u> LDH (Lactate Dehydrogenase) release assay will be used to document apoptosis.

Results and Interpretation

BRAF inhibitor-resistant BRAF mutant melanoma lines are susceptible to PKCδ inhibition
In the 50-70% of melanomas bearing BRAF mutations, the BRAF inhibitor PLX4032 vemurafenib) produces dramatic clinical responses, but the inevitable development of resistance to the drug remains an ongoing challenge. One of the proposed models of PLX4032 resistance involves secondary mutations of NRAS, or alternative mechanisms of activation of the RAS-MEK/ERK mitogenic pathway.[7] Because our studies have demonstrated the effectiveness of PKCδ inhibitors in NRAS mutant cells, we sought to investigate whether PKCδ inhibition could be similarly effective in those BRAF mutant melanoma cells that have become refractory to a BRAF inhibitor (PLX4032). To test this hypothesis, we first generated BRAF

Figure 12: PKCδ inhibitors suppress tumor cell growth of PLX4032-resistant melanoma cells with BRAF mutation. (A) Establishment of PLX4032-resistant cell sub-lines. To establish PLX4032 resistant cell lines, two individual melanoma cell lines with BRAF mutations, A375 and SKMEL5 cells were continuously exposed to increasing concentrations of PLX4032 up to 10µM (A375) and 2µM (SKMEL5). To confirm resistance to PLX4032, the viability of PLX4032-resistant cells and their parental cells was measured by MTS assay during treatment with PLX4032 at 1µM.
(B): Mechanism of resistance. PLX4032-resistant cells (A375 PLX-R3 and PLX-R5, SKMEL5 PLX-R1 and PLX-R4) were maintained in PLX4032 containing medium (4µM: A375, 2µM: SKMEL5). Fresh PLX4032-containing medium (4µM: A375, 2µM: SKMEL5) was replaced with normal medium (no PLX4032) in parental cell plates and with PLX4032-containing medium in PLX-R cell plates 6 hours before lysing. Protein lysates were subjected to immunoblot analysis for phosphorylation (T202/T204) or total expression levels of ERK proteins. Levels of ²-actin served as a loading control (from Takashima, et al, 2014).

V600E mutant melanoma cell sub-lines resistant to PLX4032 by continuously exposing A375 and SKMEL5 cells to PLX4032, with gradually increasing concentrations of the drug over weeks. The morphology of PLX4032-resistant cells (referred as "PLX-R") was flatter, and more enlarged and spindle-looking compared to their parental cells in both the A375-PLX-Rs and SKMEL5-PLX-Rs derivatives (data not shown). Resistance of PLX-Rs to PLX4032 was verified by comparing their sensitivity to the drug with that of their parental cells (**Figure 12A**). PLX-R derivative lines from both A375 and SKMEL5 grew in the presence of concentrations of PLX4032 which were cytotoxic to the parental cells. Sequencing of NRAS revealed that none of these resistant cell lines had acquired activating NRAS mutations at position 61. Immunoblot analyses demonstrated that the resistant cell sublines from either the A375 or SKMEL5 parent lines apparently have distinct mechanisms responsible for their resistance. A375-PLX-R sublines exhibited higher phosphorylation levels of ERK in the presence of PLX4032 compared to the parent A375 cells, in which ERK phosphorylation was completely suppressed in the presence of PLX4032 (**Figure 12B**), indicating that the A375-PLX-R cells became resistant to PLX4032 treatment by bypassing BRAF inhibition by the drug, leading to reactivation of ERK pathway. Conversely, SKMEL5-PLX-Rs remained responsive to ERK-MAPK pathway inhibition by

PLX4032 (**Figure 12B**), and yet were capable of surviving under the drug-treatment conditions, suggesting that these cells employ an alternative pathway for survival to compensate for mutant BRAF/ERK inhibition by the drug. Despite the differences in apparent mechanisms of resistance to PLX4032 treatment, all of these resistant lines were susceptible to cytotoxicity induced by
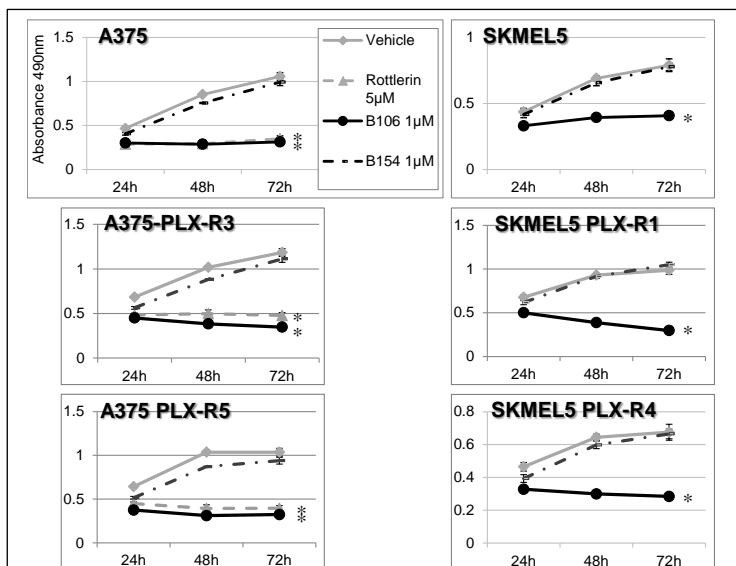
Figure 12C: PKCδ inhibitors suppress survival of PLX4032-resistant cells. Two PLX4032-resistant cell sub-lines derived from A375 (Left) and SKMEL5 (Right) parental cells were exposed to rottlerin (5µM) or B106 (1µM) for 24, 48 or 72 hours and MTS assays were performed at each time point. DMSO and B154 (1µM) served as a vehicle control and a negative compound control, respectively. Each point represents the average of triplicates and error bars indicate the standard deviations. P values (*) were calculated between DMSO (vehicle control) and rottlerin 5µM, or DMSO and B106 1µM in each cell line at 72 hours (p < 0.0002) (from Takashima, et al, 2014).

PKCδ inhibitors at concentrations comparable to the NRAS-mutant melanoma lines, compared to treatment with vehicle (DMSO) or the negative-control compound B154 (**Figure 12C**). Furthermore, PKCδ inhibitors suppress cell survival in melanoma cell lines with BRAF mutation and wt-NRAS (**Figure 13).**

We then sequenced the BRAF inhibitor-resistant derivatives to determine if they were NRAS mutant. Sequencing of NRAS revealed that these resistant cell lines retained wild-type NRAS alleles at position 61. The resistant cell sublines derived from both the A375 or SKMEL5 parent lines did acquire distinct aberrant alterations in RAS pathway signaling that may be responsible for their resistance (increased activation of ERK1,2 in the resistant A375 lines, and increased CRAF in the resistant SKMEL5 lines (Figure 12B).

Interpretation of TASK 2 results:

Collectively, these results strongly support PKCδ as a potential therapeutic target in melanomas with BRAF mutations and with BRAF mutations resistant to BRAF inhibitors.

TASK 3: Test this RAS-targeted approach in *in vivo* models of human melanoma.

These studies will extend the *in vitro* studies above into proof-of-principle *in vivo* experimental models.

Figure 13: PKCδ inhibitors suppress cell survival in melanoma cell lines with BRAF mutation and wt-NRAS. A375, A2058, and SKMEL5, cells were exposed to rottlerin (5 or 10μM) or B106 (5 or 10 μM) for 24, 48 or 72 hours and MTS assays were performed at each time point. DMSO served as a vehicle control and a negative compound control, respectively. Each point represents the average of triplicates and error bars indicate the standard deviations. P values (*) were calculated between DMSO (vehicle control) and rottlerin, or DMSO and B106 in each cell line at 72 hours (p < 0.0002) (from Takashima, et al, 2014).

3a) High-purity synthesis of quantities of selected new PKCδ inhibitors sufficient for *in vivo* studies.

Status: Completed for B106 and B154

3b) Obtain ACURO approval for *in vivo* studies

Status: Completed

3c) Establish a xenograft model with the N-RAS-mutant SBCl2 cell line, and test at least two PKCδ inhibitors (*e.g.,* "B106" and a derivative of B106) for anti-tumor activity, at one or more doses, depending upon tumor responses or safety of the drug. Estimate 7 cohorts of 15 animals plus 5 controls = 110 animals

Status: Tumor model established and B106 tested, see below

3d) Establish a xenograft model with the BRAF-mutant A375 cell line, and test the lead PKCδ inhibitor (*e.g.,* "B106") for anti-tumor activity, at one or more doses depending upon tumor responses or safety of the drug. Estimate 3 cohorts of 15 animals plus 5 controls = 50 animals

Status: Tumor model established but B106 was not tested, because of lack of bioavailability in other i*n vivo* studies. Awaiting a more bioavailable inhibitor

3e) Establish a xenograft model with the BRAF-inhibitor-resistant A375 cell lines, and test the lead PKCδ inhibitor (*e.g.,* "B106") for anti-tumor activity, at one or more doses. Estimate 4 cohorts of 15 animals = 60 animals

Status: Not yet initiated. Awaiting a more bioavailable PKCδ inhibitor (either 4th generation, described below, or packaging in nanoparticles (below).

Methods: Models employed are xenograft models, utilizing the N-RAS-mutant SBCl2 human melanoma line, BRAF-mutant A375 cell line and a drug-resistant BRAF-mutant A375 line derived in Aim/Task 2 above. Drugs tested, or vehicle, are administered *i.p.* daily, and tumor size is quantitated over time.

This task has been initiated. We initially established the MTD for B106, our lead compound at this time, then tested it against a xenograft model.
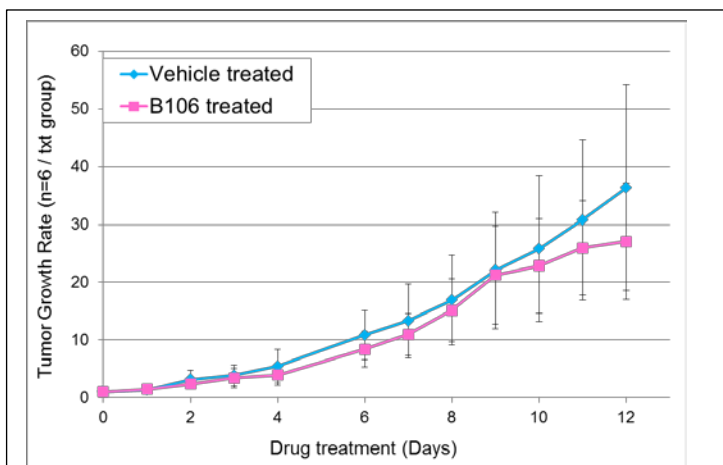
Figure 14: Mouse xenograft model with B106 daily dosing. Donor athymic nude mice were subcutaneously injected with 3 x 10^6 cells of the SBcl2 cell line and tumors were grown. The resulting tumors were harvested, dissected into small blocks (approximately 3 mm^3) and frozen for later use. For the xenograft study, tumor blocks were implanted subcutaneously into 12 mice (1 block / implantation) and 8 days later, when tumor growth was apparent, dosing was initiated. 6 mice were treated with vehicle (DMSO) administered intraperitoneally and the other 6 mice were treated with B106 (40 mg/kg) daily for 12 consecutive days. Tumor size was measured daily using a caliper and tumor growth rate was calculated. Each point represents the average tumor growth rate of 6 mice and error bars indicate the standard deviations.

Methods: Test this targeted approach in *in vivo* models of human melanoma. A xenograft model has been employed, utilizing a human melanoma cell line with aberrantly-activated N-Ras-signaling (SBcl2). Prior to the experiment to test B106 for anti-tumor efficacy in mice, tumors were grown and harvested from donor animals for future implantation. Athymic nude mice (Crl:NU(NCr)-Foxn1nu homozygous, Charles River) were injected subcutaneously with 3 x 10^6 cells of the SBcl2 cell line and tumors were grown. Approximately 3 months later, these tumors were harvested, dissected into small blocks (approximately 3 mm3) and frozen in 10% DMSO/medium. For the xenograft study, tumor blocks were implanted subcutaneously into 12 mice and 8 days later, when tumor growth was apparent, dosing was started. 6 mice were administered vehicle (DMSO) intraperitoneally and the other 6 mice were administered B106 (40mg/kg) daily for 12 consecutive days. Tumor size was documented daily and tumor growth rate was calculated.

Results:

Based on the potent anti-tumor activity of B106 in the melanoma cell culture systems, we proceeded to test the efficacy of B106 *in vivo* in a mouse xenograft tumor model. Tumor blocks of SBcl2 cells were implanted into 12 mice and dosing was started 8 days after tumor implantation; 6 mice received B106 intraperitoneally at 40 mg/kg and the other 6 mice were given DMSO, the vehicle solvent of B106, daily for 12 consecutive days. Tumor size was measured daily and tumor growth rate was calculated. Treatment of B106 did not produce any difference in tumor growth compared to the DMSO-treated group (**Figure 14**).

Interpretation: There was no statistically-significant effect of B106 on tumor growth compared to vehicle (DMSO) controls (**Fig. 14**). There are, however, two concerns remaining at this point regarding pharmacokinetics of B106. First, it is unclear whether the drug entered into the systemic circulation and delivered to the local areas, as B106 is extremely hydrophobic and could not be diluted with hydrophilic solvent. Secondly, there is no information regarding how fast the drug is metabolized at this time.

Two strategies are being used to circumvent this problem.

1) A new generation of compounds with hydrophilic modification of the B106 structure is currently being synthesized (see below). When any of these compounds is revealed to be as potent as B106 in the cell culture system, its *in vivo* efficacy and pharmacokinetics will be tested.

27

Figure 15: Nanoparticle encapsulation of B106 in PLGA np.

2) We are encapsulating B106 into a nanoparticle conformation PLGA to facilitate delivery and overcome solubility issues in vivo.

The encapsulation efficiency is almost 100%. Average size is 45nm (diameter) for the whole sample (without filtration) (**Figure 15**). Release characteristics in tissue culture are being explored prior to testing *in vivo*.

TASK 3 Plans for the future: Chemical modifications of B106 to improve drug-like properties.

Figure 16: Proposed modifications to B106 to explore Structure-Activity relationships and improve pharmaceutical properties. R_1; R_2 = H or OH; n= 0,1,2,3; W, X, Y, Z, = N or CH; R_3 = H, cinnamoyl, other R; R_4 = H; OH; NH_2
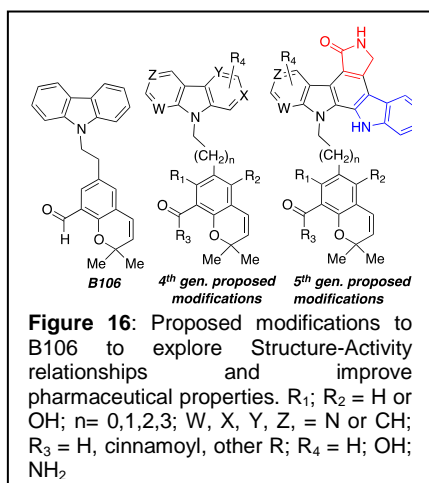
Structural modifications to the core B106 lead compound have been made to improve their solubility and metabolic stability (**Fig. 16**) using the synthetic approaches noted in **Scheme 2**. We will start by simply adding polar groups to the B106 scaffold, which is thus far the most promising analog. Thus, as shown in **Fig. 16**, R_1 and R_2, which are hydroxyl groups in rottlerin and are hydrogen atoms in B106, will be sequentially substituted with OH groups which should improve water solubility. In addition, we performed an isosteric replacement of the aromatic CH groups (X and Z) with basic nitrogen atoms which will be protonated at physiological pH providing for additional water solubility and perhaps improved potency. Based on the functional group modifications we are currently examining to increase water-solubility in just the 4th generation structural framework illustrated in Figure 12, the number of possible analogs will be expand considerably. For example, just taking the minimal set of possible unique structures embodied by the 4th generation species, there are at least 810 possible structural embodiments. We do not propose to make all of these combinations, but rather, will endeavor to substitute the more polar functional residues such as the hydroxyl residues at R_1 and R_2 and the nitrogen atoms into the "staurosporine" heterocycle to develop an SAR around the most promising new analogs. Single substitutions will be evaluated initially, and then combinations of substitutions on the B106 core will be prepared. The 5th
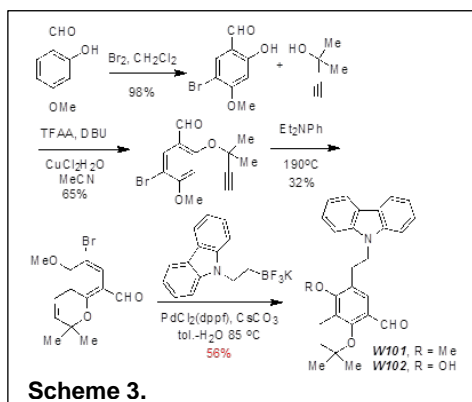
Scheme 3.

generation species will be evaluated to sequentially introduce the fused pyrrolidinone (red) and then fused indole moieties (blue) of the staurosporine cap group. Here again, the number of possible unique structural possibilities rapidly expands covering hundreds and possibly thousands of compounds. As in any synthetic investigation, we shall begin with those

heterocycle and polar group substitutions that are the most readily accessible, test these substances as they are prepared to guide the design and synthesis of subsequent analogs. A total of 50-100 compounds per year will be synthesized and evaluated. They will be evaluated for solubility and octanol:water partitioning coefficient (logP). Further characterization of the pharmaceutical properties of these analogs will be carried out following evaluation of enzyme selectivity. The synthesis of our latest hybrid molecules **W101** and **W102** with potentially improved solubility properties are shown below in **Scheme 3**. These compounds have been synthesized and evaluated.

The potency and selectivity of the new analogs were initially evaluated for PKCδ and PKCα inhibitory activity using recombinant PKCδ or PKCα (Invitrogen) and the Omnia Kinase Assays (Invitrogen) with a 'PKC kinase-specific' peptide substrate. Incorporation of a chelation-enhanced fluorophore results in an increase in fluorescence ($\lambda_{ex}360/\lambda_{em}485$) upon phosphorylation. The kits were used according to the manufacturer's instructions.

The IC_{50}s for PKCδ for W101 and W102 are approximately 0.05 μM and >50 μM, respectively. The IC_{50}s for PKCα for W101 and W102 are approximately >50 μM and >50 μM, respectively. Additional molecules (W102-W107) have also been synthesized and characterized, but none are as potent and PKCδ-selective as W101.

The W101 molecule looks promising (*e.g.,* low nM potency and >1000x selectivity *vs.* PKCα, although solubility was only minimally improved. Their effect on additional closely related kinases will be evaluated including PKCβI, PKCβII, PKCγ, PKCε, PKCη, PKCθ, PKCζ and PKCι. The molecules with the optimal potency and selectivity will be further characterized. Criteria for advancement include at least 1000 fold selectivity versus PKCα, which is important in many cellular processes and is a fundamental regulator of cardiac contractility and Ca^{2+} handling in myocytes, improved solubility of at least 10 ng/mL and octanol:water partitioning coefficient (logP) in the 1.5 – 3.5 range. Compounds that exhibit these characteristics will then be evaluated for their selectivity against other PKC family members. As B106 has already been shown to be safe when administered to mice at therapeutically active doses, this compound will be profiled against the other PKC family members (PKCβI, PKCβII, PKCγ, PKCε, PKCη, PKCθ, PKCζ and PKCι). The profile of B106 will act as a template against which other compounds will be compared. Regardless of those results, compounds will be sought with at least 100-fold selectivity against the most biologically important other protein kinase C family members, including PKCγ (important in neuronal function) and PKCε (important in apoptosis, cardioprotection from ischemia, heat shock response, as well as insulin exocytosis). Inhibitory activity against the other PKC family members will also be evaluated to fully profile the compounds.

Compounds with at least 1000 fold selectivity against PKCδ, a logP of 1.5– 3.5 and solubility of at least 10 mg/mL will be further characterized for their biological activity. The ability of selected inhibitors to induce cytotoxicity in human prostate cancer cells will be assessed as we did for the 3rd generation compounds (Tasks I and II above). These compounds will also be evaluated for cytotoxicity on normal human melanocytes and endothelial cells (human microvascular endothelial cells), using dye exclusion as well as other primary normal human cells, as described in Task I above.

TASK 4   Data Analysis and Preparation of Report

Status: Completed for Year 2.

Discussion of Findings from this Work.

Current obstacles in melanoma therapy

Approval of the BRAF inhibitor PLX4032 (vemurafenib), one of the first targeted therapies in melanoma, represented a major advance in the treatment of this disease. BRAF-V600E-mutant tumors, the target of vemurafenib, account for 50-70% of melanoma cases.[8] Despite the remarkably high response rate and tumor regression in responders, however, the tumors eventually and inevitably relapse due to the development of resistance to this class of drugs. Ironically, the complexity and redundancy of RAS/MAPK signaling pathways provide the tumor cells many opportunities for drug resistance, which rapidly develops. There are no targeted therapies available for melanomas harboring NRAS mutations, the second most frequent genotype after BRAF mutations. The MEK inhibitors currently in clinical trials are not likely to become an important option in NRAS-mutant melanomas due to their unexpectedly preferential activity against BRAF-mutant melanomas.[9] Moreover, there are potential risks with respect to the use of BRAF inhibitor in RAS-mutant melanomas,[10-13] including their potential to cause secondary tumors with RAS mutations,[14,15] further highlighting the need to explore therapeutic options other than BRAF inhibitors. Melanomas with NRAS mutations and BRAF-mutant melanomas resistant to BRAF inhibitors therefore represent unmet medical needs, and constitute a large proportion of the melanoma cases.

PKCδ as a therapeutic target in melanomas with NRAS mutations or BRAF inhibitor resistance

Somatic point mutations of *RAS* genes at codons 12, 13, and 61 are the most common dominant oncogenic lesions in human cancer,[8,9] making aberrant Ras signaling an important therapeutic target in these cancers. The rationale for a PKCδ-targeted therapy against tumors with aberrant RAS signaling is based on prior findings by our group and later others. Inhibition of PKCδ was shown to preferentially inhibit the growth of cancer cell lines with genomic mutations in KRAS or HRAS genes, oncogenic activation of KRAS proteins, or aberrant activation of RAS signaling pathways.[3,4,16-18] In addition, PKCδ was demonstrated to be non-essential for the survival and proliferation of normal cells and animals,[19] suggesting that a therapeutic approach targeting PKCδ would likely spare normal cells, but inhibit proliferation of tumor cells whose survival depends on PKCδ activity: that is, provide a tumor-specific therapeutic approach. Furthermore, one of the proposed mechanisms of BRAF inhibitor-resistance is the evolution of secondary mutations in NRAS,[1] suggesting a potential link between BRAF-resistant melanoma and RAS mutations. Taken together, these reports above underline the potential of PKCδ-targeted therapy as a cancer-specific therapy targeting tumors with NRAS mutations in melanoma. Accordingly, we sought to determine if tumors with oncogenic mutations in NRAS, specifically melanomas with activating mutations of NRAS at position 61, would be dependent upon PKCδ for survival.

The present study supports the potential of PKCδ as a therapeutic target in melanomas. Cell proliferation and clonogenic assays demonstrated that inhibition of PKCδ suppressed cell growth in multiple melanoma cell lines with NRAS mutations as well as in PLX4032-resistant cell lines. The cell lines with NRAS mutation that were used in this study had different amino acid substitutions of NRAS codon 61, the most frequently mutated codon in NRAS (data not shown), suggesting the effect of PKCδ inhibitors does not depend on a specific NRAS mutation for their activity (unlike BRAF inhibitors, some of which are selective to only the most common mutation, V600E). Similarly, PKCδ inhibition was effective in the PLX4032-resistant cell lines tested herein, regardless of the differences in their apparent resistance mechanisms, further supporting the potential of this approach. Sequencing of the NRAS genes in these resistant

sublines revealed no activating mutations at position 61, despite the evidence of constitutive MEK/ERK pathway signaling. Constitutive MEK/ERK signaling (even in the absence of new activating mutations in NRAS) appears to mediate the majority of acquired resistance to BRAF inhibitors.[7] [A comprehensive analysis of resistance mechanism in these derived sublines is being reported separately.] We have previously reported that aberrant activation of the MEK/ERK arm of the RAS signaling pathway, by introduction of a constitutively-activated CRAF gene, is sufficient to render cells susceptible to PKCδ inhibition, even in the absence of activating mutations of RAS alleles.[3]

The novel PKCδ inhibitor B106, which showed 1000-fold selectivity against PKCδ over PKCα in preliminary *in vitro* kinase assay, was active at nanomolar concentrations, ten times lower than for rottlerin. These results in cell culture systems suggest the potential of the newest PKCδ inhibitors as targeted agents, although the *in vivo* efficacy of B106 is yet to be determined. (The hydrophobicity of the B106 molecule makes it unsuitable for testing in tumor xenograft models.)

PKCδ inhibition induces caspase-dependent apoptosis via the JNK-H2AX pathway

Induction of apoptosis is one of the most desirable mechanisms for cytotoxic therapeutic action, as theoretically it selectively kills cells in which an apoptotic signal is introduced without adversely affecting surrounding cells and hence limits inflammation or tissue scarring. One of the downstream targets of PKCδ, stress-activated protein kinase/c-Jun N-terminal kinase (SAPK/JNK) is activated in response to cellular stresses, including genotoxic stresses [*e.g.,* ionizing radiation (IR), ultraviolet radiation (UV)), chemotherapeutic agents, or reactive oxygen species (ROS)] and is involved in a variety of cellular activities, such as cell proliferation, differentiation, inflammatory response, DNA repair, motility, metabolism and apoptosis.[20] The JNK pathway comprises one of the three major MAPK pathways. The JNK family is on the MAPK tier and consists of three isozymes: JNK1, JNK2 and JNK3. JNK1 and JNK2 are ubiquitously expressed while JNK3 is restricted to brain, heart and testis.[20] Alternative splicing yields multiple splicing variants of all three isozymes: each of JNK1 and 2 genes contributes both a short form (46kDa) and a long form (54kDa), and a minor 52kDa form is believed to derive mostly to JNK3.[20] Upon activation of the JNK pathway, both the 46kDa and 54kDa forms become phosphorylated at Thr183/Tyr185 by two upstream MAPKKs, SEK1/MKK4 and MKK7. MKK4 appears to preferentially phosphorylate Tyr185 and MKK7 favors Thr183.[21] While MKK7 is a JNK-selective MAPKK, MKK4 is capable of activating both JNK and the other closely related MAPK, p38. The pro-apoptotic JNK pathway, initially discovered as a UV radiation-responsive signaling kinase cascade, induces apoptosis in part through regulating Bcl2 family members in the cytosol. In response to apoptotic signals, JNK activates the pro-apoptotic Bcl-2 family proteins Bax and Bad, possibly in part through regulating BH3-only members of the Bcl-2 family including Bim, Bid or Bif, 14-3-3 or the FOXO transcription factor.[22] Alternatively, JNK also activates transcription factors including the components of activator protein 1 (AP-1), a transcription factor complex containing c-Jun, JunD or ATF2. In turn, AP-1 activates transcription of pro-apoptotic facilitators, such as TNF± or Fas-L (death receptor ligands) or Bak (a pro-apoptotic Bcl2 member).[23] Supporting the critical role of JNK in apoptosis, mouse embryonic fibroblasts with JNK1/2 knocked-down were resistant to apoptosis induced by various apoptotic stimuli.[24] Many chemotherapeutic agents, including paclitaxel, cisplatin or doxorubicin, employ the JNK pathway for their cytotoxic activity.[25,26] This study demonstrated that PKCδ inhibition activated the JNK pathway through MMK4 to mediate caspase-dependent apoptosis. This was somewhat unexpected, as MKK7 activation was anticipated because of its more selective ability to activate JNK relative to p38. Activation of JNK was consistently induced by PKCδ inhibition, either *via* siRNA or small molecule inhibitors such as B106, but the closely-related MAPKs p38 and ERK (also potential targets of PKCδ in different settings) were not activated. Furthermore, the induced absence of JNK1/2 expression in the cells significantly

31

mitigated caspase activity induced by PKCδ inhibition. These results demonstrate the functional importance and necessity of the activation of this pathway in PKCδ inhibition-induced caspase-dependent apoptosis in NRAS mutant melanoma cells. Consistent with our findings, a recent report demonstrated that knockdown of PKCδ induced apoptosis with elevated phosphorylation of JNK in NIH-3T3 cells stably transfected with HRAS.[16]

Among the known downstream effectors of JNK, a series of recent reports proposed an active role for phospho-H2AX in apoptosis. H2AX (histone H2A variant X) is a minor subtype of the H2A family. Approximately 10% of histone H2A proteins are H2AX in normal fibroblasts, although the proportion varies in different tissues (ranging up to 20%).[27] H2AX in its phosphorylated form (phospho-H2AX, also called ³H2AX) is primarily known for its role in DNA double strand break (DSB) repair, and has long been utilized as a marker of DSB. Upon DSB formation, PI$_3$K-like kinases [ataxia telangiectasia mutated (ATM), ataxia telangiectasia and Rad3-related (ATR) and DNA-dependent protein kinase (DNA-PK)], are activated and phosphorylate H2AX at Ser 139.[28] Phosphorylated H2AX is one of the first proteins recruited to DSB sites during the DNA damage response, and facilitates the access of repair proteins to the site.[28]

In the context of apoptosis, earlier studies reported that H2AX phosphorylation can occur as a consequence of apoptosis. DSBs generated from DNA fragmentation during the apoptotic process were reported to produce phosphorylated H2AX.[29] DNA-PK and ATM were shown to be responsible for the phosphorylation of H2AX in this process.[30] However, a series of recent reports have instead proposed a more active role of phospho-H2AX in induction of apoptosis. In this model, phosphorylation of H2AX at Ser 139 provokes apoptosis by inducing DNA fragmentation in UV-damaged cells.[6] Supporting this model, several studies reported phospho-H2AX-mediated apoptosis, some of which are involved in apoptosis induced by chemotherapeutic agents.[31-33] PKCδ inhibition by B106 treatment evoked phosphorylation of H2AX subsequent to JNK activation. Specific knockdown of PKCδ using siRNA verified the role of PKCδ: JNK phosphorylation occurred by 24 hours after siRNA transfection and H2AX phosphorylation was observed subsequently. The phosphorylation of H2AX induced by B106 treatment was mitigated in the absence of JNK expression, positioning H2AX phosphorylation downstream of JNK after PKCδ inhibition. Caspase activation caused by PKCδ inhibition was significantly decreased in the enforced absence of H2AX expression. Furthermore, as a direct readout of apoptosis, DNA fragmentation was almost completely abrogated by knockdown of H2AX prior to PKCδ inhibition. Collectively, these results demonstrate the importance of H2AX as an active apoptotic mediator, providing functional evidence showing it to be a necessary component of apoptosis initiated by PKCδ inhibition.

The concept of targeting cancer therapeutics towards specific mutations or abnormalities in tumor cells which are not found in normal tissues has the potential advantages of high selectivity for the tumor and correspondingly low secondary toxicities. We have previously demonstrated that knockdown of PKCδ, or its inhibition by previous generations of small molecules, was not toxic to non-transformed murine and human cell lines, or to tumor lines without aberrant activation of the RAS signaling pathway.[5,34,35] In unpublished work, we have shown that B106 does not inhibit the growth of primary murine mesenchymal cells, primary human endothelial cells and human epithelial cells at concentrations which are profoundly cytotoxic to melanoma lines bearing NRAS mutations (0.5-2.5 uM). In addition, continuous local infusion of B106 at 5 μM concentrations is not cytotoxic to dermal and subdermal tissues in mice (Trojanowska and Faller, in preparation). Derivatives of the 3rd generation PKCδ inhibitor B106 are being generated, using structure function analysis of the 36 compounds in that cohort and medicinal chemistry to enhance "drug-like properties, to facilitate future *in vivo* studies. Collectively, these studies suggest that PKCδ suppression may represent a tumor-targeted

approach to a subpopulation of melanomas for which there is currently no targeted treatment.

4. **KEY RESEARCH ACCOMPLISHMENTS:** Bulleted list of key research accomplishments emanating from this research.

- Demonstrated the sensitivity human melanomas to PKCδ inhibition
- Designed and synthesized 36 new compounds as PKCδ inhibitors
- Tested the activity of these 36 new compounds against PKCδ and PKCα
- Tested the activity of these 36 new compounds against human melanoma cells
- Established MTD for our lead compound
- Determined the duration of exposure to PKCδ inhibitor drug necessary to achieve maximal cytotoxicity
- Demonstrated that our lead 3rd generation compound (B106) has 5-10 greater potency in inducing cytotoxicity against a panel of human melanoma cells than LC-1.
- Demonstrated that our lead 3rd generation compound (B106) has 5-10 greater potency than LC-1 in inducing cytotoxicity against BRAF mutant melanomas resistant to BRAF inhibitors.
- Demonstrated that our lead 3rd generation compound (B106) has cytotoxic activity against NRAS-mutant melanoma cancer stem cells (CSC).
- Designed a strategy for synthesis of more hydrophilic analogs of our 3rd generation lead compound, and synthesized 7 4th generation PKCδ inhibitors.
- Tested the activity of these 7 4th generation compounds against PKCδ and PKCα

5. **CONCLUSION:**

In our 2 years of work, we have accomplished nearly all of the tasks we proposed. We have succeeded in demonstrating that multiple types of NRAS mutant human melanoma cells are susceptible to PKCδ inhibition, using siRNA as a "specificity" test, and multiple structurally-distinct small molecule PKCδ inhibitors. These findings validate PKCδ as a target in melanoma, and provide proof-of-principle for the use of PKCδ inhibitors as potential therapeutics. Furthermore, we have shown the utility of PKCδ-inhibition as a strategy for the elimination of BRAF-mutant melanomas which are resistant to BRAF inhibitors. We have refined the initial PKCδ inhibitor lead compound now through 2 generations, producing small molecules of

increasing potency and PKCδ specificity. Our next generation will be optimized for "drug-like" properties, to facilitate moving into *in vivo* testing of tumor xenografts.

This *in vivo* testing of 3rd generation compounds in animal models has not yet proven successful due to the chemical properties of the lead 3rd generation molecule, but refinement of the lead compound is progressing. Furthermore, we are pursuing the alternative strategy of nanoparticle encapsulation for enhancing drug delivery *in vivo*. Results of such studies will demonstrate the efficacy of this approach, provide informal toxicology, and informal PK.

6. PUBLICATIONS, ABSTRACTS, AND PRESENTATIONS

Takashima, A. and Faller, D.V. Targeting the RAS oncogene. Expert Opinion on Therapeutic Targets, 2013, 17(5):507-31.

Takashima A, Williams RM, Faller DV. Targeting N-Ras in malignant melanoma. Proceedings of the Annual Meeting of the AACR (2013) Oral Presentation.

Takashima, A., Chen, Z., English, B., Williams, R.A., Faller, D.V. Protein kinase C δ is a therapeutic target in malignant melanoma with NRas mutation or BRaf inhibitor-resistance. 2014. ACS Chemical Biology, 2014 9(4):1003-14. PMC4160068

Chen, Z., Forman, L.W., Williams, R.M. Faller, D.V. Protein Kinase C-delta Inactivation Inhibits the Proliferation and survival of Cancer Stem Cells in culture and in vivo. 2014. BMC Cancer, 14: 90-98. PMC3927586.

Sarkar, S and Faller, DV: Novel TGFδ receptor inhibitors block both canonical and non-canonical signaling to prevent tumor progression. In preparation.

7. INVENTIONS, PATENTS AND LICENSES

None

8. REPORTABLE OUTCOMES: Provide a list of reportable outcomes that have resulted from this research to include:

Takashima, A. and Faller, D.V. Targeting the RAS oncogene. Expert Opinion on Therapeutic Targets, 2013, 17(5):507-31.

Takashima A, Williams RM, Faller DV. Targeting N-Ras in malignant melanoma. Proceedings of the Annual Meeting of the AACR (2013) Oral Presentation.

Takashima, A., Chen, Z., English, B., Williams, R.A., Faller, D.V. Protein kinase C δ is a therapeutic target in malignant melanoma with NRas mutation or BRaf inhibitor-resistance. 2014. ACS Chemical Biology, 2014 9(4):1003-14. PMC4160068

Chen, Z., Forman, L.W., Williams, R.M. Faller, D.V. Protein Kinase C-delta Inactivation Inhibits the Proliferation and survival of Cancer Stem Cells in culture and in vivo. 2014. BMC Cancer, 14: 90-98. PMC3927586.

Sarkar, S and Faller, DV: Novel TGFδ receptor inhibitors block both canonical and non-canonical signaling to prevent tumor progression. In preparation.

9. OTHER ACHIEVEMENTS

none

10. REFERENCES:

1. Nazarian R et al. Melanomas acquire resistance to B-RAF(V600E) inhibition by RTK or N-RAS upregulation. Nature. 468:973-977 (2010).

2. Malumbres M and Barbacid M. RAS oncogenes: the first 30 years. Nat.Rev.Cancer. 3:459-465 (2003).

3. Xia S, Forman LW, and Faller DV. Protein Kinase C{delta} is required for survival of cells expressing activated p21RAS. J Biol.Chem. 282:13199-13210 (2007).

4. Chen Z et al. The proliferation and survival of human neuroendocrine tumors is dependent upon protein kinase C-delta. Endocr.Relat Cancer 18:759-771 (2011).

5. Xia S et al. PKCdelta survival signaling in cells containing an activated p21Ras protein requires PDK1. Cell Signal. 21:502-508 (2009).

6. Lu C et al. Cell apoptosis: requirement of H2AX in DNA ladder formation, but not for the activation of caspase-3. Mol.Cell. 23:121-132 (2006).

7. Trunzer K et al. Pharmacodynamic effects and mechanisms of resistance to vemurafenib in patients with metastatic melanoma. J Clin.Oncol. 31:1767-1774 (2013).

8. Inamdar GS, Madhunapantula SV, and Robertson GP. Targeting the MAPK pathway in melanoma: why some approaches succeed and other fail. Biochem.Pharmacol. 80:624-637 (2010).

9. Takashima A and Faller DV. Targeting the RAS oncogene. Expert.Opin.Ther.Targets. (2013).

10. Hatzivassiliou G et al. RAF inhibitors prime wild-type RAF to activate the MAPK pathway and enhance growth. Nature. 464:431-435 (2010).

11. Heidorn SJ et al. Kinase-dead BRAF and oncogenic RAS cooperate to drive tumor progression through CRAF. Cell. 140:209-221 (2010).

12. Kaplan FM et al. Hyperactivation of MEK-ERK1/2 signaling and resistance to apoptosis induced by the oncogenic B-RAF inhibitor, PLX4720, in mutant N-RAS melanoma cells. Oncogene. 30:366-371 (2011).

13. Poulikakos PI et al. RAF inhibitors transactivate RAF dimers and ERK signalling in cells with wild-type BRAF. Nature. 464:427-430 (2010).

14. Su F et al. RAS mutations in cutaneous squamous-cell carcinomas in patients treated with BRAF inhibitors. N.Engl.J Med. 366:207-215 (2012).

15. Callahan MK et al. Progression of RAS-mutant leukemia during RAF inhibitor treatment. N.Engl.J Med. 367:2316-2321 (2012).

16. Zhu T et al. Synthetic Lethality Induced by Loss of PKC delta and Mutated Ras. Genes Cancer. 1:142-151 (2010).

17. Symonds JM et al. Protein kinase C delta is a downstream effector of oncogenic K-ras in lung tumors. Cancer Res. 71:2087-2097 (2011).

18. Zhu T, Tsuji T, and Chen C. Roles of PKC isoforms in the induction of apoptosis elicited by aberrant Ras. Oncogene. 29:1050-1061 (2010).

19. Leitges M et al. Exacerbated vein graft arteriosclerosis in protein kinase Cdelta-null mice. J.Clin.Invest. 108:1505-1512 (2001).

20. Johnson GL and Nakamura K. The c-jun kinase/stress-activated pathway: regulation, function and role in human disease. Biochim.Biophys.Acta. 1773:1341-1348 (2007).

21. Bode AM and Dong Z. The functional contrariety of JNK. Mol.Carcinog. 46:591-598 (2007).

22. Weston CR and Davis RJ. The JNK signal transduction pathway. Curr.Opin.Cell Biol. 19:142-149 (2007).

23. Turjanski AG, Vaque JP, and Gutkind JS. MAP kinases and the control of nuclear events. Oncogene. 26:3240-3253 (2007).

24. Tournier C et al. Requirement of JNK for stress-induced activation of the cytochrome c-mediated death pathway. Science 288:870-874 (2000).

25. Lee LF et al. Paclitaxel (Taxol)-induced gene expression and cell death are both mediated by the activation of c-Jun NH2-terminal kinase (JNK/SAPK). J Biol.Chem. 273:28253-28260 (1998).

26. Koyama T et al. Apoptosis induced by chemotherapeutic agents involves c-Jun N-terminal kinase activation in sarcoma cell lines. J Orthop.Res. 24:1153-1162 (2006).

27. Bonner WM et al. GammaH2AX and cancer. Nat.Rev.Cancer. 8:957-967 (2008).

28. Yuan J, Adamski R, and Chen J. Focus on histone variant H2AX: to be or not to be. FEBS Lett. 584:3717-3724 (2010).

29. Rogakou EP et al. Initiation of DNA fragmentation during apoptosis induces phosphorylation of H2AX histone at serine 139. J Biol.Chem. 275:9390-9395 (2000).

30. Mukherjee B et al. DNA-PK phosphorylates histone H2AX during apoptotic DNA fragmentation in mammalian cells. DNA Repair (Amst). 5:575-590 (2006).

31. Wen W et al. MST1 promotes apoptosis through phosphorylation of histone H2AX. J Biol.Chem. 285:39108-39116 (2010).

32. Liu Y et al. Histone H2AX is a mediator of gastrointestinal stromal tumor cell apoptosis following treatment with imatinib mesylate. Cancer Res. 67:2685-2692 (2007).

33. Jane EP and Pollack IF. Enzastaurin induces H2AX phosphorylation to regulate apoptosis via MAPK signalling in malignant glioma cells. Eur.J Cancer. 46:412-419 (2010).

34. Chen Z et al. The proliferation and survival of human neuroendocrine tumors is dependent upon protein kinase C-delta. Endocr.Relat Cancer 18:759-771 (2011).

35. Xia S, Forman LW, and Faller DV. Protein Kinase C{delta} is required for survival of cells expressing activated p21RAS. J Biol.Chem. 282:13199-13210 (2007).

11. APPENDICES:

Takashima, A., Chen, Z., English, B., Williams, R.A., Faller, D.V. Protein kinase C δ is a therapeutic target in malignant melanoma with NRas mutation or BRaf inhibitor-resistance. 2014. ACS Chemical Biology, 2014 9(4):1003-14. PMC4160068

Plus supplemental data.

Chen, Z., Forman, L.W., Williams, R.M. Faller, D.V. Protein Kinase C-delta Inactivation Inhibits the Proliferation and survival of Cancer Stem Cells in culture and in vivo. 2014. BMC Cancer, 14: 90-98. PMC3927586.

Protein Kinase Cδ Is a Therapeutic Target in Malignant Melanoma with NRAS Mutation

Asami Takashima,[†] Brandon English,[‖] Zhihong Chen,[†] Juxiang Cao,[§] Rutao Cui,[†,§] Robert M. Williams,[‖,⊥] and Douglas V. Faller*[,†,‡]

[†]Cancer Center, [‡]Departments of Medicine, Biochemistry, Pediatrics, Microbiology, Pathology and Laboratory Medicine, and [§]Department of Dermatology, Boston University School of Medicine, 72 E Concord Street, Boston, Massachusetts 02118, United States

[‖]Department of Chemistry, Colorado State University, Fort Collins, Colorado 80523, United States

[⊥]University of Colorado Cancer Center, Aurora, Colorado 80045, United States

S *Supporting Information*

ABSTRACT: NRAS is the second most frequently mutated gene in melanoma. Previous reports have demonstrated the sensitivity of cancer cell lines carrying KRAS mutations to apoptosis initiated by inhibition of protein kinase Cδ (PKCδ). Here, we report that PKCδ inhibition is cytotoxic in melanomas with primary NRAS mutations. Novel small-molecule inhibitors of PKCδ were designed as chimeric hybrids of two naturally occurring PKCδ inhibitors, staurosporine and rottlerin. The specific hypothesis interrogated and validated is that combining two domains of two naturally occurring PKCδ inhibitors into a chimeric or hybrid structure retains biochemical and biological activity and improves PKCδ isozyme selectivity. We have devised a potentially general synthetic protocol to make these chimeric species using Molander trifluorborate coupling chemistry. Inhibition of PKCδ, by siRNA or small molecule inhibitors, suppressed the growth of multiple melanoma cell lines carrying NRAS mutations, mediated *via* caspase-dependent apoptosis. Following PKCδ inhibition, the stress-responsive JNK pathway was activated, leading to the activation of H2AX. Consistent with recent reports on the apoptotic role of phospho-H2AX, knockdown of H2AX prior to PKCδ inhibition mitigated the induction of caspase-dependent apoptosis. Furthermore, PKCδ inhibition effectively induced cytotoxicity in BRAF mutant melanoma cell lines that had evolved resistance to a BRAF inhibitor, suggesting the potential clinical application of targeting PKCδ in patients who have relapsed following treatment with BRAF inhibitors. Taken together, the present work demonstrates that inhibition of PKCδ by novel small molecule inhibitors causes caspase-dependent apoptosis mediated *via* the JNK-H2AX pathway in melanomas with NRAS mutations or BRAF inhibitor resistance.
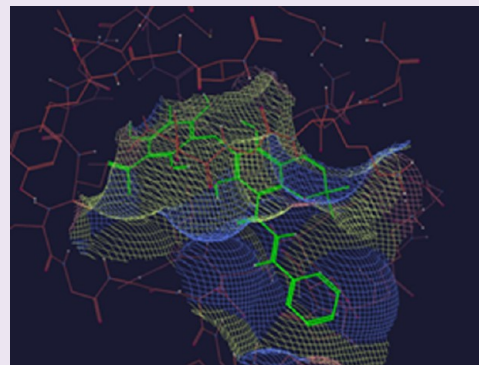
Although melanomas account for less than 5% of skin cancer cases, they were responsible for more than 75% of estimated skin cancer deaths in 2012, and the incidence rate has been increasing for the last 30 years.[1] While chemotherapeutic treatments have improved response rates in metastatic melanoma, there has been no significant impact on survival for decades.[1]

Melanoma is highly dependent upon the RAS/RAF/MEK/ERK pathway, one of the three major mitogen-activated protein kinase (MAPK) pathways. The components of this pathway, therefore, can serve as the targets of drugs for late-stage melanomas. BRAF (one of the three RAF isoforms) is the most commonly mutated gene in melanoma (45−55% of melanoma cases), while mutations in NRAS (one of the three RAS isoforms) are observed in 15−30% of melanoma cases.[2,3] The BRAF inhibitor PLX4032 (vemurafenib) shows high activity in patients with BRAF-V600E mutation; however, responders eventually and inevitably became resistant to this drug and relapsed.[4] One of the proposed mechanisms of acquired resistance to vemurafenib is reactivation of MEK/ERK signaling independently of BRAF, the suppression of which had been the goal of PLX4032 action, through a variety of compensatory alterations.[5,6] In contrast to BRAF, the oncogenic RAS/GAP switch is an exceedingly difficult target for rational drug discovery and is now widely considered "undrugable".[3,7,8] An "indirect" approach, targeting a survival pathway required by tumor cells bearing an activated RAS allele, may represent an alternative strategy for NRAS mutant melanomas.

We previously demonstrated that cancer cells carrying oncogenic KRAS mutations undergo apoptosis when protein kinase C δ (PKCδ) activity is inhibited by means of a chemical inhibitor, RNA interference, or a dominant-negative var-
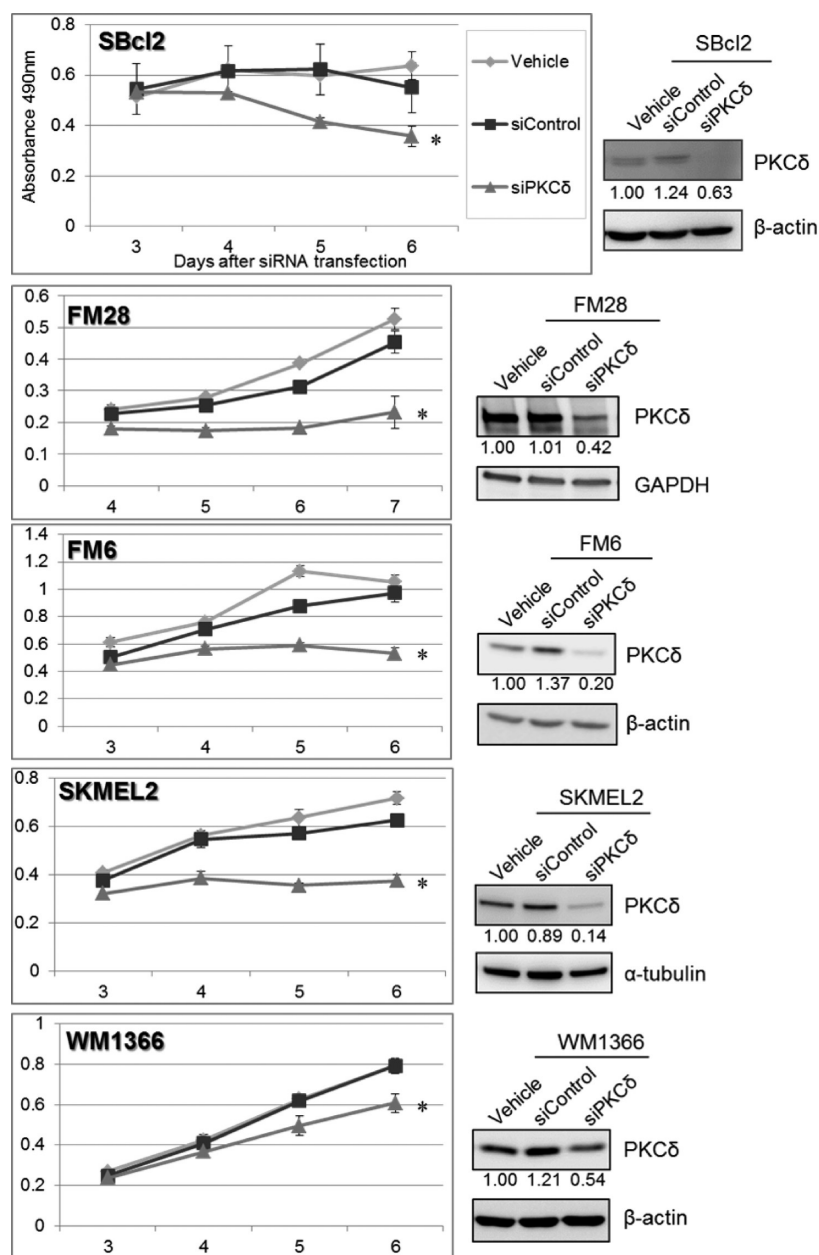
Figure 1. Downregulation of PKCδ suppresses cell survival in melanoma cell lines with NRAS mutation. siRNA targeting PKCδ ("siPKCδ") or nontargeting siRNA ("siControl") were transfected into SBcl2 and FM28 (50 nM), SKMEL2 (10 nM), and FM6 and WM1366 (5 nM), after establishing cell line-specific optimal transfection conditions. As a vehicle control, cells were treated in parallel with transfection reagent alone ("vehicle"). MTS assays were performed at 3 or 4 days after siRNA transfection. Each point represents the average of triplicates, and error bars indicate the standard deviations. p values (*) were calculated between vehicle control and siPKCδ on the last assay day ($p < 0.006$). Downregulation of PKCδ protein on the first assay day was assessed by immunoblot analysis. The relative band intensity of PKCδ is indicated below the image (normalized to loading controls, β-actin, α-tubulin, or GAPDH).

iant.[9−12] Other groups also subsequently validated PKCδ as a target in cancer cells of multiple types with aberrant activation of KRAS signaling.[13,14]

PKCδ belongs to the PKC family of serine/threonine protein kinases, which are involved in diverse cellular functions, such as proliferation, tumor promotion, differentiation, and apoptotic cell death.[15] The PKC family is categorized into three subfamilies based on structural, functional, and biochemical differences and activators: the classical/conventional PKCs (α, βI, βII, γ), the novel PKCs (δ, ε, θ, μ), and the atypical PKCs (ζ, λ). The novel PKCs, including PKCδ, are characteristically activated by diacylglycerol (DAG) and are independent of the

need for the secondary messenger Ca^{2+}. PKCδ functions as either a pro-apoptotic or an antiapoptotic/pro-survival regulator depending upon cellular context, such as the specific stimulus or its subcellular localization.[15] PKCδ is implicated as an early regulator in certain antiapoptotic/pro-survival signaling cascades through induction or suppression of downstream substrates, including ERK, AKT, and NF-κB. Other context-dependent effectors of PKCδ include JNK, glycogen synthase kinase-3 (GSK3), FLICE-like inhibitory protein (FLIP), cIAP2, and p21$^{Cip1/WAF1}$. A role for PKCδ as an antiapoptotic/pro-survival regulator has been reported in various types of cancer cells, including non-small cell lung cancer, pancreatic, and colon

A

B
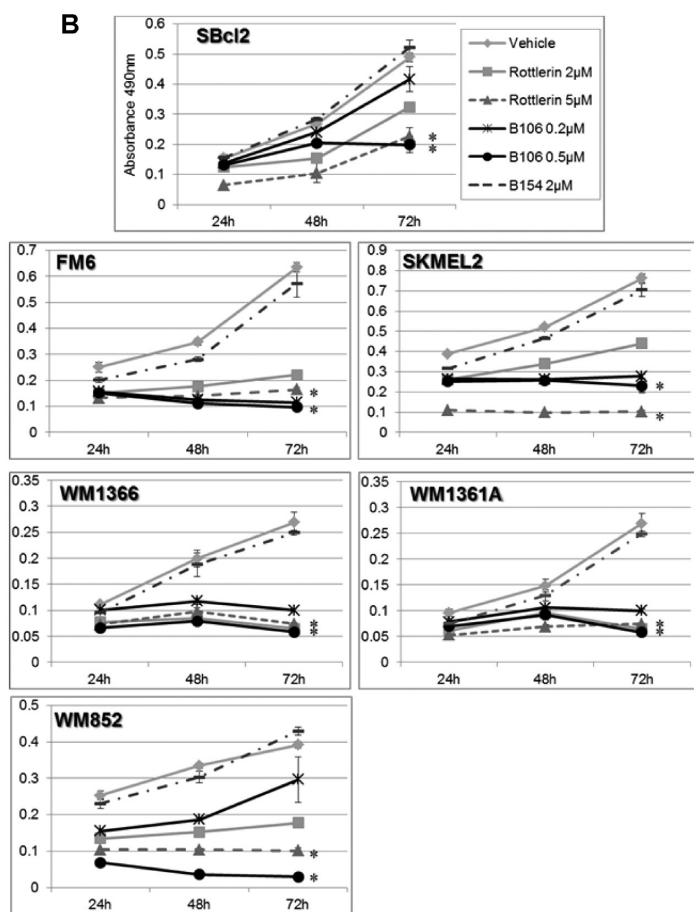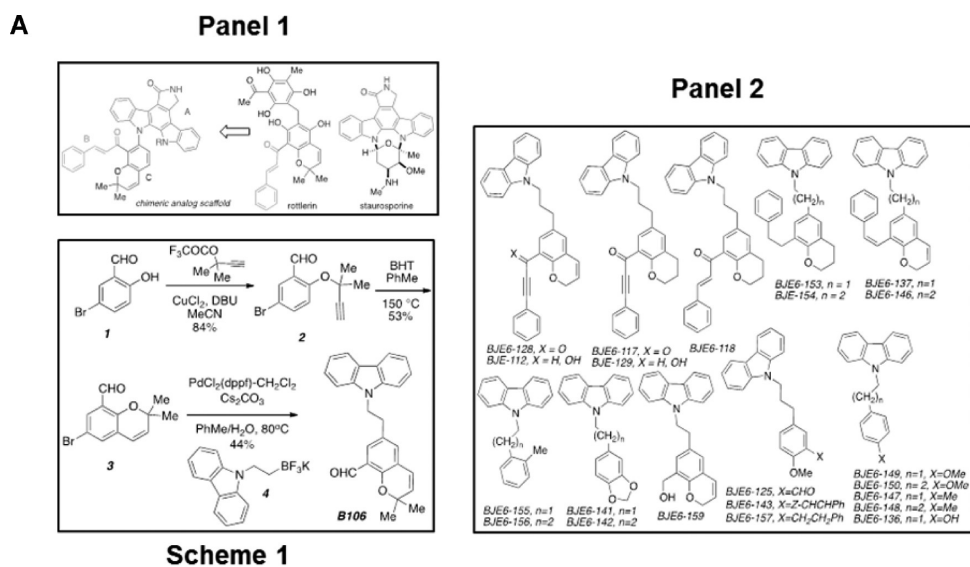
Figure 2. continued
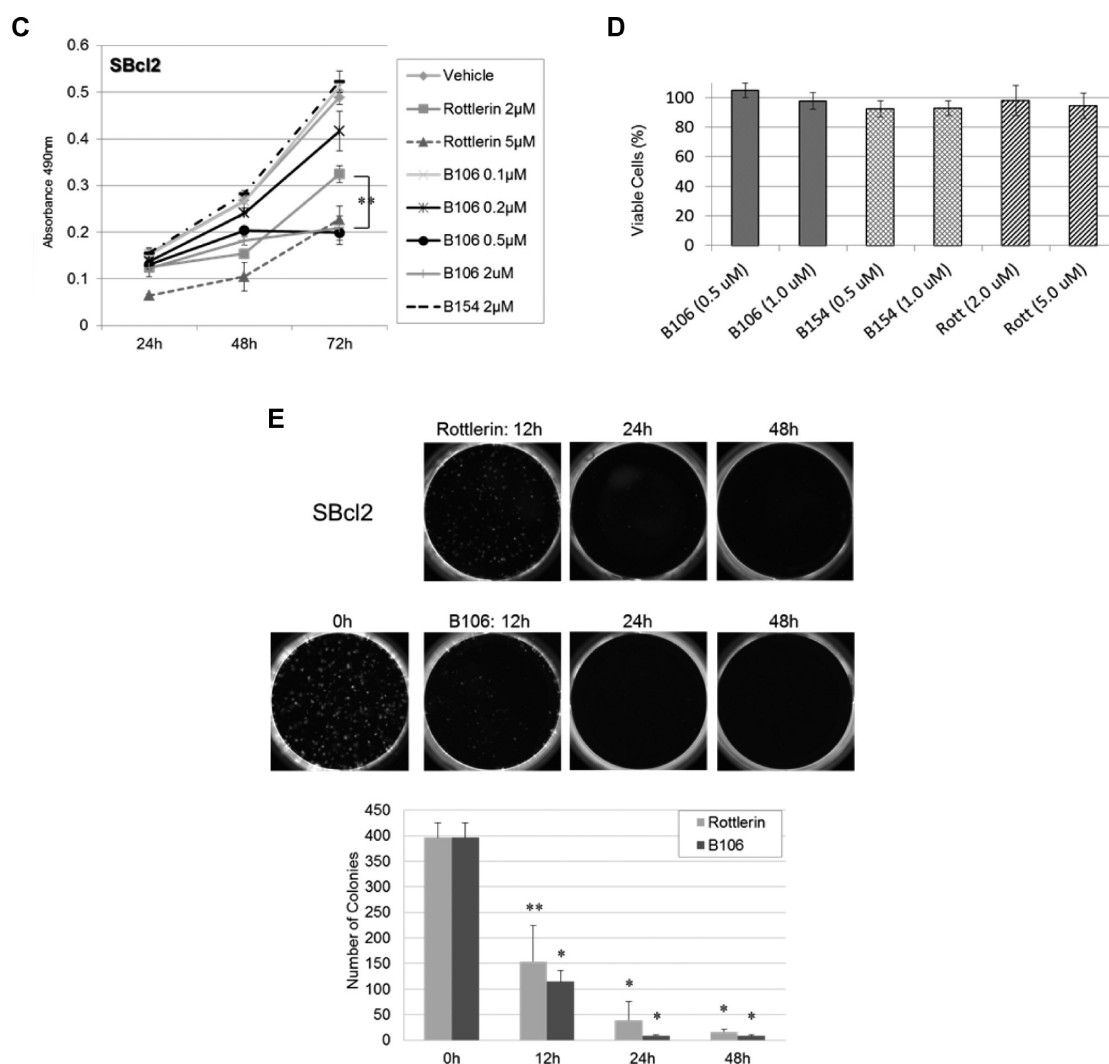
Figure 2. PKCδ inhibitors suppress survival in melanoma cell lines with NRAS mutations. (A) Structure and synthesis of PKCδ inhibitors. Panel 1: Design of mallotoxin/rottlerin-staurosporine hybrids. Scheme 1: Synthesis of B106. Panel 2: 3rd generation compounds. (B) PKCδ inhibitors suppress cell survival in melanoma cell lines with NRAS mutations. SBcl2, FM6, SKMEL2, WM1366, WM1361A, and WM852 cells were exposed to rottlerin (2 or 5 μM) or B106 (0.2 or 0.5 μM) for 24, 48, or 72 h, and MTS assays were performed at each time point. DMSO and B154 (2 μM) served as a vehicle control and a negative compound control, respectively. Each point represents the average of triplicates and error bars indicate the standard deviations. p values (*) were calculated between DMSO (vehicle control) and rottlerin 5 μM or DMSO and B106 0.5 μM in each cell line at 72 h ($p < 0.0002$). (C) Titration of PKCδ inhibitor treatment. The expanded doses of B106 (0.1 μM and 2 μM) in the MTS assay in SBcl2 in Figure 2A are shown. ** indicates a p value < 0.5 between treatment of 2 μM of rottlerin and B106. (D) Effects of PKCδ inhibitors on primary human melanocytes. Cell survival of human primary melanocytes exposed to the indicated concentrations of the compounds for 72 h (relative to DMSO-treated controls; mean $\pm$ SD, $n = 3$). (E) PKCδ inhibitors induce irreversible effects on cell growth. SBcl2 cells were treated with rottlerin or B106 at 1 μM for 0, 12, 24, or 48 h. After these exposure times, the same number of viable cells from each treatment condition was replated at low cell density and cells were cultured in medium without inhibitors for 8 days. Cell colonies were counted. Each point represents the average of triplicates and error bars indicate the standard deviations. p values: ** $p < 0.01$, * $p < 0.001$ compared to time 0 h.

cancers.[16−20] Interestingly, these types of cancers are correlated with high rates of activating mutations in KRAS genes.[7,8] Importantly, unlike many other PKC isozymes, PKCδ is not required for the survival of normal cells and tissues, and PKCδ-null mice are viable, fertile, and develop normally.[21]

Our previous studies demonstrating the synthetic lethal activity of PKCδ inhibition in pancreatic, lung, neuroendocrine, and breast cancers, and cancer stem-like cells (CSCs) with KRAS mutations[9−12] suggested the potential of targeting PKCδ in melanomas with an activating NRAS mutation. In this study, we demonstrate that inhibition of PKCδ by siRNA or novel chemical compounds suppresses the growth of melanoma lines with NRAS mutations through induction of caspase-dependent apoptosis. A novel PKCδ inhibitor developed through pharmacophore modeling exerted cytotoxic activity on NRAS mutant tumors at concentrations 1 log lower than commercially available PKCδ inhibitors. This cytotoxicity was mediated by activation of stress-responsive JNK-H2AX pathway, which involves a novel function of phospho-H2AX in mediating the apoptotic response. Furthermore, this study also showed that PKCδ inhibition can effectively inhibit the growth of PLX4032-resistant melanoma cells with BRAF mutations, demonstrating the potential of an approach targeting PKCδ in the substantial fraction of patients with melanoma who currently have only limited treatment options.

Table 1. Comparison of Properties of PKCδ Inhibitors[a]

cmpds.	generation	PKCδ IC$_{50}$	PKCα IC$_{50}$	PKCδ/PKCα selectivity	"Ras-specific" cytotoxicity
Rottlerin	1st	3−5 μM	75 μM	28-fold	3−5 μM
KAM1	2nd	3 μM	157 μM	56-fold	3 μM
B106	3rd	0.05 μM	50 μM	1000-fold	0.5 μM
B154	3rd	>40 μM	>100 μM		none

[a]*In vitro* kinase assays demonstrated that third generation PKCδ inhibitor B106 is more potent and more selective for PKCδ over PKCα than rottlerin/mallotoxin or the 2nd generation PKCδ inhibitor KAM1. B154 is used as an inactive (negative control) compound.

■ RESULTS AND DISCUSSION

PKCδ Is a Potential Therapeutic Target in Melanoma with NRAS Mutation. To validate the potential of this approach targeting PKCδ in melanomas with NRAS mutations, we first examined the effect of PKCδ-selective inhibition on cell growth by specifically and selectively knocking down PKCδ protein expression in multiple melanoma cell lines harboring NRAS mutations, using siRNA. The specificity of the PKCδ-specific siRNAs employed herein for PKCδ among all the other PKC isoforms has been previously demonstrated.[9−11] Even partial knockdown of PKCδ protein significantly inhibited the proliferation of multiple melanoma cell types with NRAS mutations, including SBcl2, FM28, FM6, and SKMEL2 cells (Figure 1). Interestingly, the degree of protein knockdown did not appear to be the sole factor in determining the degree of growth inhibitory effect by siRNA transfection; some cell lines were more susceptible than others to cell growth inhibition resulting from PKCδ downregulation. No viable cells with chronic suppression of PKCδ could ever be isolated, consistent with our previous demonstration of a requirement for PKCδ activity for the viability in cells bearing mutationally activated RAS.

These cell survival assays verified that PKCδ is essential for survival of NRAS mutant melanoma cells.

Development of Novel PKCδ Inhibitor BJE6-106 (B106). Potent small molecule inhibitors of PKCδ have not previously been available. Broad (pan) inhibitors of PKC isozymes are generally toxic, as certain PKC isozymes are required for normal physiological functions, and inhibition of such isozymes by a nonselective PKCδ inhibitor can damage normal cells.[22,23] We therefore pursued development of a more potent PKCδ inhibitor with higher PKCδ selectivity in order to explore the therapeutic potential of this approach of targeting PKCδ.

We initially generated a pharmacophore model based on molecular interactions of small molecules with "novel" class PKC isozymes. In the initial pharmacophore model for PKCδ inhibitors, mallotoxin/rottlerin, a naturally occurring product, with moderate aqueous solubility, and oral bioavailability,[24] was used as a prototype structure for a molecule with PKCδ-inhibitory activity (IC$_{50}$ = 5 μM). Protein structural data for PKCθ, another "novel" PKC isozyme, which is also inhibited by mallotoxin/rottlerin, was incorporated (Supporting Information). Mallotoxin/rottlerin is relatively selective for PKCδ over PKCα (PKCδ IC$_{50}$:PKCα IC$_{50}$ is approximately 30:1). We and others have also shown that mallotoxin/rottlerin, at the concentrations employed herein, is not cytostatic or cytotoxic to normal primary cells or cell lines and is well-tolerated when administered orally or intraperitoneally to mice.[9−12,24] This favorable toxicity profile, combined with its *in vivo* efficacy, made mallotoxin/rottlerin attractive as a starting point for modification and drug development. We further developed the pharmacophore model using a prototype chimeric structure

based on mallotoxin/rottlerin and a more general class of protein kinase C inhibitors (the natural product staurosporine), and incorporating protein structural data for "novel" class PKCs. The strategy was to retain most of the "bottom" part of mallotoxin/rottlerin (Figure 2A, panel 1), which is assumed to give mallotoxin/rottlerin its PKCδ specificity, but to vary the "head group", which is assumed to bind to the hinge region of the kinase active site. Numerous "head groups" from known potent kinase inhibitors were tested in the PKCδ model.[11] The criteria for selection was that the resulting molecule should form favorable interactions with the hinge region while the "bottom part" retained interactions with the binding site similar to that of staurosporine (from the X-ray crystallographic studies) and mallotoxin/rottlerin (from docking studies into PKCδ). In these second generation of PKCδ inhibitors, the "head" group was made to resemble that of staurosporine, a potent general PKC inhibitor, and other bisindoyl maleimide kinase inhibitors, with domains B (cinnamate side chain) and C (benzopyran) conserved from the mallotoxin/rottlerin scaffold to preserve isozyme specificity. The chromene portion of mallotoxin was combined with the carbazole portion of staurosporine to produce chimeric molecule including KAM1.[11] KAM1 was indeed active and more PKCδ-specific than rottlerin/mallotoxin and showed activity against cancer cells with activation of RAS or RAS signaling, including human neuroendocrine tumors, pancreatic cancers, and H460 lung cancer cells.[11] KAM1 had an IC$_{50}$ of 3 μM for PKCδ (similar to mallotoxin/rottlerin) and better isozyme selectivity (IC$_{50}$ > 150 μM for PKCα) (Table 1).[11]

On the basis of structure−activity relationship (SAR) analysis of KAM1 and other second generation compounds, we then generated 36 new third generation compounds (Figure 2A, panel 2). These derivatives showed a broad range of PKCδ-inhibitory activity, ranging from IC$_{50}$ > 40 μM to IC$_{50}$ < 0.05 μM (Supporting Information Table 1). BJE6-106 (B106) (Figure 2A, Scheme 1), our current lead third generation compound, has an IC$_{50}$ for PKCδ of <0.05 μM and targeted selectivity over classical PKC isozymes (a 1000-fold PKCδ selectivity over PKCα) (Table 1). BJE6-154 (B154) was among the least potent of the 36 compounds studied (PKCδ IC$_{50}$ > 40 μM) and was used as a negative-control compound with minimal inhibitory activity against PKCδ.

Inhibition of PKCδ Activity Induces Cell Growth Inhibition in Melanoma Cell Lines with NRAS Mutations. To investigate the effect of PKCδ inhibition by small molecule compounds on tumor cell growth, tumor cell survival was assessed in the presence of mallotoxin/rottlerin or B106 using a panel of melanoma cell lines with Q61 NRAS mutations, including SBcl2, FM6, SKMEL2, WM1366, WM1361A, and WM852 (Figure 2B, Table 2). Cells were exposed to rottlerin (2 or 5 μM) or B106 (0.2 or 0.5 μM) and viable cells were quantitated at 24, 48, and 72 h after treatment. Rottlerin consistently inhibited proliferation of all cell lines at 5 μM, and

E

dx.doi.org/10.1021/cb400837t | ACS Chem. Biol. XXXX, XXX, XXX−XXX

Table 2. Confirmed NRAS Q61 Mutations of the Cell Lines

cell line	allele	amino acid	type
SBcl2	C181A	Q61K	homozygous
FM6	C181A	Q61K	heterozygous
FM28	C181A	Q61K	homozygous
SKMEL2	A182G	Q61R	heterozygous
WM-1361A	A182G	Q61R	heterozygous
WM-1366	A182T	Q61L	heterozygous
WM852	A182G	Q61R	homozygous

intermediate inhibitory effects were observed at 2 μM. The third generation PKCδ inhibitor B106 effectively inhibited growth of all cell lines tested at 0.5 μM, and at 0.2 μM in some cell lines, which is at least 10 times lower than the concentration of rottlerin required to exert the same magnitude of cytotoxic effect. Both inhibitors demonstrated dose-dependent cytotoxic effects, and B106 at 0.5 μM was significantly more active than rottlerin at 2 μM (Figure 2C). Exposure to B154 at 2 μM produced a proliferation curve similar to vehicle (DMSO) treatment in all cell lines, consistent with our hypothesis that the cell growth inhibition induced by B106 resulted from the inhibition of PKCδ activity. Furthermore, B106 produced no statistically significant effects on the proliferation of primary human melanocytes at concentrations of 0.5 and 1.0 μM, indicating the tumor-specific effect of B106 (Figure 2D).

To assess the irreversible damage done to the cells by PKCδ inhibition in a different manner, clonogenic colony assays were performed using SBcl2 melanoma cells to determine the kinetics of the action of PKCδ inhibitors on the growth and proliferative characteristics of the cells. In contrast to a proliferation assay, which examines potentially temporary and reversible effects on proliferation and survival, clonogenic assays assess irreversible effects of a compound on cell viability and proliferative capacity. Cells were exposed to mallotoxin/ rottlerin or B106 for 12, 24, or 48 h and then replated in medium without inhibitors, and the difference in colony-forming ability of cultures was assessed. Both mallotoxin/ rottlerin and B106 treatment significantly decreased the number of colonies formed in SBcl2 cells after as little as 12 h of treatment, and approximately 40-fold reduction in the number of colonies was observed with 48 h of drug exposure (Figure 2E). These results demonstrate an irreversible cytotoxic effect of these PKCδ inhibitors on tumor cell growth, even after limited and transient exposure to the compounds.

Collectively, these results supported PKCδ as a potential therapeutic target in melanomas with NRAS mutation. The new PKCδ inhibitor B106 demonstrated activity at nanomolar concentrations, and may serve as a lead compound for future modifications.

Inhibition of PKCδ Activity Triggers Caspase-Dependent Apoptosis. We next determined how PKCδ inhibition results in suppression of tumor cell growth in melanoma. Activated caspase 3 and caspase 7, the ultimate executioners of apoptosis, trigger proteolytic cleavage of crucial key apoptotic proteins, which in turn leads to late apoptotic events, including DNA fragmentation. The activity of effector caspases 3 and 7 was assessed in cells treated with PKCδ inhibitors. Twenty-four hours of exposure to rottlerin (5 μM) or B106 (0.2 and 0.5 μM) significantly increased the activity of caspase 3/7 in SBcl2 cells compared to vehicle (DMSO) (Figure 3A). The effect of B106 on caspase 3/7 activation was greater than that of
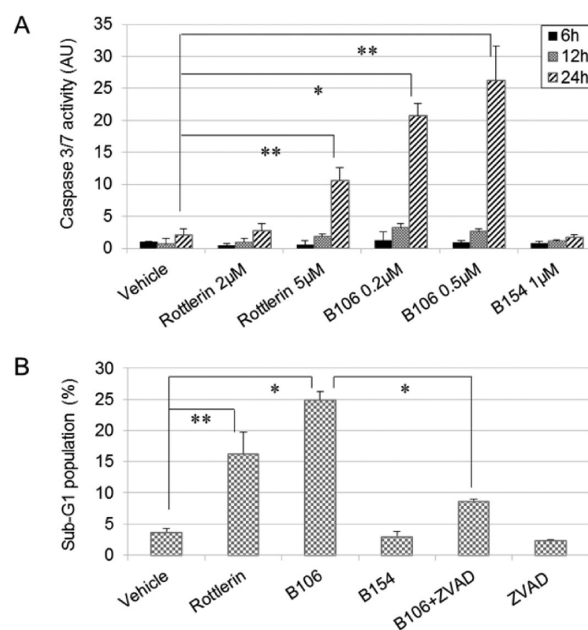
Figure 3. Inhibition of PKCδ induces caspase-dependent apoptosis. (A) Effector caspase 3/7 activation by PKCδ inhibition. SBcl2 cells were exposed to rottlerin (2 or 5 μM) or B106 (0.2 or 0.5 μM) for 6, 12, or 24 h and caspase 3/7 activity was measured. DMSO and B154 (1 μM) served as a vehicle control and a negative compound control, respectively. The average values of triplicates were normalized to those of vehicle-treated sample at 6 h. Error bars indicate the standard deviations. p values: ** $p < 0.003$, * $p < 0.0002$. (B) DNA fragmentation induced by PKCδ inhibition. SBcl2 cells were treated with rottlerin (5 μM), B106 (0.5 μM) alone, or B106 (0.5 μM) plus the pan-caspase inhibitor Z-VAD-FMK (100 μM) together for 24 h. The proportion of sub-G1 population was measured by flow cytometry. Values represent the average of duplicates and error bars indicate the standard deviations. p values: ** $p < 0.04$, * $p < 0.004$.

rottlerin: a 10-fold increase at 0.2 μM and a 12.5-fold increase at 0.5 μM of B106, in contrast to a 5-fold increase by rottlerin at 5 μM. These findings indicated the potential involvement of caspase 3/7-mediated apoptosis in response to PKCδ inhibition.

As evidence of apoptosis, induction of DNA fragmentation, a hallmark of late events in the sequence of the apoptotic process, in the presence or absence of PKCδ inhibitors was assessed by flow cytometric analysis. The proportion of cells containing a DNA content of less than 2n (fragmented DNA), categorized as the "sub-G1" population and considered in the late apoptotic phase, was significantly higher after treatment with rottlerin at 5 μM and even higher after treatment with B106 at 0.5 μM, whereas B154, a negative-control compound for B106, lacking PKCδ-inhibitory activity, produced no more fragmented DNA than did vehicle control (DMSO), suggesting the effect of B106 on DNA fragmentation was related to inhibition of PKCδ activity (Figure 3B). To determine whether activation of caspases by PKCδ inhibitors was necessary for the observed apoptosis, the pan-caspase inhibitor Z-VAD-FMK (carbobenzoxy-valyl-alanyl-aspartyl-[Omethyl]-fluoromethylketone) was employed. Pretreatment of cells with Z-VAD-FMK (50 μM) prevented B106-induced caspase 3 cleavage in immunoblot analysis (data not shown). B106-induced DNA fragmentation was significantly abrogated when SBcl2 cells were pretreated with Z-VAD-FMK (100 μM) (Figure 3B). Taken together, these data suggest that PKCδ inhibition attenuates tumor cell
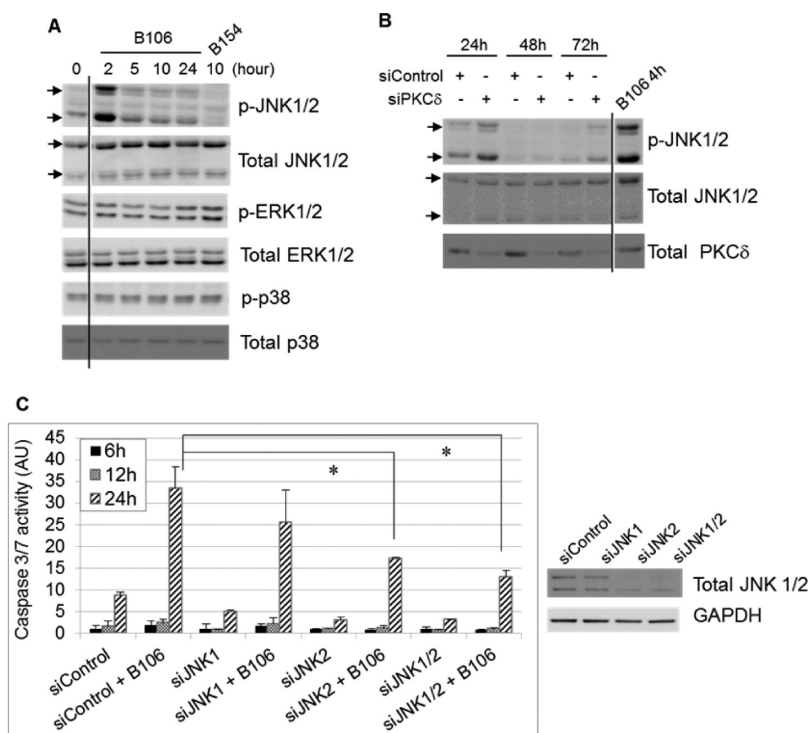
Figure 4. PKCδ inhibition triggers an apoptotic response through activation of JNK. PKCδ inhibition activates JNK. (A, B) SBcl2 cells were exposed to B106 (1 μM) or the negative control compound B154 (1 μM) for indicated times (A) or transfected with siRNA targeting PKCδ ("siPKCδ") or nontargeting siRNA ("siControl") at 5 nM for the indicated times (B). Protein lysates were subjected to immunoblot analysis for levels of phosphorylated or total MAPK proteins. (C) Activation of caspase 3/7 is mitigated by knockdown of JNK prior to B106 treatment. SBcl2 cells were transfected with siRNA targeting JNK1 or JNK2 alone (5 nM), or the combination of JNK1 and JNK2 siRNA (5 nM each), or nontargeting siRNA (10 nM) for 72 h, and subsequently exposed to B106 (0.5 μM) or vehicle (DMSO) for 6, 12, and 24 h. Caspase 3/7 activity was measured. The average values of triplicates were normalized to those of the vehicle-treated sample at 6 h between the pairs exposed to the same siRNA. Error bars indicate the standard deviations. p values: * $p < 0.005$. Downregulation of JNK1/2 proteins were confirmed by immunoblot analysis at 72 h. In panels A and B, certain lanes not relevant to this discussion were excised, as indicated by the vertical lines.

growth by inducing caspase-dependent apoptosis in NRAS mutant melanoma cells.

PKCδ Inhibition Triggers Apoptotic Response via the Stress-Responsive JNK Pathway. To identify which intracellular signaling pathway PKCδ inhibition employs to induce cytotoxicity, the activation status of known downstream targets of PKCδ was examined after PKCδ inhibition, including MAPKs (ERK, p38, and JNK), AKT, NFκB pathway, cyclin-dependent kinase inhibitors, p53, IAPs, GSK3β, or c-Abl. Inhibition of PKCδ activity in SBcl2 cells by B106 induced phosphorylation (activation) of JNK1/2 (T183/Y185) most strongly after 2 h of exposure (Figure 4A). In contrast, phosphorylation of the closely related MAPKs p38 and ERK was not affected by PKCδ inhibitors (Figure 4A). Consistent with these observations generated using chemical inhibitors, selective downregulation of PKCδ by transfection of PKCδ-specific siRNA induced phosphorylation of JNK1/2 at 24 h, (when effects of siRNA on PKCδ levels were first observed) (Figure 4B). Transfection of PKCδ-specific or negative control siRNA did not affect phosphorylation levels of ERK or p38.

Among its pleiotropic cellular activities, JNK is an effector in certain apoptotic responses, and some chemotherapeutic agents, including paclitaxel, cisplatin and doxorubicin, employ the JNK pathway for their cytotoxic activity.[25,26] Because of the data demonstrating that PKCδ inhibition causes caspase-dependent apoptosis (Figure 3) and JNK activation (Figures 4A and B), the effect of inhibition of the JNK pathway during B106 treatment was explored to determine if there is a

functional relationship. SBcl2 cells were transfected with nonspecific siRNA or siRNA specific for JNK1 or JNK2 alone, or cotransfected with JNK1- plus JNK2-specific siRNA for 72 h, and then exposed to B106 or DMSO (vehicle) for 6, 12, or 24 h, followed by measurement of caspase activity (Figure 4C). Analysis at 24 h after B106 treatment showed that knockdown of JNK2 alone, and coknockdown of JNK1 and 2, mitigated B106-induced caspase 3/7 activation in rough proportion to the knockdown efficiency of JNK1/2 proteins. These data indicated that JNK is a necessary mediator of the apoptotic response induced by PKCδ inhibition.

PKCδ Inhibition Activates the MKK4-JNK-H2AX Pathway. We tested for involvement of known upstream and downstream effectors of the JNK pathway following PKCδ inhibition. The MAPKK kinases MKK4 and MKK7 lie one tier above JNK. MKK4 was activated by B106 (Figure 5A), whereas MKK7 was not phosphorylated in response to B106 (data not shown). Activation of the canonical JNK substrate, c-Jun, was also observed in response to B106 exposure, confirming the activation of the JNK pathway by PKCδ inhibitors (Figure 5A). Furthermore, activation of H2AX (histone H2A variant X), another downstream effector of JNK associated with its apoptotic actions,[27] was noted at later time points in response to B106 treatment (Figure 5A). B106 consistently induced H2AX phosphorylation as early as after 10 h of exposure. The effect of PKCδ inhibition on H2AX activation was further confirmed by selective downregulation of PKCδ with siRNA. Phosphorylation of H2AX was observed at 72 h after PKCδ
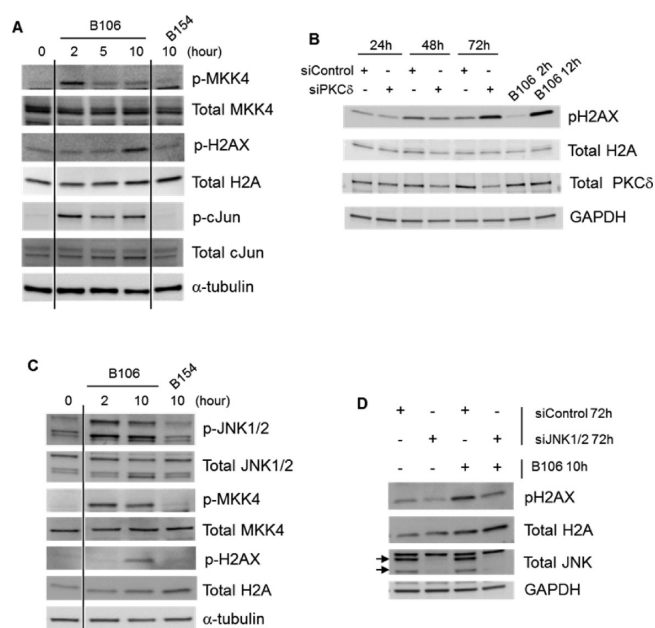
Figure 5. PKCδ inhibition activates the MKK4-JNK-H2AX pathway. (A) Activation of upstream and downstream components of the JNK pathway by B106. SBcl2 cells were exposed to B106 or the negative control compound B154 at 1 μM for the indicated times. Protein lysates were subjected to immunoblot analysis. (B) Selective downregulation of PKCδ results in phosphorylation of H2AX. SBcl2 cells were transfected with siRNA targeting PKCδ ("siPKCδ") or nontargeting ("siControl") at 50 nM for the indicated times. Protein lysates were subjected to immunoblot analysis. In panels A and B, certain lanes not relevant to this discussion were excised, as indicated by the vertical lines. (C) PKCδ inhibition activates H2AX through JNK. SBcl2 cells were transfected with siRNA targeting JNK1 and JNK2 together (5 nM each) or nontargeting siRNA (10 nM) for 72 h and subsequently exposed to B106 (0.5 μM) or vehicle (DMSO) for 10 h. Protein lysates were subjected to immunoblot analysis. Arrows indicate JNK1/2.

siRNA transfection (Figure 5B). PKCδ inhibition by B106 treatment similarly induced phosphorylation of MKK4, JNK and H2AX in NRAS mutant melanoma WM1366 cells (Figure 5C).

Because JNK affects diverse downstream effectors, we next determined whether JNK activation caused by PKCδ inhibition is directly linked to B106-induced H2AX activation. Knockdown of JNK1/2 itself slightly reduced basal phospho-H2AX (pH2AX) expression, indicating that basal phosphorylation of H2AX is regulated by JNK (Lane 2, Figure 5D). B106 exposure robustly induced phosphorylation of H2AX in control siRNA-treated cells (Lane 3, Figure 5D); in comparison, prior downregulation of JNK1/2 protein by siRNA attenuated B106-induced H2AX phosphorylation (Lane 4, Figure 5D). Collectively, these data suggest that PKCδ inhibition directly or indirectly activates MKK4 in cells containing mutated NRAS, which in turn activates JNK1/2 and subsequently H2AX.

H2AX is a Critical Regulator of Caspase-Dependent Apoptosis Induced in Response to PKCδ inhibition. Although phosphorylation of H2AX is best known as a consequence of DNA double-stranded breaks in the DNA-damage response, facilitating repair,[28−30] recent studies have demonstrated that phosphorylation of H2AX at Ser 139 resulting from JNK activation actively mediates the induction of apoptosis by inducing DNA fragmentation in UV- or

chemotherapy-damaged cells.[31−34] Accordingly, the direct involvement of H2AX in apoptotic response to PKCδ inhibition was examined. SBcl2 cells were transfected with siRNA targeting H2AX, or nontargeting siRNA, for 72 h and then exposed to B106 for 6, 12, or 24 h, with subsequent assay of caspase 3/7 activation. Downregulation of H2AX prior to B106 treatment greatly decreased the level of caspase 3/7 activation at 24 h of B106 exposure (Figure 6A).
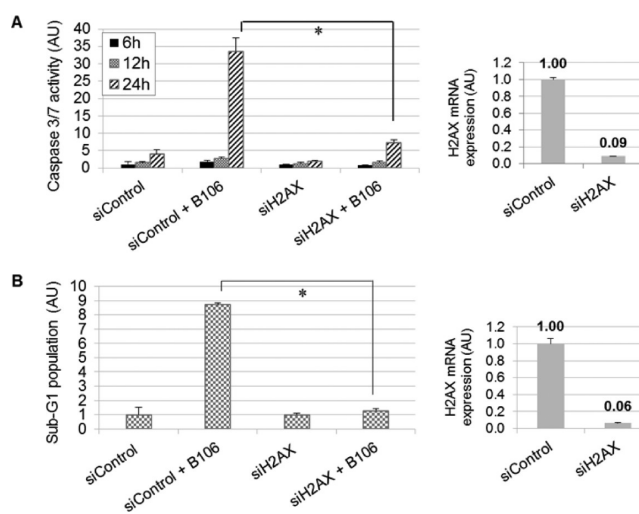
Figure 6. H2AX is a critical apoptotic regulator in apoptosis induced by PKCδ inhibition. (A) Activation of caspases 3/7 is mitigated by knockdown of H2AX prior to B106 treatment. SBcl2 cells were transfected with siRNA targeting H2AX or nontargeting siRNA at 5 nM for 72 h, and subsequently exposed to B106 (0.5 μM) or vehicle for 6, 12, or 24 h. Caspase 3/7 activity was measured. The average values of triplicates were normalized to those of the vehicle-treated sample at 6 h between the pairs exposed to the same siRNA. Error bars indicate the standard deviations. p values: * p < 0.005. Downregulation of H2AX at 72 h was confirmed by quantitative PCR. (B) Induction of DNA fragmentation is mitigated by knockdown of H2AX prior to B106 treatment. SBcl2 cells were transfected with siRNA targeting H2AX, or nontargeting siRNA, at 5 nM for 72 h, and subsequently exposed to B106 (0.5 μM) or vehicle for 24 h. The proportion of sub-G1 population was measured by flow cytometry. The average values of duplicates were normalized to those of the vehicle-treated samples between the pairs exposed to the same siRNA. Error bars indicate the standard deviations. p value: * p < 0.0004. Downregulation of H2AX at 96 h was confirmed by quantitative PCR.

To explore a direct link between H2AX and the execution of apoptosis, PKCδ inhibition-induced DNA fragmentation was examined in the presence or absence of H2AX. SBcl2 cells were transfected with either negative-control siRNA or siRNA targeting H2AX for 72 h, and then subjected to PKCδ inhibition by exposure to B106 for 24 h. PKCδ inhibition by B106 treatment increased DNA fragmentation 8.5-fold in the cells transfected with negative control siRNA (Figure 6B). In contrast, PKCδ inhibition by B106 treatment failed to induce DNA fragmentation in the absence of H2AX (Figure 6B), indicating that H2AX is necessary for B106-induced apoptosis (Figure 6B). Collectively, these results suggest that inhibition of PKCδ by B106 treatment triggers caspase-dependent apoptosis through activation of the JNK-H2AX stress-responsive signaling pathway.

BRAF Inhibitor-Resistant BRAF Mutant Melanoma Lines Are Susceptible to PKCδ Inhibition. The inevitable

H

dx.doi.org/10.1021/cb400837t | ACS Chem. Biol. XXXX, XXX, XXX−XXX
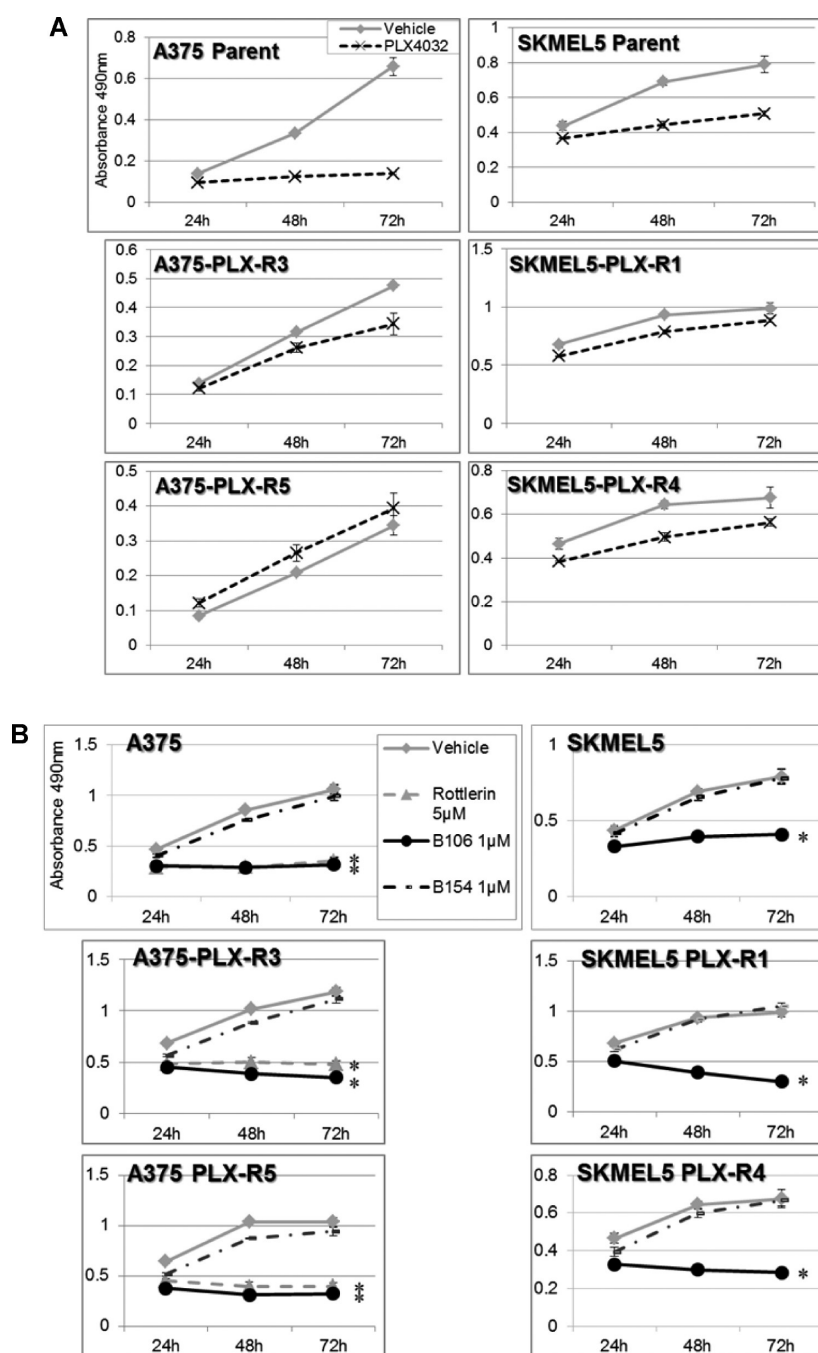
Figure 7. PKCδ inhibitors suppress growth of PLX4032-resistant BRAF mutant melanoma cells. (A) Establishment of PLX4032-resistant cell sublines. To establish PLX4032 resistant cell lines, two individual melanoma cell lines with BRAF mutations, A375 and SKMEL5, were continuously exposed to increasing concentrations of PLX4032 up to 10 μM (A375) and 2 μM (SKMEL5). To confirm resistance to PLX4032, the viability of PLX4032-resistant cells and their parental cells was measured by MTS assay during treatment with PLX4032 at 1 μM. (B) PKCδ inhibitors suppress survival of PLX4032-resistant cells. Two PLX4032-resistant cell sublines derived from A375 (left) and SKMEL5 (right) cells were exposed to rottlerin (5 μM) or B106 (1 μM) for 24, 48, or 72 h, and MTS assays were performed at each time point. DMSO and B154 (1 μM) served as a vehicle control and a negative compound control, respectively. Each point represents the average of triplicates and error bars indicate the standard deviations. p values (*) were calculated between DMSO (vehicle control) and rottlerin 5 μM, or DMSO and B106, 1 μM in each cell line at 72 h ($p < 0.0002$).

development of resistance to the BRAF inhibitor PLX4032 (vemurafenib) in melanomas bearing BRAF mutations remains an ongoing clinical challenge. Several proposed models of PLX4032 resistance involve reactivation of RAS-MEK/ERK mitogenic pathway, induced, for example, by the secondary mutations of NRAS at position 61, or activation of alternative pathways leading to reactivation of ERK signaling, such as

IGF1R or AKT.[6] Our previous studies have demonstrated the effectiveness of PKCδ inhibitors in the cells with the aberrant CRAF-ERK activation even in the absence of mutations in RAS oncogenes.[9−12] We therefore investigated whether PKCδ inhibition could be similarly effective in those BRAF mutant melanoma cells that have become refractory to a BRAF inhibitor (PLX4032). We generated BRAF-V600E mutant

I

dx.doi.org/10.1021/cb400837t | ACS Chem. Biol. XXXX, XXX, XXX−XXX

melanoma cell sublines resistant to PLX4032 by continuously exposing A375 and SKMEL5 cells to PLX4032, with gradually increasing concentrations of the drug over weeks. Resistance to PLX4032 was verified by comparing their sensitivity to the drug with that of their parental cells (Figure 7A). PLX-R derivative lines from both A375 and SKMEL5 grew in the presence of concentrations of PLX4032 which were cytotoxic to the parental cells. Sequencing revealed that these resistant cell lines retained wild-type NRAS alleles at position 61. The resistant cell sublines derived from both the A375 or SKMEL5 parent lines acquired distinct aberrant alterations in RAS pathway signaling that may be responsible for their resistance (increased activation of ERK1,2 in the resistant A375 lines, and increased CRAF in the resistant SKMEL5 lines). All of these PLX4032-resistant lines were susceptible to cytotoxicity induced by PKCδ inhibitors at concentrations comparable to the NRAS mutant melanoma lines (Figure 7B). The parental cell lines A375 and SKEML5 (both BRAF-V600E mutant) were also susceptible to PKCδ inhibition (Figure 7B); this finding is consistent with our previous report that cells with aberrant activation/mutation of RAF signaling, and consequent activation of this RAS effector pathway (even in the presence of normal RAS alleles) require PKCδ activity for survival.[9−12]

PKCδ as a Therapeutic Target in Melanomas with NRAS Mutations or BRAF Inhibitor Resistance. Somatic point mutations of RAS genes at codons 12, 13, and 61 are the most common dominant oncogenic lesions in human cancer,[2,3] making aberrant RAS signaling an important therapeutic target. Inhibition of PKCδ preferentially inhibits the growth of cancer cell lines with genomic mutations in KRAS or HRAS genes, or oncogenic activation of KRAS proteins.[9−12,35,36] While initially characterized as a specific synthetic lethal interaction between PKCδ and RAS, further work disclosed that aberrant activation of certain RAS effector pathways, PI$_3$K-AKT and CRAF-MEK, would also confer sensitivity to PKCδ inhibition.[9−12] Importantly, PKCδ was demonstrated to be nonessential for the survival and proliferation of normal cells and animals,[21] suggesting that a therapeutic approach targeting PKCδ would likely spare normal cells, but inhibit the proliferation of tumor cells whose survival depends on PKCδ activity. This report underlines the potential of PKCδ-targeted therapy as a cancer-specific therapy targeting melanoma with NRAS mutations. Cell proliferation and clonogenic assays demonstrated that inhibition of PKCδ suppressed cell growth in multiple melanoma cell lines with NRAS mutations, as well as in PLX4032-resistant cell lines. The cell lines with NRAS mutation that were used in this study had different amino acid substitutions of NRAS codon 61, suggesting the effect of PKCδ inhibitors does not depend on a specific NRAS mutation for their activity. Similarly, PKCδ inhibition was effective in the PLX4032-resistant cell lines tested herein, regardless of the differences in their apparent resistance mechanisms, further supporting the potential of this approach. Constitutive MEK/ERK signaling appears to mediate the majority of acquired resistance to BRAF inhibitors,[6] and we have previously reported that aberrant activation of the MEK/ERK arm of the RAS signaling pathway is sufficient to render cells susceptible to PKCδ inhibition, even in the absence of activating mutations of RAS alleles.[9−11] Furthermore, we have recently demonstrated that cancer "stem-like" cells (CSCs) derived from a variety of human tumors, including melanomas, are susceptible to PKCδ inhibition.[12]

The novel PKCδ inhibitor B106, which showed 1000-fold selectivity against PKCδ over PKCα in preliminary *in vitro* kinase assays, was active at nanomolar concentrations, 10 times lower than for rottlerin. These results in cell culture systems suggest the potential of the newest PKCδ inhibitors as targeted agents, although the *in vivo* efficacy of B106 is yet to be determined. The hydrophobicity of B106 molecule and its rapid metabolism, requiring continuous infusion to generate a pharmacodynamic signal, makes it unsuitable for testing in tumor xenograft models.

Induction of apoptosis is one of the most desirable mechanisms for cytotoxic therapeutic action. The stress-activated protein kinase/c-Jun N-terminal kinase (SAPK/JNK), a downstream targets of PKCδ, is activated in response to cellular stresses, including genotoxic stresses.[37] Many chemotherapeutic agents employ the JNK pathway for their cytotoxic activity.[38,39] This study demonstrates that PKCδ inhibition activates the JNK pathway through MMK4 to mediate caspase-dependent apoptosis. Consistent with our findings, a recent report demonstrated that knockdown of PKCδ induced apoptosis with elevated phosphorylation of JNK in NIH-3T3 cells stably transfected with HRAS.[35] Among the known downstream effectors of JNK, a series of recent reports proposed an active role for phospho-H2AX in apoptosis.[31−34] PKCδ inhibition evoked phosphorylation of H2AX subsequent to JNK activation, positioning H2AX phosphorylation downstream of JNK after PKCδ inhibition. Collectively, these results demonstrate the importance of H2AX as an active apoptotic mediator, providing functional evidence showing it to be a necessary component of apoptosis initiated by PKCδ inhibition.

The concept of targeting cancer therapeutics toward specific mutations or aberrations in tumor cells that are not found in normal tissues has the potential advantages of high selectivity for the tumor and correspondingly low secondary toxicities. We have previously demonstrated that knockdown of PKCδ, or its inhibition by previous generations of small molecules, was not toxic to nontransformed primary murine and human cell lines, primary human endothelial cells, or to tumor lines without aberrant activation of the RAS signaling pathway, at concentrations which are profoundly cytotoxic to melanoma lines bearing NRAS mutations (0.5−2.5 μM).[9−11] Herein, we show that human primary melanocytes are not affected by B106. In addition, continuous local infusion of B106 at 5 μM concentrations is not cytotoxic to dermal and subdermal tissues in mice. Derivatives of the third generation PKCδ inhibitor B106 are being generated, using structure function analysis of the 36 compounds in that cohort and medicinal chemistry to enhance drug-like properties, to facilitate future *in vivo* studies. Collectively, our studies suggest that PKCδ suppression may offer a promising tumor-specific option for a subpopulation of melanomas for which we have currently a limited number of effective therapeutics.

■ ASSOCIATED CONTENT

Ⓢ Supporting Information

Synthesis data. PKCδ-inhibitory activity data. This material is available free of charge *via* the Internet at http://pubs.acs.org.

■ AUTHOR INFORMATION

Corresponding Author

*Phone: 617-638-4173. Fax: 617-638-4176. E-mail: dfaller@bu.edu.

Notes

■ ACKNOWLEDGMENTS

■ REFERENCES

(1) Siegel, R., Naishadham, D., and Jemal, A. (2013) Cancer statistics, 2013. *Ca−Cancer J. Clin. 63*, 11−30.

(2) Inamdar, G. S., Madhunapantula, S. V., and Robertson, G. P. (2010) Targeting the MAPK pathway in melanoma: Why some approaches succeed and other fail. *Biochem. Pharmacol. 80*, 624−637.

(3) Takashima, A., and Faller, D. V. (2013) Targeting the RAS oncogene. *Expert. Opin. Ther. Targets 17*, 507−531.

(4) Chapman, P. B., Hauschild, A., Robert, C., Haanen, J. B., Ascierto, P., Larkin, J., Dummer, R., Garbe, C., Testori, A., Maio, M., Hogg, D., Lorigan, P., Lebbe, C., Jouary, T., Schadendorf, D., Ribas, A., O'Day, S. J., Sosman, J. A., Kirkwood, J. M., Eggermont, A. M., Dreno, B., Nolop, K., Li, J., Nelson, B., Hou, J., Lee, R. J., Flaherty, K. T., and McArthur, G. A. (2011) Improved survival with vemurafenib in melanoma with BRAF V600E mutation. *N. Engl. J. Med. 364*, 2507−2516.

(5) Nazarian, R., Shi, H., Wang, Q., Kong, X., Koya, R. C., Lee, H., Chen, Z., Lee, M. K., Attar, N., Sazegar, H., Chodon, T., Nelson, S. F., McArthur, G., Sosman, J. A., Ribas, A., and Lo, R. S. (2010) Melanomas acquire resistance to B-RAF(V600E) inhibition by RTK or N-RAS upregulation. *Nature 468*, 973−977.

(6) Trunzer, K., Pavlick, A. C., Schuchter, L., Gonzalez, R., McArthur, G. A., Hutson, T. E., Moschos, S. J., Flaherty, K. T., Kim, K. B., Weber, J. S., Hersey, P., Long, G. V., Lawrence, D., Ott, P. A., Amaravadi, R. K., Lewis, K. D., Puzanov, I., Lo, R. S., Koehler, A., Kockx, M., Spleiss, O., Schell-Steven, A., Gilbert, H. N., Cockey, L., Bollag, G., Lee, R. J., Joe, A. K., Sosman, J. A., and Ribas, A. (2013) Pharmacodynamic effects and mechanisms of resistance to vemurafenib in patients with metastatic melanoma. *J. Clin. Oncol. 31*, 1767−1774.

(7) Schubbert, S., Shannon, K., and Bollag, G. (2007) Hyperactive Ras in developmental disorders and cancer. *Nat. Rev. Cancer 7*, 295−308.

(8) Malumbres, M., and Barbacid, M. (2003) RAS oncogenes: The first 30 years. *Nat. Rev. Cancer 3*, 459−465.

(9) Xia, S., Forman, L. W., and Faller, D. V. (2007) Protein kinase Cδ is required for survival of cells expressing activated p21RAS. *J. Biol. Chem. 282*, 13199−13210.

(10) Xia, S., Chen, Z., Forman, L. W., and Faller, D. V. (2009) PKCδ survival signaling in cells containing an activated p21Ras protein requires PDK1. *Cell Signal. 21*, 502−508.

(11) Chen, Z., Forman, L. W., Miller, K. A., English, B., Takashima, A., Bohacek, R. A., Williams, R. M., and Faller, D. V. (2011) The proliferation and survival of human neuroendocrine tumors is dependent upon protein kinase Cδ. *Endocr. Relat. Cancer 18*, 759−771.

(12) Chen, Z., Forman, L. W., Williams, R. M., and Faller, D. V. (2014) Protein kinase Cδ inactivation inhibits the proliferation and survival of cancer stem cells in culture and *in vivo*. *BMC Cancer*, in press.

(13) Zhu, T., Chen, L., Du, W., Tsuji, T., and Chen, C. (2010) Synthetic lethality induced by loss of PKCδ and mutated Ras. *Genes Cancer 1*, 142−151.

(14) Symonds, J. M., Ohm, A. M., Carter, C. J., Heasley, L. E., Boyle, T. A., Franklin, W. A., and Reyland, M. E. (2011) Protein kinase Cδ is a downstream effector of oncogenic K-Ras in lung tumors. *Cancer Res. 71*, 2087−2097.

(15) Basu, A., and Pal, D. (2010) Two faces of protein kinase Cδ: The contrasting roles of PKCδ in cell survival and cell death. *Sci. World J. 10* (2272−84), 2272−2284.

(16) Lonne, G. K., Masoumi, K. C., Lennartsson, J., and Larsson, C. (2009) Protein kinase Cδ supports survival of MDA-MB-231 breast cancer cells by suppressing the ERK1/2 pathway. *J. Biol. Chem. 284*, 33456−33465.

(17) Wang, Q., Wang, X., Zhou, Y., and Evers, B. M. (2006) PKCδ-mediated regulation of FLIP expression in human colon cancer cells. *Int. J. Cancer 118*, 326−334.

(18) Baudot, A. D., Jeandel, P. Y., Mouska, X., Maurer, U., Tartare-Deckert, S., Raynaud, S. D., Cassuto, J. P., Ticchioni, M., and Deckert, M. (2009) The tyrosine kinase Syk regulates the survival of chronic lymphocytic leukemia B cells through PKCδ and proteasome-dependent regulation of Mcl-1 expression. *Oncogene 28*, 3261−3273.

(19) Clark, A. S., West, K. A., Blumberg, P. M., and Dennis, P. A. (2003) Altered protein kinase C (PKC) isoforms in non-small cell lung cancer cells: PKCδ promotes cellular survival and chemotherapeutic resistance. *Cancer Res. 63*, 780−786.

(20) Mauro, L. V., Grossoni, V. C., Urtreger, A. J., Yang, C., Colombo, L. L., Morandi, A., Pallotta, M. G., Kazanietz, M. G., Bal de Kier Joffe, E. D., and Puricelli, L. L. (2010) PKCδ promotes tumoral progression of human ductal pancreatic cancer. *Pancreas 39*, e31−e41.

(21) Leitges, M., Mayr, M., Braun, U., Mayr, U., Li, C., Pfister, G., Ghaffari-Tabrizi, N., Baier, G., Hu, Y., and Xu, Q. (2001) Exacerbated vein graft arteriosclerosis in protein kinase Cδ-null mice. *J. Clin. Invest. 108*, 1505−1512.

(22) Soloff, R. S., Katayama, C., Lin, M. Y., Feramisco, J. R., and Hedrick, S. M. (2004) Targeted deletion of protein kinase Cλ reveals a distribution of functions between the two atypical protein kinase C isoforms. *J. Immunol. 173*, 3250−3260.

(23) Mochly-Rosen, D., Das, K., and Grimes, K. V. (2012) Protein kinase C, an elusive therapeutic target? *Nat. Rev. Drug Discov. 11*, 937−957.

(24) Chou, W. H., Choi, D. S., Zhang, H., Mu, D., McMahon, T., Kharazia, V. N., Lowell, C. A., Ferriero, D. M., and Messing, R. O. (2004) Neutrophil protein kinase Cδ as a mediator of stroke-reperfusion injury. *J Clin. Invest. 114*, 49−56.

(25) Hatzivassiliou, G., Song, K., Yen, I., Brandhuber, B. J., Anderson, D. J., Alvarado, R., Ludlam, M. J., Stokoe, D., Gloor, S. L., Vigers, G., Morales, T., Aliagas, I., Liu, B., Sideris, S., Hoeflich, K. P., Jaiswal, B. S., Seshagiri, S., Koeppen, H., Belvin, M., Friedman, L. S., and Malek, S. (2010) RAF inhibitors prime wild-type RAF to activate the MAPK pathway and enhance growth. *Nature 464*, 431−435.

(26) Heidorn, S. J., Milagre, C., Whittaker, S., Nourry, A., Niculescu-Duvas, I., Dhomen, N., Hussain, J., Reis-Filho, J. S., Springer, C. J., Pritchard, C., and Marais, R. (2010) Kinase-dead BRAF and oncogenic RAS cooperate to drive tumor progression through CRAF. *Cell 140*, 209−221.

(27) Lu, C., Zhu, F., Cho, Y. Y., Tang, F., Zykova, T., Ma, W. Y., Bode, A. M., and Dong, Z. (2006) Cell apoptosis: Requirement of H2AX in DNA ladder formation but not for the activation of caspase-3. *Mol. Cell 23*, 121−132.

(28) Yuan, J., Adamski, R., and Chen, J. (2010) Focus on histone variant H2AX: To be or not to be. *FEBS Lett. 584*, 3717−3724.

(29) Rogakou, E. P., Nieves-Neira, W., Boon, C., Pommier, Y., and Bonner, W. M. (2000) Initiation of DNA fragmentation during apoptosis induces phosphorylation of H2AX histone at serine 139. *J. Biol. Chem. 275*, 9390−9395.

(30) Mukherjee, B., Kessinger, C., Kobayashi, J., Chen, B. P., Chen, D. J., Chatterjee, A., and Burma, S. (2006) DNA-PK phosphorylates

histone H2AX during apoptotic DNA fragmentation in mammalian cells. *DNA Repair (Amst) 5,* 575−590.

(31) Kaplan, F. M., Shao, Y., Mayberry, M. M., and Aplin, A. E. (2011) Hyperactivation of MEK-ERK1/2 signaling and resistance to apoptosis induced by the oncogenic B-RAF inhibitor, PLX4720, in mutant N-RAS melanoma cells. *Oncogene 30,* 366−371.

(32) Jane, E. P., and Pollack, I. F. (2010) Enzastaurin induces H2AX phosphorylation to regulate apoptosis via MAPK signalling in malignant glioma cells. *Eur. J. Cancer 46,* 412−419.

(33) Liu, Y., Tseng, M., Perdreau, S. A., Rossi, F., Antonescu, C., Besmer, P., Fletcher, J. A., Duensing, S., and Duensing, A. (2007) Histone H2AX is a mediator of gastrointestinal stromal tumor cell apoptosis following treatment with imatinib mesylate. *Cancer Res. 67,* 2685−2692.

(34) Wen, W., Zhu, F., Zhang, J., Keum, Y. S., Zykova, T., Yao, K., Peng, C., Zheng, D., Cho, Y. Y., Ma, W. Y., Bode, A. M., and Dong, Z. (2010) MST1 promotes apoptosis through phosphorylation of histone H2AX. *J. Biol. Chem. 285,* 39108−39116.

(35) Zhu, T., Chen, L., Du, W., Tsuji, T., and Chen, C. (2010) Synthetic lethality induced by loss of PKCδ and mutated Ras. *Genes Cancer 1,* 142−151.

(36) Symonds, J. M., Ohm, A. M., Carter, C. J., Heasley, L. E., Boyle, T. A., Franklin, W. A., and Reyland, M. E. (2011) Protein kinase Cδ is a downstream effector of oncogenic K-Ras in lung tumors. *Cancer Res. 71,* 2087−2097.

(37) Johnson, G. L., and Nakamura, K. (2007) The c-jun kinase/ stress-activated pathway: Regulation, function, and role in human disease. *Biochim. Biophys. Acta 1773,* 1341−1348.

(38) Lee, L. F., Li, G., Templeton, D. J., and Ting, J. P. (1998) Paclitaxel (Taxol)-induced gene expression and cell death are both mediated by the activation of c-Jun NH2-terminal kinase (JNK/ SAPK). *J. Biol. Chem. 273,* 28253−28260.

(39) Koyama, T., Mikami, T., Koyama, T., Imakiire, A., Yamamoto, K., Toyota, H., and Mizuguchi, J. (2006) Apoptosis induced by chemotherapeutic agents involves c-Jun N-terminal kinase activation in sarcoma cell lines. *J. Orthop. Res. 24,* 1153−1162.

L

dx.doi.org/10.1021/cb400837t | *ACS Chem. Biol.* XXXX, XXX, XXX−XXX

Supplemental Table 1:

PKCδ Inhibitory Activity of BJE6 compounds

Compound	IC$_{50}$ (*in vitro*)[1]			IC$_{50}$ (*in culture*)[3]
	PKCδ IC$_{50}$ (μM)	PKCα IC$_{50}$ (μM)	PKCδ/PKCα (IC$_{50}$ ratio)[2]	
Rottlerin	4.4	75	28	10
KAM-1	3.6	177	56	5
B058	5.8	NA[4]	-	>50
B071	3	NA	-	>100
B095	8	NA	-	>100
B097	9.5	NA	-	>100
B106	0.08	15	200	1
B108	3	NA	-	>100
B109	0.09	75	800	>100
B111	2.5	25	100	40
B112	6	NA	-	>50
B117	4.5	NA	-	>100
B118	10	NA	-	>100
B121	4	NA	-	>100
B125	0.25	20	800	>100
B128	6.5	NA	-	>100
B129	6.5	NA	-	>50
B130	4	NA	-	40
B131	10	NA	-	>100
B136	14	NA	-	>100
B137	3	NA	-	>100
B141	4.8	NA	-	>50
B142	3.5	NA	-	>100
B143	6	NA	-	>100
B146	5	NA	-	>100
B147	5.8	NA	-	20
B148	4	NA	-	>100
B149	0.31	>300	>1000	20
B150	0.625	500	800	30
B151	< 0.05	50	>1000	>100
B152	< 0.05	50	>1000	>100
B153	3	NA	-	>100
B154	23	NA	-	>100

B155	3	NA	-	>100
B156	7.5	NA	-	>100
B157	5	NA	-	>100
B158	4.5	NA	-	>100
B159	7	NA	-	40

[1] IC$_{50}$ measured using recombinant PKCδ or PKCα

[2] Ratio of PKCδ IC$_{50}$ to PKCα IC$_{50}$

[3] IC$_{50}$ for cytotoxicity on a KRAS-mutant cell line H460.

[4] NA = not assayed (PKCα inhibitory activity was only assayed on compounds with an IC$_{50}$ for PKCδ of <2.5 μM).

SUPPLEMENTAL INFORMATION FOR REVIEW

There are few substrates established to be "unique" to PKCδ. One such is the phosphorylation of transcription factor Fli1 after TGFβ or CTGF stimulation. We have carried out those studies to demonstrate the action of B106 on PKCδ *in vivo*. We attach these data here for Reviewer 2 (panel E in Figure below).

Figure. PKCδ inhibitor B106 inhibits collagen production and Fli1 phosphorylation. Dermal fibroblasts were stimulated with TGFβ for 24 hr in the presence or absence of the indicated concentration of B106. Secretion of collagen protein was examined by immunoblot (**A**). Bar graph represents Mean±SD from two independent experiments. COL1A1 mRNA was analyzed by qPCR (**B**). SSc fibroblasts were treated with the indicated doses of B106. Secretion of collagen was examined by Western blot (**C**) and COL1A1 mRNA was analyzed by qPCR (**D**). Dermal fibroblasts were stimulated with TGFβ or CTGF for 2 h. Fli1 phosphorylation was assessed by Western blot with the phospho-specific Fli1 Ab as previously described [5] (**E**).

Analysis of BJE6-106 Inhibitory Activity on Selected SER/THR and Other Kinases

Kinase	IC$_{50}$ (μM) [1]	IC$_{50}$ relative to PKCδ [2]
PKCδ	0.1	-
PKCα	22	220
PKCθ	12	120
cRAF	>25	>250
cABL	>25	>250
JAK1/2	>25	>250
MAPK	>25	>250
ERK	>25	>250
p38	>25	>250
JNK1/2	>25	>250
PKA	>25	>250
PDGF-R [3]	>25	>250
EGF-R [3]	>25	>250

[1] B106 (and all the 4th generation compounds of this series which were tested) produced inconsistent results in two different commercially-available kinome assays, because of variable but significant precipitation when the 100% DMSO solution containing the compounds was diluted with the aqueous buffers in the assays. The presence of protein or lipid in the buffers prevented this precipitation, but it was not possible to employ these hydrophobic agents in the commercial assays. Accordingly, the IC$_{50}$ of B106 had to be measured individually for each kinase, either using a recombinant or purified kinase, and an artificial substrate (InVitrogen). Kinases were chosen for analysis based on their similarity to PKCδ, or their involvement in RAS signaling pathways.

[2] The data generated here for each kinase cannot be compared to other kinases with absolute precision, as different substrates were utilized, and this ratio should be considered only an estimate.

[3] Ligand-induced autophosphorylation
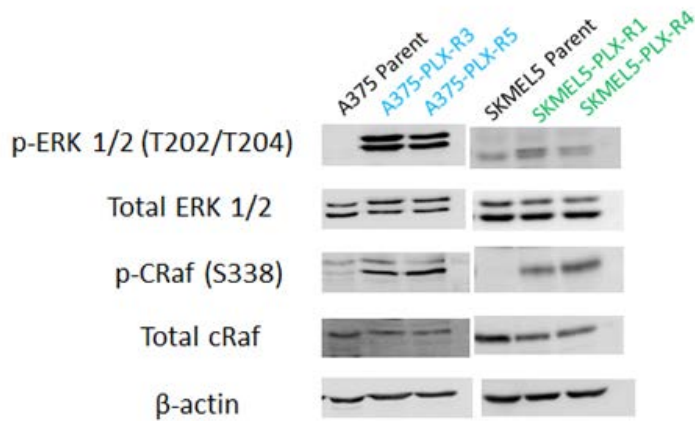
Figure: RAF/MEK/ERK pathway activation in PLX4032-resistant melanoma cell line derivatives.

Parental A375 cells, SKMEL5 cells, and their PLX4032-resistant derivatives in log phase growth were lysed and the lysates were subjected to immunoblot analysis. Antibodies to total ERK1/2, pERK (T202/T204), total CRAF, and phospho-cRaf (S338) were used. β-actin served as a loading control.

PROTEIN KINASE C δ IS A THERAPEUTIC TARGET IN MALIGNANT MELANOMA WITH NRAS MUTATION OR BRAF INHIBITOR-RESISTANCE

Asami Takashima[1], Brandon English[2], Zhihong Chen[1], Rutao Cui[1,3], Juxiang Cao[3], Robert M. Williams[2,4], Douglas V. Faller[1,5]

[1]Cancer Center and [5]Departments of Medicine, Biochemistry, Pediatrics, Microbiology, Pathology and Laboratory Medicine, and [3]Department of Dermatology,
Boston University School of Medicine, 72 E Concord St. Boston MA, 02118
[2]Department of Chemistry, Colorado State University, Fort Collins, Colorado 80523
[4]University of Colorado Cancer Center, Aurora, Colorado 80045

Supporting Information

Preparation of BJE6-154

Unless otherwise noted, all reagents were obtained from commercial suppliers and were used without further purification. All air or moisture sensitive reactions were performed under a positive pressured of argon in flame-dried glassware. Tetrahydrofuran (THF), toluene, diethyl ether (Et$_2$O), dichloromethane, benzene (PhH), acetonitrile (MeCN), triethylamine (NEt$_3$), pyridine, diisopropyl amine, methanol (MeOH), dimethylsulfoxide (DMSO), and N,N-dimethylformamide (DMF) were obtained from a dry solvent system (Ar degassed solvents delivered through activated alumina columns, positive pressure of argon). Column chromatography was performed on Merck silica gel Kieselgel 60 (230-400 mesh). ^{1}HNMR and ^{13}CNMR spectra were recorded on Varian 300, or 400 MHz spectrometers. Chemical shifts are reported in ppm relative to CHCl$_3$ at δ 7.27 (^{1}HNMR) and δ 77.23 (^{13}CNMR). Mass spectra were obtained on Fisons VG Autospec. IR spectra were obtained from thin films on a NaCl plate using a Perkin-Elmer 1600 series FT-IR spectrometer.

Synthesis of 9-(3-(trifluoro-»^{4}-boranyl)propyl)-9*H*-carbazole, potassium salt:

To 3.83 mL (26.5 mmol, 5.5 equiv) 2,5-dimethylhexa-2,4-diene dissolved in 10.0 mL dry THF in a flame dried 100 mL round bottomed flask at 0°C was added 12.06 mL of a 1.0M solution of BH$_3$ dissolved in THF. The reaction was stirred at 0°C for 3hr before the addition of 1.00 g (4.82 mmol, 1 equiv.) 9-allylcarbazole dissolved in a minimum amount of dry THF. The reaction was allowed to warm to ambient temperature with stirring over 3hr before being cooled to 0°C. To this mixture was added 1.7 mL deionized H$_2$O. The reaction was then stirred for 1.5hr at ambient temperature before the addition of 4.3 mL of a 37% solution of CH$_2$O$_{(aq)}$. The reaction was stirred at ambient temperature for 16hr before being added to brine, extracted into EtOAc, dried over Na$_2$SO$_4$, and concentrated. The resulting residue was taken up in a mixture of 17.0 mL acetone and 6.5 mL H$_2$O before the addition of 1.51 g (19.3 mmol, 4 equiv.) KHF$_2$. The resulting mixture was stirred at ambient temperature for 4hr before being concentrated under reduced pressure. The resulting residue was recrystallized from acetone and Et$_2$O yielding 1.10 g (72%) of a white crystalize solid which was utilized below without characterization or further purification.
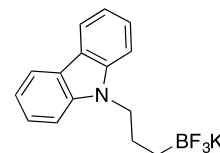
Synthesis of 6-bromo-2,2-dimethyl-2*H*-chromene-8-carbaldehyde:

To a 100 mL flame dried round bottomed flask containing 5.54 mL (57.2 mmol, 1.15 equiv) 2-methylbut-3-yn-2-ol dissolved in 50 mL dry MeCN at 0°C was added 11.1 mL (74.6 mmol, 1.5 equiv.) DBU followed by the dropwise addition of 8.08 mL (57.2 mmol, 1.15 equiv.) freshly distilled TFAA. The reaction was stirred at 0°C for 30 min before being added via cannula to a 250 mL round bottomed flask containing 10.0 g (49.7 mmol, 1 equiv.) 5-bromo-2-hydroxybenzaldehyde, 9.65 mL (64.6 mmol, 1.3 equiv.) DBU, and 8.5 mg (0.050 mmol, 0.001 equiv.) CuCl$_2$-2H$_2$O dissolved in dry MeCN at -5°C. The reaction was stirred for 16hr at ambient temperature before being concentrated under reduced pressure. The resulting residue was taken up in EtOAc, washed once with H$_2$O, once with 1 M HCl, and once with brine before being dried over Na$_2$SO$_4$, and concentrated. This residue was subjected to silica gel flash chromatography eluting with 19 : 1 to 4 : 1 hex/EtOAc to yield 11.17g (84%) of the desired product as a pale yellow solid.
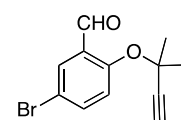
^{1}HNMR (300MHz, CDCl$_3$) δ 10.27(s, 1H), 7.88 (s, 1H), 7.55 (d, J = 8.4, 1H), 7.38 (d, J = 8.4, 1H), 2.63 (s, 1H), 1.67 (s, 6H);); ^{13}CNMR (75MHz, CDCl$_3$) δ 188.8, 157.4, 137.5, 130.9, 130.2, 122.8, 116.1, 84.7, 76.3, 74.5, 29.7; IR (NaCl, film) 3294, 1687, 1588, 1471 cm^{-1}; HRMS (+TOF) 267.0015 calcd for C$_{12}$H$_{12}$BrO$_2$ [M+H]$^+$, found: 267.0016; R$_f$ = 0.38 (9 : 1 hex./ EtOAc). Ref. KAM1-415, BJE6-094

^{1}H NMR (300 MHz) CDCl$_3$

^{13}C NMR (75 MHz) CDCl$_3$

2
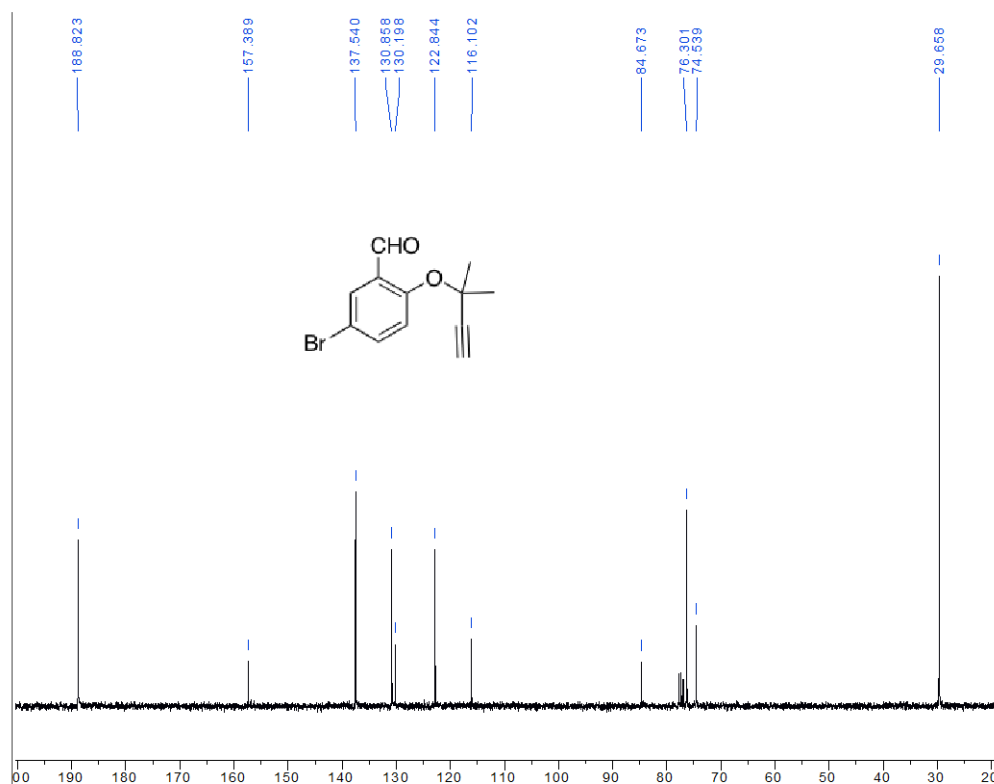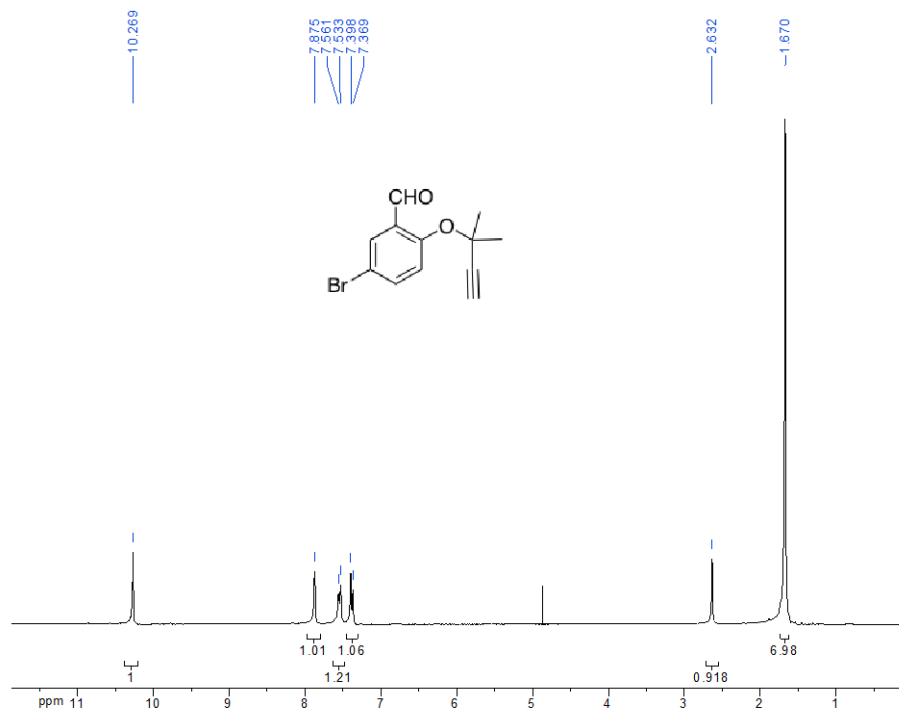
Synthesis of 6-bromo-2,2-dimethyl-2*H*-chromene-8-carbaldehyde: To an 80 mL microwave reaction vessel containing 4.00 g (14.8 mmol, 1 equiv.) 5-bromo-2-((2-methylbut-3-yn-2-yl)oxy)benzaldehyde dissolved in 60 mL dry MeCN was added 66.0 mg (0.300 mmol, 0.02 equiv.) BHT. The reaction was heated in a microwave reactor to 180°C for 20 min before being concentrated and purified by silica gel flash chromatography eluting with 19 : 1 hex./EtOAc to yield 2.10 g (53%) of the desired product as a yellow oil.
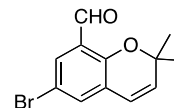
^{1}HNMR (300MHz, CDCl$_3$) δ 10.35 (s,1H), 7.73 (d, *J* = 2.7, 1H), 7.27 (dd, *J* = 2.7, 0.3, 1H), 6.29 (d, *J* = 9.9, 1H), 5.75 (d, *J* = 9.9, 1H), 1.50 (s, 3H); ^{13}CNMR (75MHz, CDCl$_3$) δ 188.0, 155.3, 134.3, 132.8, 129.4, 125.6, 124.6, 120.8, 113.4, 78.4, 28.4; IR (NaCl, film) 2863, 1678, 1574 cm^{-1}; HRMS (+TOF) 267.0015 calcd for C$_{12}$H$_{12}$BrO$_2$ [M+H]$^+$, found: 267.0012; R$_f$ = 0.33 (9 : 1 hex./ EtOAc).Ref. KAM1-419, BJE6-105

^{1}H NMR (300 MHz) CDCl$_3$

3

^{13}C NMR (75 MHz) CDCl$_3$
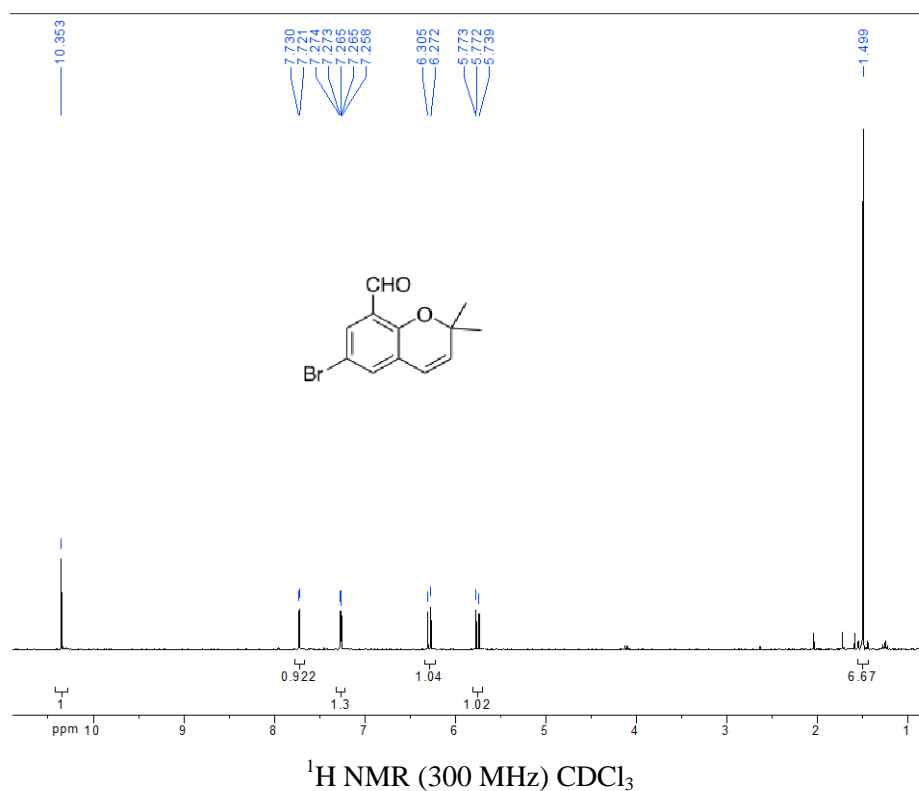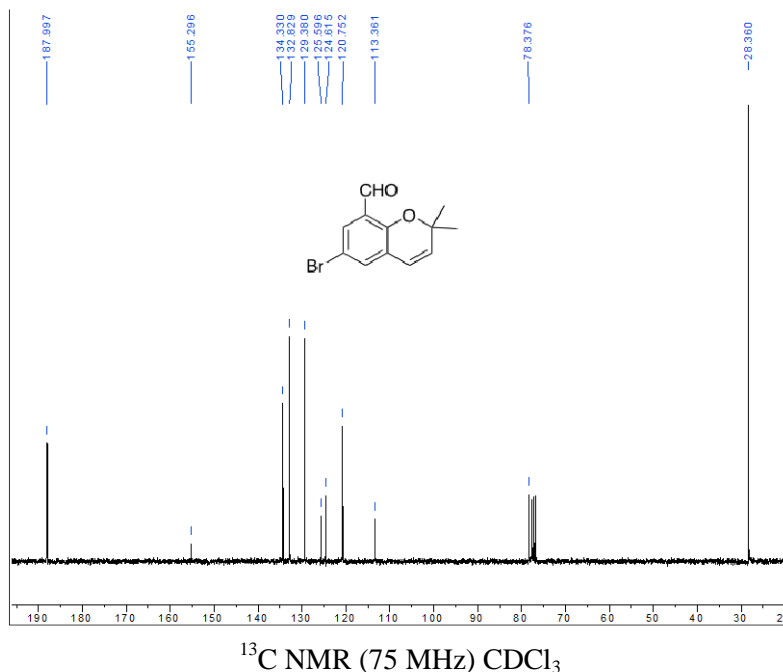
Synthesis of 1-(6-bromo-2,2-dimethyl-2*H*-chromen-8-yl)-3-phenylprop-2-yn-1-ol: To a flame dried 100 mL round bottomed flask containing 745 mg (7.30 mmol, 1.3 equiv.) ethynylbenzene dissolved in 30 mL dry THF at -78°C was dropwise added 4.2 mL (6.7 mmol, 1.2 equiv) of a 1.6 M solution of *n*-BuLi in hexanes. The reaction was allowed to stir at -78°C for 30 min before the addition of 1.50 g (5.62 mmol, 1 equiv.) 6-bromo-2,2-dimethyl-2*H*-chromene-8-carbaldehyde dissolved in 10 mL dry THF. After stirring for 30 min at -78°C the reaction was poured into saturated NH$_4$Cl$_{(aq.)}$, extracted into EtOAc, dried over Na$_2$SO$_4$, and concentrated. The resulting residue was purified by silica gel flash chromatography eluting with 4 : 1 hex./EtOAc yielding 2.1 g (99%) of the desired product as a yellow oil.
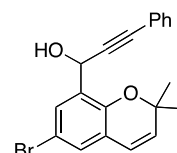
^{1}HNMR (300MHz, CDCl$_3$) δ 7.52 (d, *J* = 2.4, 1H), 7.46 (m, 2H), 7.33 (m, 3H), 7.10 (d, *J* = 2.4, 1H), 6.27 (d, *J* = 9.9, 1H), 5.78 (s, 1H), 5.69 (d, *J* = 9.6, 1H), 3.06 (bs, 1H), 1.49 (s, 3H), 1.48 (s, 3H); ^{13}CNMR (75MHz, CDCl$_3$) δ 149.5, 132.2, 132.0, 130.3, 130.1, 129.1, 128.7, 128.5, 123.6, 122.7, 121.4, 113.1, 88.2, 86.3, 77.8, 61.3, 28.2, 28.2; IR (NaCl, film) 3428 br, 2230 cm^{-1}; HRMS (+TOF) 351.0379 calcd. for C$_{20}$H$_{16}$BrO [M-H$_2$O]$^+$, found: 351.0389; R$_f$ = 0.40 (4 : 1 hex./ EtOAc). Ref. KAM1-420, BJE6-107

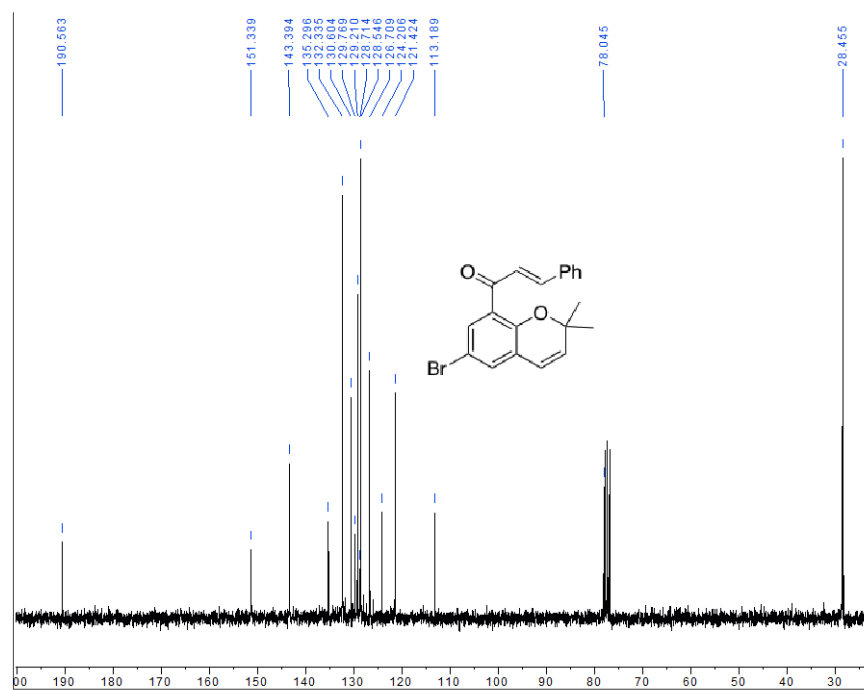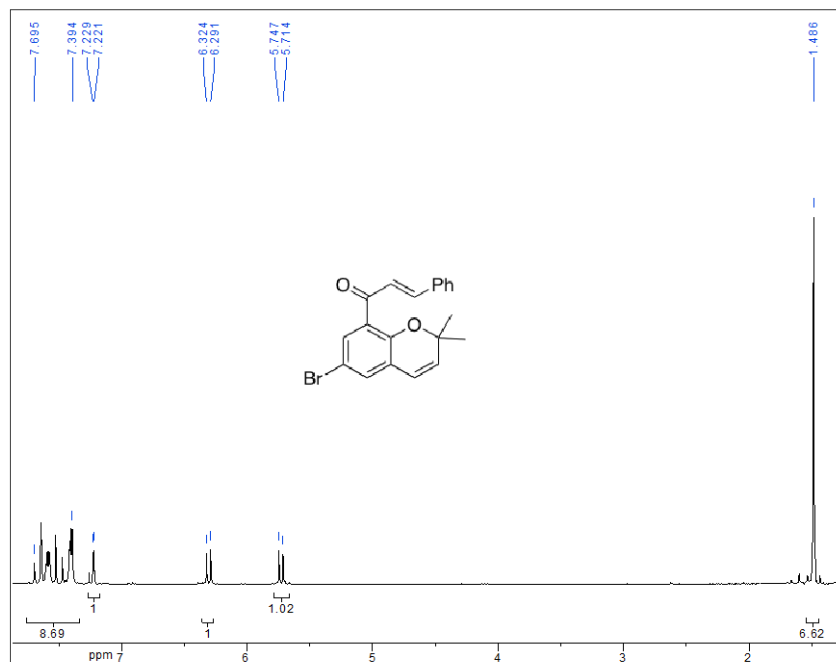**¹H NMR (300 MHz) CDCl₃**

¹³C NMR (75 MHz) CDCl₃
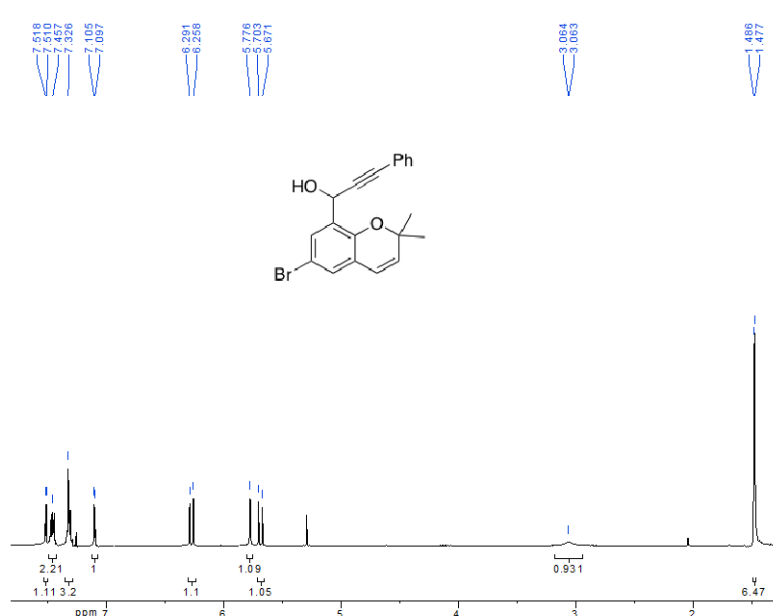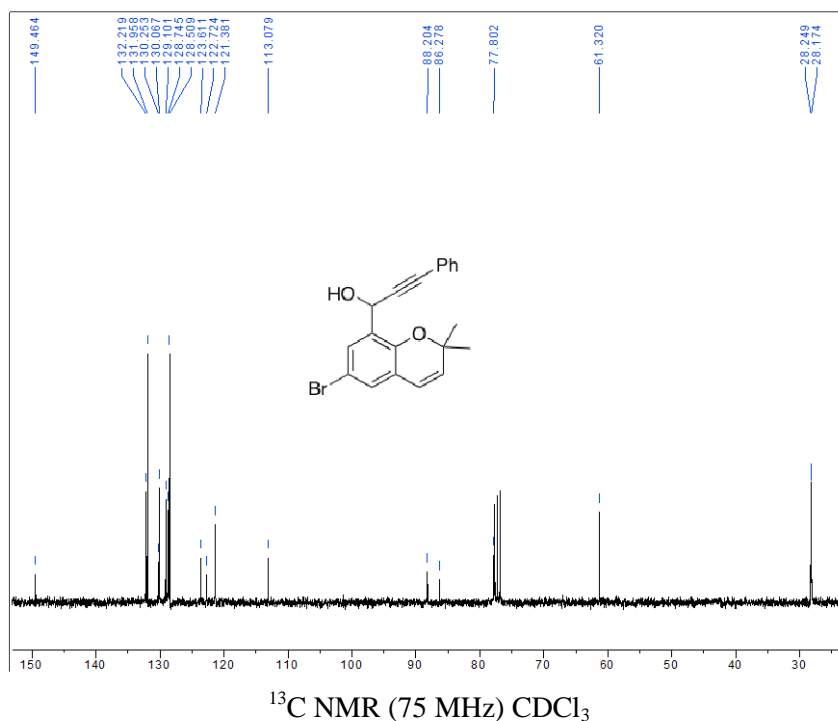
Synthesis of (*E*)-1-(6-bromo-2,2-dimethyl-2*H*-chromen-8-yl)-3-phenylprop-2-en-1-ol: To a 10 mL round bottomed flask containing 100 mg (0.271 mmol, 1 equiv.) 1-(6-bromo-2,2-dimethyl-2*H*-chromen-8-yl)-3-phenylprop-2-yn-1-ol dissolved in 1.5 mL dry THF was added 12 mg (0.33 mmol, 1.2 equiv.) LiAlH₄. The reaction was heated to reflux for 1 hr and cooled to ambient temperature. The reaction was quenched by addition of H_2O followed by 15% NaOH$_{(aq.)}$ and then EtOAc. The organic layer was separated and then filtered through a short silica gel plug before being concentrated to yield 100 mg (99%) of the desired product as a yellow oil.
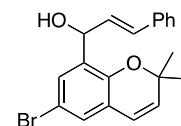
¹HNMR (300MHz, CDCl₃) δ 7.40-7.24 (m, 6H), 7.06 (d, *J* = 2.4, 1H), 6.70 (d, *J* = 15.9, 1H), 6.38 (dd, *J* = 15.9, 5.4, 1H), 6.26 (d, *J* = 9.9, 1H), 5.66 (d, *J* = 9.9, 1H), 5.50 (m, 1H), 1.44(s, 3H), 1.42 (s, 3H); ¹³CNMR (75MHz, CDCl₃) δ 149.0, 136.9, 132.5, 132.0, 130.6, 129.5, 128.8, 128.8, 128.3, 127.9, 126.8, 123.5, 121.6, 113.3, 77.4, 70.7, 28.3, 28.2; IR (NaCl, film) 3416 br cm⁻¹; HRMS (+TOF) 353.0536 calcd for C₁₁H₁₅O₃ [M-H₂O]⁺, found: 353.0548; R$_f$ = 0.26 (9 : 1 hex./EtOAc). Ref. KAM1-421, BJE110

5

^{1}H NMR (300 MHz) CDCl$_3$

^{13}C NMR (75 MHz) CDCl$_3$
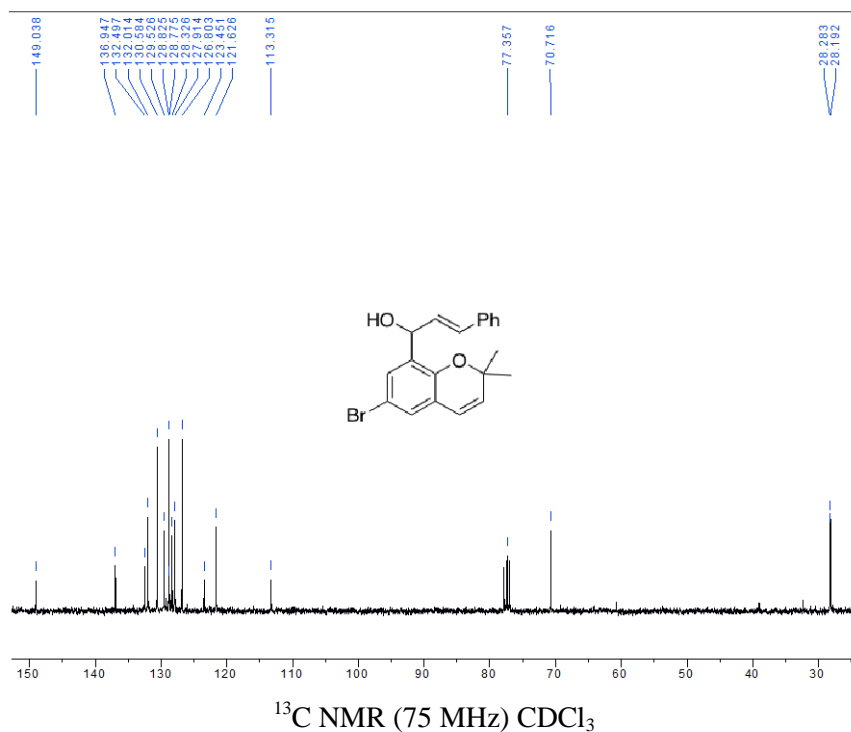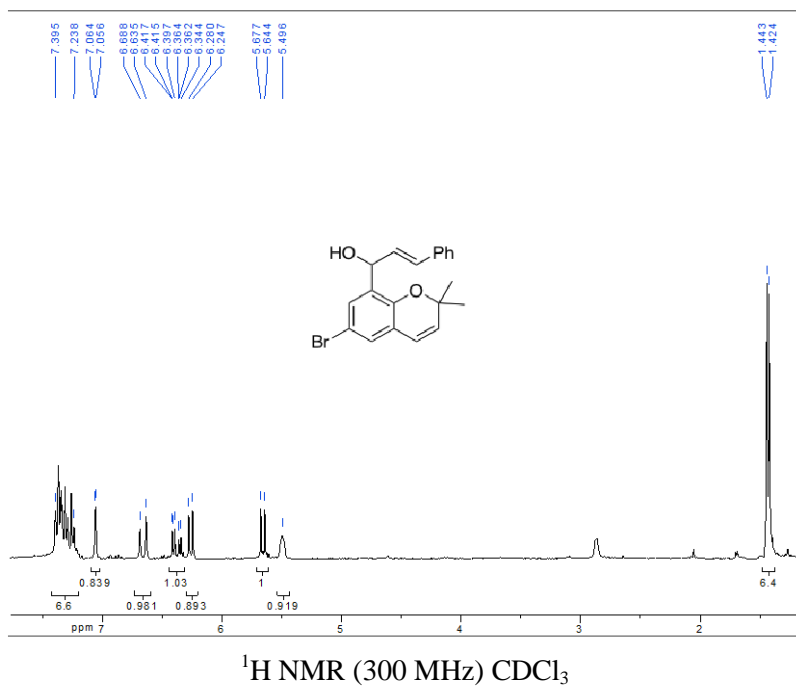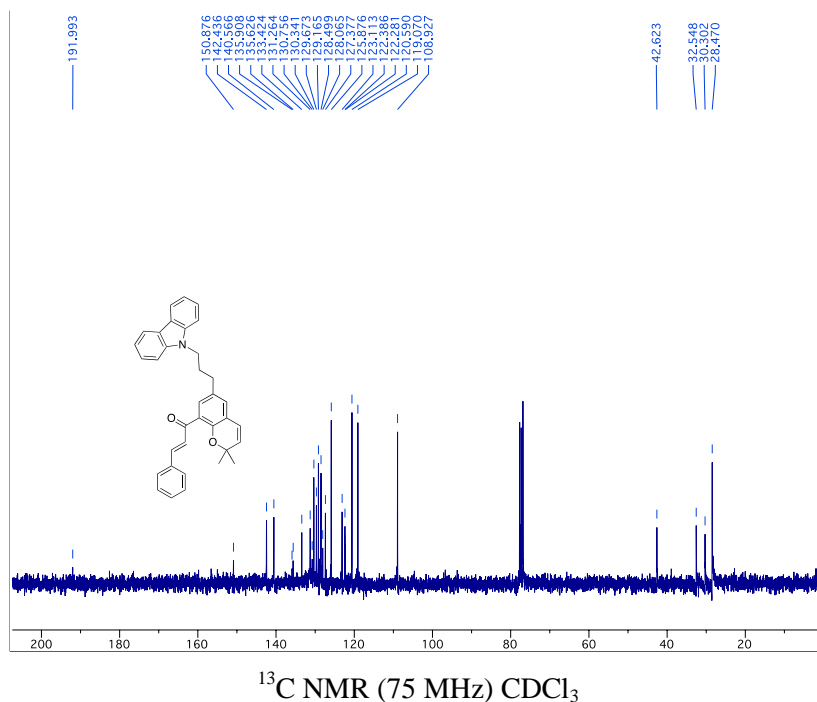
Synthesis of (*E*)-1-(6-bromo-2,2-dimethyl-2*H*-chromen-8-yl)-3-phenylprop-2-en-1-one: To a 50 ml round bottomed flask containing 1.41 g (3.80 mmol, 1 equiv.) (*E*)-1-(6-bromo-2,2-dimethyl-2*H*-chromen-8-yl)-3-phenylprop-2-en-1-ol dissolved in 20 mL dry CH$_2$Cl$_2$ was added 1.98 g (22.8 mmol, 6 equiv.) MnO$_2$ and the reaction was stirred at ambient temperature for 2 hr. The reaction was filtered through celite and concentrated. The resulting residue was purified by silica gel flash chromatography eluting with 19 : 1 to 4 : 1 hex./EtOAc yielding 1.25 g (89%) of the desired product as a yellow oil.

^{1}HNMR (300MHz, CDCl$_3$) δ 7.70-7.39 (m, 8H), 7.22 (d, *J* = 2.4, 1H), 6.31 (d, *J* = 9.9, 1H), 5.72 (d, *J* = 9.9, 1H), 1.49 (s, 6H); ^{13}CNMR (75MHz, CDCl$_3$) δ 190.6, 151.3, 143.4, 135.3, 132.3, 130.6, 129.8, 129.2, 128.7, 128.5, 126.7, 124.2,

6
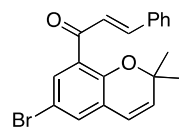
121.4, 113.2, 78.0, 28.5; IR (NaCl, film) 1654, 1603, 1435 cm^{-1}; HRMS (+TOF) 369.0485 calcd for C$_{20}$H$_{18}$BrO$_2$ [M+H]$^{+}$, found: 369.0489; R$_f$ = 0.50 (4 :1 hex./ EtOAc). Ref. KAM1-422, BJE6-113

^{1}H NMR (300 MHz) CDCl$_3$

^{13}C NMR (75 MHz) CDCl$_3$

Synthesis of (*E*)-1-(6-(3-(9*H*-carbazol-9-yl)propyl)-2,2-dimethyl-2*H*-chromen-8-yl)-3-phenylprop-2-en-1-one: To a 10 mL round bottomed flask containing 76 mg (0.206 mmol, 1 equiv.) (*E*)-1-(6-bromo-2,2-dimethyl-2*H*-chromen-8-yl)-3-phenylprop-2-en-1-one and 65 mg (0.206 mmol, 1 equiv.) of 9-(3-(trifluoro-»^{4}-boranyl)propyl)-9*H*-carbazole, potassium salt was added 8 mg (0.010 mmol, 0.05 equiv.) PdCl$_2$(dppf)-CH$_2$Cl$_2$ and 201 mg (0.618 mmol, 3 equiv.) Cs$_2$CO$_3$ followed by 1.5 mL dry PhMe and 0.5 mL H$_2$O. The reaction was heated to 80°C for 12 hr, filtered through cotton and concentrated. Purification by silica gel flash chromatography eluting with 9 : 1 hex./EtOAc to 1 : 1 hex./EtOAc yielded 46 mg (45%) of the desired product as a yellow oil.

^{1}HNMR (300MHz, CDCl$_3$) δ 8.13 (m, 2H), 7.64 (m, 4H), 7.42 (m, 8H), 7.25 (m, 2H), 6.88 (s, 1H), 6.29 (d, *J* = 9.9, 1H), 5.68 (d, *J* = 9.9, 1H), 4.36 (t, *J* = 7.2, 2H), 2.65 (t, *J* = 8.1, 2H), 2.23 (m, 2H), 1.51 (s, 6H); ^{13}CNMR (75MHz, CDCl$_3$) δ 192.0, 150.9, 142.4, 140.6, 135.9, 135.6, 133.4, 131.3, 130.8, 130.3, 129.7, 129.2, 128.5, 128.1, 127.4, 125.9, 123.1, 122.4, 122.3, 120.6, 119.1, 108.9, 42.6, 32.5, 30.3, 28.5; HRMS (+TOF) 498.2433 calcd for C$_{35}$H$_{32}$NO$_2$ [M+H]$^+$, found: 498.2431; R$_f$ = 0.14 (9 : 1 hex./ EtOAc). Ref. BJE6-118
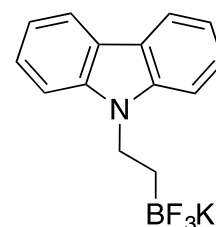

^{1}H NMR (300 MHz) CDCl$_3$

¹³C NMR (75 MHz) CDCl₃
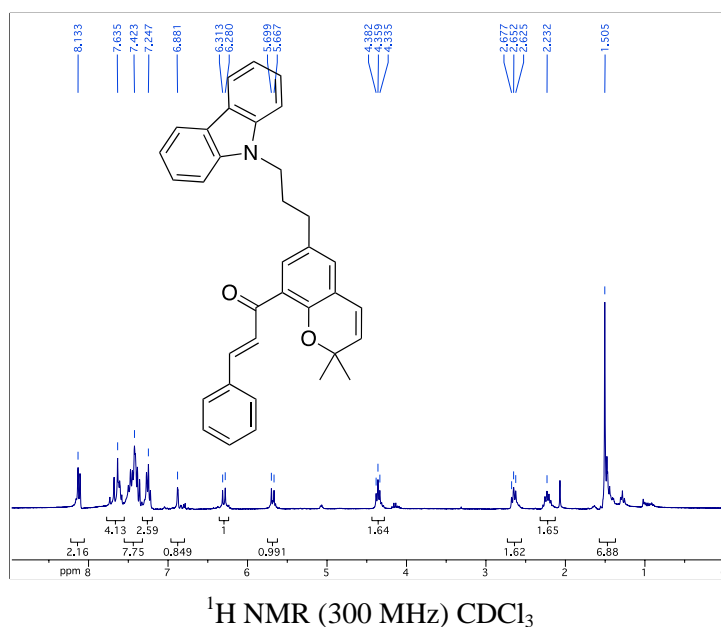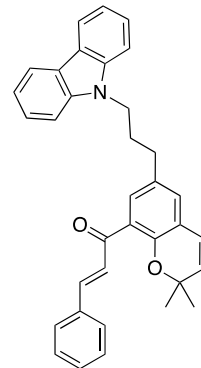
Synthesis of 1-(6-(3-(9*H*-carbazol-9-yl)propyl)-2,2-dimethylchroman-8-yl)-3-phenylpropan-1-one (BJE6-154): To a 10 mL round bottomed flask containing 20.0 mg (0.0401 mmol, 1 equiv.) (*E*)-1-(6-(3-(9*H*-carbazol-9-yl)propyl)-2,2-dimethyl-2*H*-chromen-8-yl)-3-phenylprop-2-en-1-one dissolved in 1 mL dry THF was added a spatula tip of 10% Pd/C. H₂ gas was bubbled through the mixture for 2 min and the reaction was stirred at ambient temperature under balloon pressure of H₂(g) for 2 hr before being filtered through celite and concentrated to yield 18 mg (90%) of the desired product as a colorless film. The NMR and mass spectra were fully consistent with the structure of the desired product.
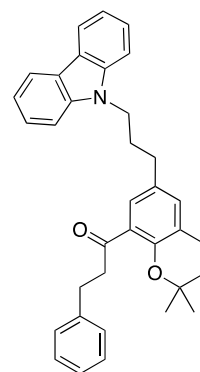
Preparation and Spectra for B106

Synthesis of Molander Salt *1* (9-(2-(trifluoro-»⁴-boranyl)ethyl)-9*H*-carbazole, potassium salt): To 4.11 mL (28.4 mmol, 5.5 equiv) 2,5-dimethylhexa-2,4-diene dissolved in 10.0 mL dry THF in a flame dried 100 mL round bottomed flask at 0°C was added 12.9 mL of a 1.0M solution of BH₃ dissolved in THF. The reaction was stirred at 0°C for 3hr before the addition of 1.00 g (5.17 mmol, 1 equiv.) 9-vinylcarbazole dissolved in a minimum amount of dry THF. The reaction was allowed to warm to ambient temperature with stirring over 3hr before being cooled to 0°C. To this mixture was added 1.7 mL deionized H₂O. The reaction was then stirred for 1.5hr at ambient temperature before the addition of 4.3 mL of a 37% solution of CH₂O(aq). The reaction was stirred at ambient temperature for 16hr before being added to brine, extracted into EtOAc, dried over Na₂SO₄, and concentrated. The resulting residue was taken up in a mixture of 17.0 mL acetone and 6.5 mL H₂O before the addition of 1.62 g (20.7 mmol, 4 equiv.) KHF₂. The resulting mixture was stirred at ambient temperature for 4hr before being concentrated under reduced pressure. The resulting residue was recrystallized from acetone and Et₂O yielding 1.06 g (68%) of a white crystalize solid which was utilized below without characterization or further purification.
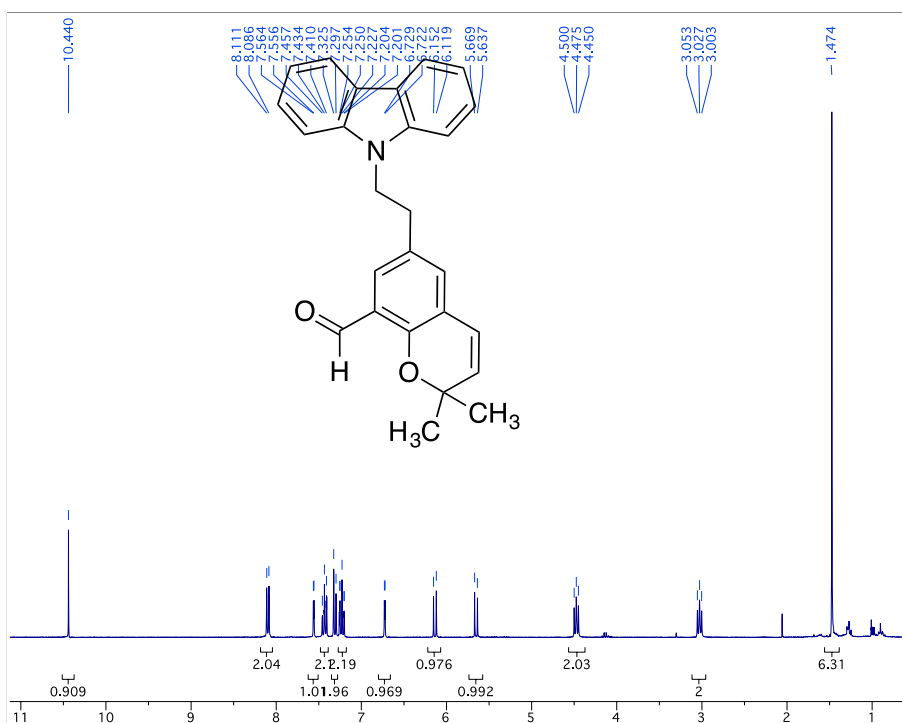
Synthesis of 6-(2-(9*H*-carbazol-9-yl)ethyl)-2,2-dimethyl-2*H*-chromene-8-carbaldehyde (BJE6-106): To a flame dried 10 mL round bottomed flask containing 57.0mg (0.213 mmol, 1 equiv.) 6-bromo-2,2-dimethyl-2*H*-chromene-8-carbaldehyde, 64.0mg (0.213 mmol, 1 equiv.) Molander Salt *1* (9-(2-(trifluoro-»[4]-boranyl)ethyl)-9*H*-carbazole, potassium salt), 8.0 mg (0.011 mmol, 0.05 equiv.) PdCl$_2$(dppf)-CH$_2$Cl$_2$, and 208 mg (0.639 mmol, 3 equiv.) anhydrous Cs$_2$CO$_3$ was added 1.5 mL dry toluene and 0.5 mL deionized H$_2$O. The reaction was heated to 80°C for 16hr, added to brine, extracted into EtOAc, dried over Na$_2$SO$_4$, and concentrated under reduced pressure. The resulting residue was purified by silica gel flash chromatography eluting with 19 : 1 hex./EtOAc to 1 : 1 hex./EtOAc yielding 36 mg (44%) of the desired product as a colorless oil.

^{1}HNMR (300MHz, CDCl$_3$) δ 10.44 (s, 1H), 8.09 (d, *J* = 7.5, 2H), 7.56 (d, *J* = 2.4, 1H), 7.43 (t, *J* = 6.9, 2H), 7.32 (t, *J* = 8.4, 2H), 7.23 (t, *J* = 6.9, 2H), 6.73 (d, *J* = 2.1, 1H), 6.14 (d, *J* = 9.9, 1H), 5.65 (d, *J* = 9.6, 1H), 4.48 (t, *J* = 7.5, 2H), 3.03 (t, *J* = 7.5, 2H), 1.47 (s, 6H); ^{13}CNMR (75MHz, CDCl$_3$) δ 189.5, 155.4, 140.3, 133.0, 131.8, 131.0, 126.8, 125.9, 124.3, 123.1, 122.8, 121.5, 120.6, 119.2, 117.8, 108.8, 44.8, 34.3, 28.3; IR (NaCl, film) 2861, 1679 cm^{-1}; HRMS (+TOF) 382.1802 calcd for C$_{26}$H$_{23}$NO$_2$ [M+H]$^+$, found: 382.1799; R$_f$ = 0.25 (9 : 1 hex./ EtOAc).

Ref. BJE6-106

^{1}H NMR Spectrum (300MHz, CDCl$_3$)

^{13}C NMR (75 MHz) CDCl$_3$

11
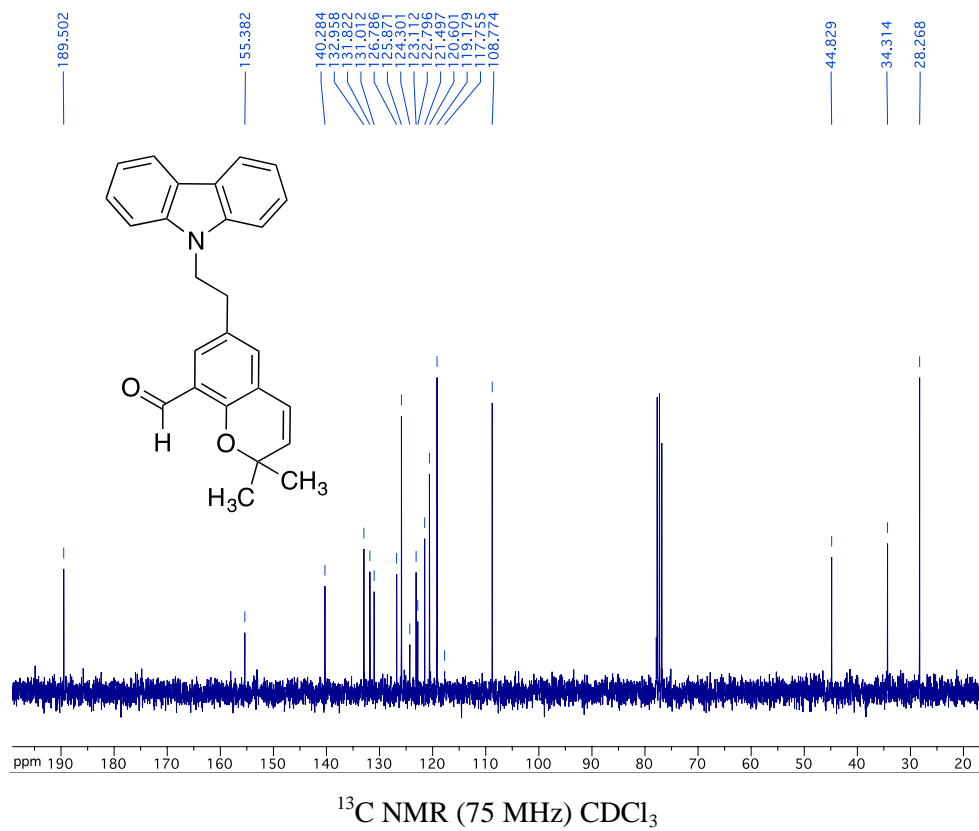
Pharmacophore Modeling of Novel PKC–delta inhibitors.

Numerous docking studies were conducted to predict how mallotoxin/rottlerin binds to PKC-delta. Since a structure of PKC-delta was not available, rottlerin was docked into the catalytic binding site of several different PKC crystal structures. The structure of PKC-theta complexed with staurosporine (pdb code 1XJD) was selected as the most suitable model.

The TFIT program within FLO molecular modeling software [1] was used to construct pharmacophores, as we have previously described.[2-4] An ensemble of low energy conformers was computed for mallotoxin/rottlerin and staurosporine, optimized to simultaneously minimize the internal energy and maximize the match of chemically similar atoms (**Fig. S1**). There has been excellent agreement between the bio-active conformations of inhibitors calculated by TFIT and that found experimentally.[5,6]
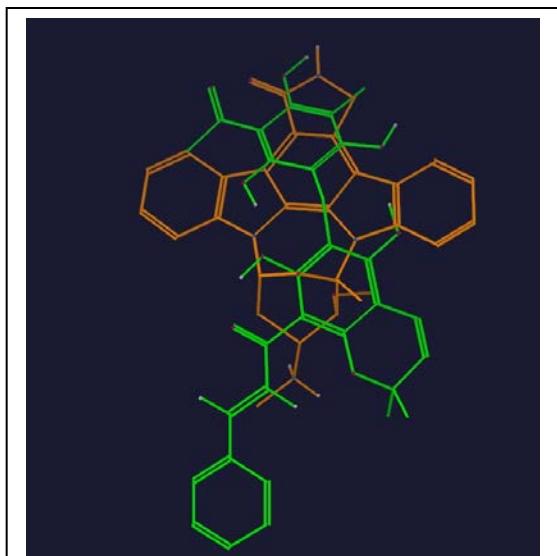
Fig. S1: "Best-fit" superimposition of staurosporine (brown and mallotoxin/rottlerin (green) structures using TFIT.

Dockmin+ is an energy minimization procedure developed for the FLO+ molecular modeling package, which uses a molecular mechanics force field to find the nearest minimum to the original structure. Then dockmin+ uses a scoring function to evaluate the ligand/binding site interactions. The scoring function used by the FLO+ suite of programs uses a potential function containing the following terms: Contact Energy; Hydrogen Bond energy, Entropy, Polar Desolvation, Internal Free Energy,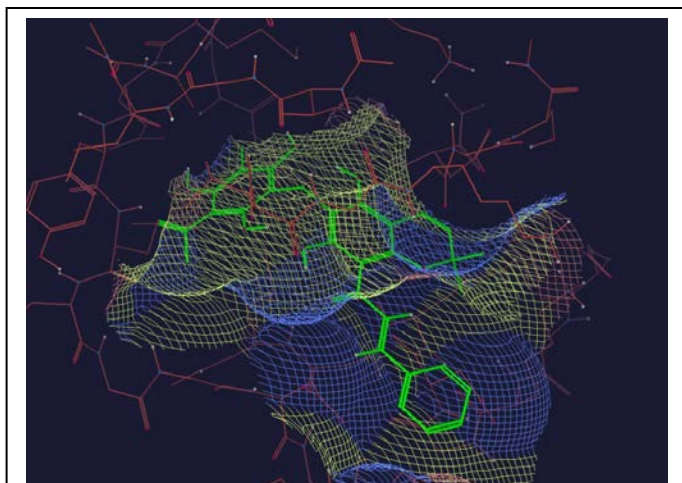 and Repulsion. It is known from crystal structures of many kinase/inhibitor complexes that the kinase active site is flexible. Therefore, regions known to be flexible were allowed to be free during the docking procedures. Eventually a reasonable binding mode of rottlerin bound to PKC-delta was obtained (**Fig. S2**). However, because rottlerin is structurally so different from typical kinase inhibitors whose binding mode is now know from x-ray data, the binding mode of rottlerin obtained in this study was taken as an initial hypothesis.

Figure S2: Model of rottlerin bound to PKC-delta

Lzm is the graphical interface used in part of the FLO+ molecular modeling

suite. Mallotoxin/rottlerin and staurosporine were evaluated using the solvent accessible surface and the atom scores. Looking at a ligand and the solvent accessible surface mesh it becomes immediately obvious to what extent the ligand occupies the binding site and gives a sense of the quality of the protein/ligand interactions. Ligand atoms in ideal van der Waals contact with the binding site atoms lie on or near the surface mesh. Ligand atoms that form hydrogen bonds with binding site atoms, penetrate the mesh.[7] The atom scores assign a numerical energy to each ligand atom showing the contribution that atom makes to the total predicted binding energy. The solvent accessible surface of the mallotoxin-rottlerin binding site is shown in a mesh in **Fig. S3**. It is computed at the van der Waals radius of the binding site atoms plus a probe distance of 1.4 Angstroms.

Figure S3: Model of mallotoxin/rottlerin docked in PKC-delta with the solvent accessible surface of the binding site shown as a mesh.

Five molecules were designed using the PKC-delta model developed from the rottlerin docking studies. The strategy was to retain most of the "bottom" part of rottlerin (see figures below) which is assumed to give rottlerin its specificity but to vary the "head group" which is assumed to bind to the hinge region of the kinase active site. Numerous "head groups" from known potent kinase inhibitors were tested in the PKC-theta model, including staurosporine, purine-based inhibitors, a CDK2 inhibitor (pdb code: 1FVT) and an aurora kinase inhibitor (pdb code 2F4J). The criteria for selection was that the resulting molecule should form favorable interactions with the hinge region while the "bottom part" retained interactions with the binding site similar to that of staurosporine (from the x-ray crystal structure) and rottlerin (from our docking studies).

In Structures 1 and 2, the head group resembled that of staurosporine and other bisindoyl maleimide inhibitors. Ease of synthesis was a major factor in the design of this head group.

Modifications of these structures that allowed for easier synthesis produced the 2nd and 3rd generation PKCδ inhibitors described previously[8] and in this report.

"Head group"

"Bottom part"
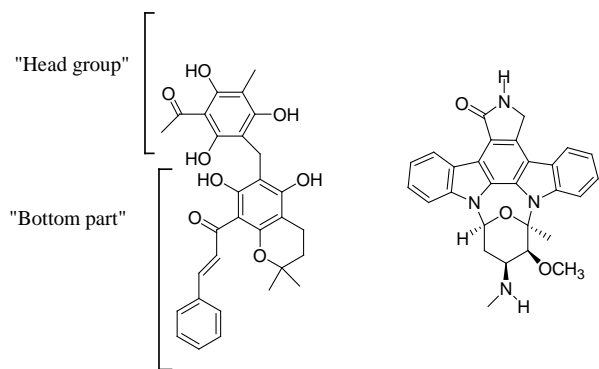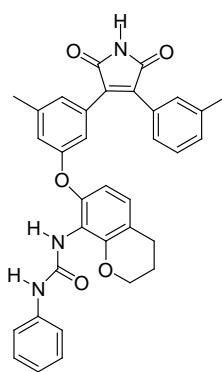
Rottlerin   Staurosporine
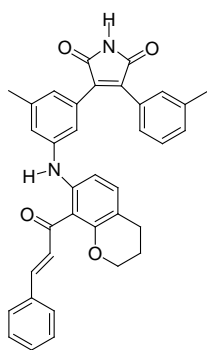
Structure 1   Structure 2

References

1. McMartin, C. and Bohacek, R. S. (1995) Flexible matching of test ligands to a 3D pharmacophore using a molecular superposition force field: comparison of predicted and experimental conformations of inhibitors of three enzymes, *J Comput. Aided Mol. Des 9*, 237-250.

2. Bohacek, R., Boosalis, M. S., McMartin, C., Faller, D. V., and Perrine, S. P. (2006) Identification of novel small-molecule inducers of fetal hemoglobin using pharmacophore and 'PSEUDO' receptor models, *Chem. Biol. Drug Des. 67*, 318-328.

3. Boosalis, M. S., Castaneda, S. A., Trudel, M., Mabaera, R., White, G. L., Lowrey, C. H., Emery, D. W., Mpollo, M. S., Shen, L., Wargin, W. A., Bohacek, R., Faller, D. V., and Perrine, S. P. (2011) Novel therapeutic candidates, identified by molecular modeling, induce gamma-globin gene expression in vivo, *Blood Cells Mol. Dis. 47*, 107-116.

4. Perrine, S. P., Castaneda, S. A., Boosalis, M. S., White, G. L., Jones, B. M., and Bohacek, R. (2005) Induction of fetal globin in beta-thalassemia: Cellular obstacles and molecular progress, *Ann. N. Y. Acad. Sci. 1054*, 257-265.

5. McMartin, C. and Bohacek, R. S. (1997) QXP: powerful, rapid computer algorithms for structure-based drug design, *J Comput. Aided Mol. Des 11*, 333-344.

6. Bohacek, R., DeLombaert, S., McMartin, C., Priestle, J., and Grutter, M. (1996) Three-dimensional models of ACE and NEP Inhibitors and their use in the design of potent dual ACE/NEP inhibitors, *J. Am. Chem. Soc. 118*, 8231-8249.

7. Bohacek, R. S. and McMartin, C. (1992) Definition and display of steric, hydrophobic, and hydrogen-bonding properties of ligand binding sites in proteins using Lee and Richards accessible surface: validation of a high-resolution graphical tool for drug design, *J Med. Chem. 35*, 1671-1684.

8. Chen, Z., Forman, L. W., Miller, K. A., English, B., Takashima, A., Bohacek, R. A., Williams, R. M., and Faller, D. V. (2011) The proliferation and survival of human neuroendocrine tumors is dependent upon protein kinase C-delta, *Endocr. Relat Cancer 18*, 759-771.

Supplemental Table 1:

PKCδ Inhibitory Activity of BJE6 compounds

Compound	IC_{50} (*in vitro*)[1]			IC_{50} (*in culture*)[3]
	PKCδ IC_{50} (µM)	PKCα IC_{50} (µM)	PKCδ/PKCα (IC_{50} ratio)[2]	
Rottlerin	4.4	75	28	10
KAM-1	3.6	177	56	5
B058	5.8	NA[4]	-	>50
B071	3	NA	-	>100
B095	8	NA	-	>100
B097	9.5	NA	-	>100
B106	0.08	15	200	1
B108	3	NA	-	>100
B109	0.09	75	800	>100
B111	2.5	25	100	40
B112	6	NA	-	>50
B117	4.5	NA	-	>100
B118	10	NA	-	>100
B121	4	NA	-	>100
B125	0.25	20	800	>100
B128	6.5	NA	-	>100
B129	6.5	NA	-	>50
B130	4	NA	-	40
B131	10	NA	-	>100
B136	14	NA	-	>100
B137	3	NA	-	>100
B141	4.8	NA	-	>50
B142	3.5	NA	-	>100
B143	6	NA	-	>100
B146	5	NA	-	>100
B147	5.8	NA	-	20
B148	4	NA	-	>100
B149	0.31	>300	>1000	20
B150	0.625	500	800	30
B151	< 0.05	50	>1000	>100
B152	< 0.05	50	>1000	>100
B153	3	NA	-	>100
B154	23	NA	-	>100

B155	3	NA	-	>100
B156	7.5	NA	-	>100
B157	5	NA	-	>100
B158	4.5	NA	-	>100
B159	7	NA	-	40

[1] IC_{50} measured using recombinant PKCδ or PKCα

[2] Ratio of PKCδ IC_{50} to PKCα IC_{50}

[3] IC_{50} for cytotoxicity on a KRAS-mutant cell line H460.

[4] NA = not assayed (PKCα inhibitory activity was only assayed on compounds with an IC_{50} for PKCδ of <2.5 μM).

METHODS

Reagents. Rottlerin/mallotoxin, PLX4032 (vemurafenib), propidium iodide, and RNase A were purchased from Axxora, LC Labs, Sigma-Aldrich and Fisher Scientific, respectively. Z-VAD-FMK was purchased from R&D Systems and Enzo Life Sciences. Antibodies against phospho-SAPK/JNK (Thr183/Tyr185) (#4668), SAPK/JNK (#9252), phospho-Histone H2A.X (Ser 139) (#2577), Histone H2A (#2578), phospho-SEK1/MKK4) (#4514), SEK1/MKK4 (#9152), phospho-MKK7 (Ser271/Thr275) (#4171), MKK7 (#4172), phospho-c-Jun (Ser63) (#9261), c-Jun (#9165), phospho-ERK1/2 (Thr202/Tyr204) (#4370), phospho-p38 (Thr180/Tyr182) (#4511) and p38 (#9212) were purchased from Cell Signaling Technologies. Antibodies against ERK1 (K-23) and PKCδ (#610398) were purchased from Santa Cruz Biotechnology and BD Biosciences, respectively. Antibodies against α-Tubulin (#T6074), β-Actin (#A1978) and GAPDH (#G8795) were purchased from Sigma-Aldrich. ON-TARGETplus SMART pool siRNA against JNK1 (L-003514), JNK2 (L-003505), H2AX (L-011682) and non-targeting scrambled siRNA #1 (D-001810-01) were purchased from Dharmacon. Silencer Select siRNA against PKCδ (PRKCD) was purchased from Life Technologies.

Synthetic Methods. BJE6-106 and BJE6-154 were synthesized using Molander trifluorborate coupling chemistry,[1,2] with the details and NMR spectra presented elsewhere in Supplemental Information. Briefly: unless otherwise noted, all reagents were obtained from commercial suppliers and were used without further purification. All air or moisture sensitive reactions were performed under a positive pressured of argon in flame-dried glassware. Tetrahydrofuran (THF), toluene, diethyl ether (Et$_2$O), dichloromethane, benzene (PhH), acetonitrile (MeCN), triethylamine (NEt$_3$), pyridine, diisopropyl amine, methanol (MeOH), dimethylsulfoxide (DMSO), and N,N-dimethylformamide (DMF) were obtained from a dry solvent system (Ar degassed solvents delivered through activated alumina columns, positive pressure of argon). Column chromatography was performed on Merck silica gel Kieselgel 60 (230-400 mesh). ^{1}HNMR and ^{13}CNMR spectra were recorded on Varian 300, or 400 MHz spectrometers. Chemical shifts are reported in ppm relative to CHCl$_3$ at δ 7.27 (^{1}HNMR) and δ 77.23 (^{13}CNMR). Mass spectra were obtained on Fisons VG Autospec. IR spectra were obtained from thin films on a NaCl plate using a Perkin-Elmer 1600 series FT-IR spectrometer.

Synthesis of Molander Salt (4): (9-(2-(trifluoro-»^{4}-boranyl)ethyl)-9H-carbazole, potassium salt): To 4.11 mL (28.4 mmol, 5.5 equiv) 2,5-dimethylhexa-2,4-diene dissolved in 10.0 mL dry THF in a flame dried 100 mL round bottomed flask at 0°C was added 12.9 mL of a 1.0M solution of BH$_3$ dissolved in THF. The reaction was stirred at 0°C for 3 hr before the addition of 1.00 g (5.17 mmol, 1 equiv.) 9-vinylcarbazole dissolved in a minimum amount of dry THF. The reaction was allowed to warm to ambient temperature with stirring over 3 hr before being cooled to 0°C. To this mixture was added 1.7 mL deionized H$_2$O. The reaction was then stirred for 1.5 hr at ambient temperature before the addition of 4.3 mL of a 37% solution of CH$_2$O$_{(aq)}$. The reaction was stirred at ambient temperature for 16 hr before being added to brine, extracted into EtOAc, dried over Na$_2$SO$_4$, and concentrated. The resulting residue was taken up in a mixture of 17.0 mL acetone and 6.5 mL H$_2$O before the addition of 1.62 g (20.7 mmol, 4 equiv.) KHF$_2$. The resulting mixture was stirred at ambient temperature for 4hr before

being concentrated under reduced pressure. The resulting residue was recrystallized from acetone and Et$_2$O yielding 1.06 g (68%) of a white crystalline solid (**4**) (see Figure 2A, Scheme 1) which was utilized below without characterization or further purification.

Synthesis of 6-bromo-2,2-dimethyl-2H-chromene-8-carbaldehyde (2): To a 100 mL flame dried round bottomed flask containing 5.54 mL (57.2 mmol, 1.15 equiv) 2-methylbut-3-yn-2-ol dissolved in 50 mL dry MeCN at 0°C was added 11.1 mL (74.6 mmol, 1.5 equiv.) DBU followed by the dropwise addition of 8.08 mL (57.2 mmol, 1.15 equiv.) freshly distilled TFAA. The reaction was stirred at 0°C for 30 min before being added via cannula to a 250 mL round bottomed flask containing 10.0 g (49.7 mmol, 1 equiv.) 5-bromo-2-hydroxybenzaldehyde (**1**), 9.65 mL (64.6 mmol, 1.3 equiv.) DBU, and 8.5 mg (0.050 mmol, 0.001 equiv.) CuCl$_2$-2H$_2$O dissolved in dry MeCN at -5°C. The reaction was stirred for 16hr at ambient temperature before being concentrated under reduced pressure. The resulting residue was taken up in EtOAc, washed once with H$_2$O, once with 1 M HCl, and once with brine before being dried over Na$_2$SO$_4$, and concentrated. This residue was subjected to silica gel flash chromatography eluting with 19:1 to 4:1 hex/EtOAc to yield 11.17g (84%) of the desired product (**2**) as a pale yellow solid.

^{1}HNMR (300MHz, CDCl$_3$) δ 10.27 (s, 1H), 7.88 (s, 1H), 7.55 (d, *J* = 8.4, 1H), 7.38 (d, *J* = 8.4, 1H), 2.63 (s, 1H), 1.67 (s, 6H);); ^{13}CNMR (75MHz, CDCl$_3$) δ 188.8, 157.4, 137.5, 130.9, 130.2, 122.8, 116.1, 84.7, 76.3, 74.5, 29.7; IR (NaCl, film) 3294, 1687, 1588, 1471 cm^{-1}; HRMS (+TOF) 267.0015 calcd for C$_{12}$H$_{12}$BrO$_2$ [M+H]$^+$, found: 267.0016; R$_f$ = 0.38 (9 : 1 hex./ EtOAc).

Synthesis of 6-bromo-2,2-dimethyl-2H-chromene-8-carbaldehyde (3): To an 80 mL microwave reaction vessel containing 4.00 g (14.8 mmol, 1 equiv.) 5-bromo-2-((2-methylbut-3-yn-2-yl)oxy)benzaldehyde (**2**) dissolved in 60 mL dry MeCN was added 66.0 mg (0.300 mmol, 0.02 equiv.) BHT. The reaction was heated in a microwave reactor to 180°C for 20 min before being concentrated and purified by silica gel flash chromatography eluting with 19:1 hex./EtOAc to yield 2.10 g (53%) of the desired product (**3**) as a yellow oil.

^{1}HNMR (300MHz, CDCl$_3$) δ 10.35 (s, 1H), 7.73 (d, *J* = 2.7, 1H), 7.27 (dd, *J* = 2.7, 0.3, 1H), 6.29 (d, *J* = 9.9, 1H), 5.75 (d, *J* = 9.9, 1H), 1.50 (s, 3H); ^{13}CNMR (75MHz, CDCl$_3$) δ 188.0, 155.3, 134.3, 132.8, 129.4, 125.6, 124.6, 120.8, 113.4, 78.4, 28.4; IR (NaCl, film) 2863, 1678, 1574 cm^{-1}; HRMS (+TOF) 267.0015 calcd for C$_{12}$H$_{12}$BrO$_2$ [M+H]$^+$, found: 267.0012; R$_f$ = 0.33 (9:1 hex./ EtOAc).

Synthesis of 6-(2-(9H-carbazol-9-yl)ethyl)-2,2-dimethyl-2H-chromene-8-carbaldehyde (B106): To a flame dried 10 mL round bottomed flask containing 57.0mg (0.213 mmol, 1 equiv.) 6-bromo-2,2-dimethyl-2*H*-chromene-8-carbaldehyde (**3**), 64.0mg (0.213 mmol, 1 equiv.) Molander Salt (**4**) (9-(2-(trifluoro-»^{4}-boranyl)ethyl)-9*H*-carbazole, potassium salt), 8.0 mg (0.011 mmol, 0.05 equiv.) PdCl$_2$(dppf)-CH$_2$Cl$_2$, and 208 mg (0.639 mmol, 3 equiv.) anhydrous Cs$_2$CO$_3$ was added 1.5 mL dry toluene and 0.5 mL deionized H$_2$O. The reaction was heated to 80°C for 16hr, added to brine, extracted into EtOAc, dried over Na$_2$SO$_4$, and concentrated under reduced pressure. The resulting residue was purified by silica gel flash chromatography eluting with 19 : 1 hex./EtOAc to 1 : 1 hex./EtOAc yielding 36 mg (44%) of the desired product (**B106**) as a colorless oil.

^{1}HNMR (300MHz, CDCl$_3$) δ 10.44 (s, 1H), 8.09 (d, *J* = 7.5, 2H), 7.56 (d, *J* = 2.4, 1H), 7.43 (t, *J* = 6.9, 2H), 7.32 (t, *J* = 8.4, 2H), 7.23 (t, *J* = 6.9, 2H), 6.73 (d, *J* = 2.1, 1H), 6.14

(d, J = 9.9, 1H), 5.65 (d, J = 9.6, 1H), 4.48 (t, J = 7.5, 2H), 3.03 (t, J = 7.5, 2H), 1.47 (s, 6H); ^{13}CNMR (75MHz, CDCl$_3$) δ 189.5, 155.4, 140.3, 133.0, 131.8, 131.0, 126.8, 125.9, 124.3, 123.1, 122.8, 121.5, 120.6, 119.2, 117.8, 108.8, 44.8, 34.3, 28.3; IR (NaCl, film) 2861, 1679 cm^{-1}; HRMS (+TOF) 382.1802 calcd for C$_{26}$H$_{23}$NO$_2$ [M+H]$^+$, found: 382.1799; R$_f$ = 0.25 (9:1 hex./ EtOAc).
Ref. BJE6-106

Cell culture, siRNA transfection, plasmid stable transfection & PLX4032-resistant sub cell lines. Human melanoma cell lines WM1366, WM1361A, WM852, FM28, FM6, SKMEL2 and SKMEL28, SBcl2, A375 and SKMEL5 were originally obtained from ATCC or the European Searchable Tumour Line Database (ESTDAB) and authenticated by these agencies using DNA fingerprinting quality control. Their respective RAS or BRAF mutations previously identified in the literature were verified by sequencing. SBcl2 and A375 and its derivative lines were maintained in Dulbecco's modified Eagle's medium (DMEM) supplemented with 10% fetal bovine serum. SKMEL5 was maintained in minimum essential medium (MEM) supplemented with 10% fetal bovine serum. All media were additionally supplemented with L-glutamine 2 mM, penicillin 100 units/ml and streptomycin 100 μg/ml. Primary human melanocytes were grown in medium 254 (Invitrogen).

siRNA transfection was performed by reverse transcription using Lipofectamine RNAiMax (Invitrogen) according to the product protocol, and media was changed the following day of transfection. PLX4032-resistant cell sublines were established according to the method described in [3]. Briefly, A375 and SKMEL5 cells were plated at low cell density and treated with PLX4032 at 1 μM or 0.5 μM, respectively. The concentration of PLX4032 was gradually increased up to 4μM (A375) or 2 μM (SKMEL5) over the course of a 3-4 week period, and clonal colonies were picked. Derived sublines of A375 and SKMEL5 were maintained in PLX4032-containing medium at 1-2 μM (A375) or 0.5 μM (SKMEL5).

Cell proliferation & Caspase assays. Cell proliferation assays (MTS assay) and caspase assays were performed with CellTiter 96 AQueous Non-Radioactive Cell Proliferation Assay kit and Caspase-Glo 3/7 Assay Systems (Promega) according to the manufacturers' protocols. Briefly, for the assays employing inhibitors, cells were plated in a 96-well plate (500-4000 cells per well depending on the cell lines and duration of the experiment), exposed to inhibitors 24 hr later and cultured for the durations indicated in the individual figure legends. For the assays employing siRNA, cells were plated the day of siRNA transfection, cultured for the duration indicated in the figure legends, and if indicated, treated with inhibitors or vehicle. After the indicated treatment times, assay reagent was added and cell plates were incubated for 1 hr at 37°C (MTS assay) or 30 min at RT (caspase assay). Absorbance at 490 nm (MTS assay) or luminescence (caspase assay) were measured using microplate readers for quantification. Human primary melanocytes were plated in triplicate on a 12-well plate. Test compounds at different concentrations or vehicle (DMSO) were added on the second day, and viable cells were enumerated 72 rh after addition of compounds. Cell survival was evaluated against the DMSO-treated controls.

Clonogenic colony assay. For the experiments depicted in Figure 2E, cells were treated with drugs for the time indicated in the figure, and then the same number of viable cells from each treatment was replated at low cell density and cultured in medium without inhibitors for 8 days, at which time colony formation was quantitated. Cell colonies were stained with ethidium bromide for visualization on an ImageQuant LAS 4000 (GE Healthcare) and colonies enumerated.

DNA fragmentation assays. Cells were harvested and fixed in 1 ml of a 35% ethanol/DMEM solution at 4°C for 30 min. Cells were then stained with a solution containing 25 μg/ml of propidium iodide/ml and 50 μg/ml of RNase A in PBS and incubated in the dark at 37°C for 30 min for flow cytometric analysis. The proportion of cells in the sub-G1 population, which contain a DNA content of less than 2N (fragmented DNA), was measured as an indicator of apoptosis.

Immunoblotting. Whole cell lysates were prepared in a buffer containing 20 mM Hepes (pH 7.4), 10% glycerol, 2 mM EDTA, 2 mM EGTA, 50 mM β-glycerophosphate and 1% Triton-X100, 1 mM dithiothreitol (DTT) and 1 mM sodium vanadate, supplemented with Halt Protease and Phosphatase Inhibitor Cocktail (100X) (Thermo Scientific). Lysates were subjected to SDS-PAGE and transferred to nitrocellulose membranes. Membranes were blocked at RT for 1-1.5 hr with 5% BSA or 5% non-fat dry milk in TBS-T (10 mM Tris [pH 7.5], 100 mM NaCl, 0.1% Tween 20) and probed with the appropriate primary antibodies (1:500-1:10,000) overnight. After washing, the blots were incubated with horseradish peroxidase-conjugated secondary antibodies (1:2000-1:10,000) and visualized using the ECL system (GE Healthcare) on an ImageQuant LAS 4000. As loading controls, either α-tubulin, β-actin or GAPDH was selected, depending on the molecular weight of the proteins being studied in each experiment or the acrylamide percentage of the gels. In some experiments, photographs of the same gel processed from the same experiment, are presented in two separate panels. In some cases, lanes not directly relevant to the particular panel have been deleted for clarity, and this is indicated in the respective figure legends.

Quantitative real-time PCR. RNA was extracted with RNeasy Mini kit purchased (Qiagen) according to the manufacturer's protocol. 1 μg of RNA was used to synthesize cDNA in a 20 μl reaction volume employing SuperScript III First-Strand Synthesis System (Invitrogen) or QuaniTect Reverse Transcription Kit (Qiagen) according to the product protocol. Quantitative real-time PCR was performed with SYBR Green PCR Master Mix (Applied Biosystems (now under Life Technologies)) according to the manufacturer's protocol. Briefly, cDNA was diluted to a final concentration of 25 ng per reaction, added to a primer set (5 μM) and SYBR Green PCR Master Mix to a final volume of reaction mixture of 20 μl, and run on an Applied Biosystems 7500 Fast Real-Time PCR system using the following thermal cycling protocol: 50°C for 2 min, 95°C for 10 min, and 40 cycles of 95°C for 15 sec and 60°C for 1 min. The relative amount of an mRNA of interest was calculated by normalizing the Ct value of the mRNA to the Ct of the internal control (β-actin). Primer sequences were: H2AX Forward: 5'-CAACAAGAAGACGCGAATCA-3', H2AX Reverse: 5'-CGGGCCCTCTTAGTACTCCT-3', β-actin Forward: 5'-

GCTCGTCGTCGACAACGGCTC-3', β-actin Reverse: 5'-CAAACATGATCTGGGTCATCTTCTC-3'

References

1. Molander, G. A. and Vargas, F. (2007) Beta-aminoethyltrifluoroborates: efficient aminoethylations via Suzuki-Miyaura cross-coupling, *Org. Lett. 9*, 203-206.

2. Molander, G. A., Yun, C. S., Ribagorda, M. et al. (2003) B-alkyl suzuki-miyaura cross-coupling reactions with air-stable potassium alkyltrifluoroborates, *J Org. Chem. 68*, 5534-5539.

3. Nazarian, R., Shi, H., Wang, Q. et al. (2010) Melanomas acquire resistance to B-RAF(V600E) inhibition by RTK or N-RAS upregulation, *Nature. 468*, 973-977.

METHODS

Reagents. Rottlerin/mallotoxin, PLX4032 (vemurafenib), propidium iodide, and RNase A were purchased from Axxora, LC Labs, Sigma-Aldrich and Fisher Scientific, respectively. Z-VAD-FMK was purchased from R&D Systems and Enzo Life Sciences. Antibodies against phospho-SAPK/JNK (Thr183/Tyr185) (#4668), SAPK/JNK (#9252), phospho-Histone H2A.X (Ser 139) (#2577), Histone H2A (#2578), phospho-SEK1/MKK4) (#4514), SEK1/MKK4 (#9152), phospho-MKK7 (Ser271/Thr275) (#4171), MKK7 (#4172), phospho-c-Jun (Ser63) (#9261), c-Jun (#9165), phospho-ERK1/2 (Thr202/Tyr204) (#4370), phospho-p38 (Thr180/Tyr182) (#4511) and p38 (#9212) were purchased from Cell Signaling Technologies. Antibodies against ERK1 (K-23) and PKCδ (#610398) were purchased from Santa Cruz Biotechnology and BD Biosciences, respectively. Antibodies against α-Tubulin (#T6074), β-Actin (#A1978) and GAPDH (#G8795) were purchased from Sigma-Aldrich. ON-TARGETplus SMART pool siRNA against JNK1 (L-003514), JNK2 (L-003505), H2AX (L-011682) and non-targeting scrambled siRNA #1 (D-001810-01) were purchased from Dharmacon. Silencer Select siRNA against PKCδ (PRKCD) was purchased from Life Technologies.

Synthetic Methods. BJE6-106 and BJE6-154 were synthesized using Molander trifluorborate coupling chemistry,[1,2] with the details and NMR spectra presented elsewhere in Supplemental Information. Briefly: unless otherwise noted, all reagents were obtained from commercial suppliers and were used without further purification. All air or moisture sensitive reactions were performed under a positive pressured of argon in flame-dried glassware. Tetrahydrofuran (THF), toluene, diethyl ether (Et$_2$O), dichloromethane, benzene (PhH), acetonitrile (MeCN), triethylamine (NEt$_3$), pyridine, diisopropyl amine, methanol (MeOH), dimethylsulfoxide (DMSO), and N,N-dimethylformamide (DMF) were obtained from a dry solvent system (Ar degassed solvents delivered through activated alumina columns, positive pressure of argon). Column chromatography was performed on Merck silica gel Kieselgel 60 (230-400 mesh). ^{1}HNMR and ^{13}CNMR spectra were recorded on Varian 300, or 400 MHz spectrometers. Chemical shifts are reported in ppm relative to CHCl$_3$ at δ 7.27 (^{1}HNMR) and δ 77.23 (^{13}CNMR). Mass spectra were obtained on Fisons VG Autospec. IR spectra were obtained from thin films on a NaCl plate using a Perkin-Elmer 1600 series FT-IR spectrometer.

Synthesis of Molander Salt (4): (9-(2-(trifluoro-»^{4}-boranyl)ethyl)-9H-carbazole, potassium salt): To 4.11 mL (28.4 mmol, 5.5 equiv) 2,5-dimethylhexa-2,4-diene dissolved in 10.0 mL dry THF in a flame dried 100 mL round bottomed flask at 0°C was added 12.9 mL of a 1.0M solution of BH$_3$ dissolved in THF. The reaction was stirred at 0°C for 3 hr before the addition of 1.00 g (5.17 mmol, 1 equiv.) 9-vinylcarbazole dissolved in a minimum amount of dry THF. The reaction was allowed to warm to ambient temperature with stirring over 3 hr before being cooled to 0°C. To this mixture was added 1.7 mL deionized H$_2$O. The reaction was then stirred for 1.5 hr at ambient temperature before the addition of 4.3 mL of a 37% solution of CH$_2$O$_{(aq)}$. The reaction was stirred at ambient temperature for 16 hr before being added to brine, extracted into EtOAc, dried over Na$_2$SO$_4$, and concentrated. The resulting residue was taken up in a mixture of 17.0 mL acetone and 6.5 mL H$_2$O before the addition of 1.62 g (20.7 mmol, 4 equiv.) KHF$_2$. The resulting mixture was stirred at ambient temperature for 4hr before

being concentrated under reduced pressure. The resulting residue was recrystallized from acetone and Et$_2$O yielding 1.06 g (68%) of a white crystalline solid (**4**) (see Figure 2A, Scheme 1) which was utilized below without characterization or further purification.

Synthesis of 6-bromo-2,2-dimethyl-2H-chromene-8-carbaldehyde (2): To a 100 mL flame dried round bottomed flask containing 5.54 mL (57.2 mmol, 1.15 equiv) 2-methylbut-3-yn-2-ol dissolved in 50 mL dry MeCN at 0°C was added 11.1 mL (74.6 mmol, 1.5 equiv.) DBU followed by the dropwise addition of 8.08 mL (57.2 mmol, 1.15 equiv.) freshly distilled TFAA. The reaction was stirred at 0°C for 30 min before being added via cannula to a 250 mL round bottomed flask containing 10.0 g (49.7 mmol, 1 equiv.) 5-bromo-2-hydroxybenzaldehyde (**1**), 9.65 mL (64.6 mmol, 1.3 equiv.) DBU, and 8.5 mg (0.050 mmol, 0.001 equiv.) CuCl$_2$-2H$_2$O dissolved in dry MeCN at -5°C. The reaction was stirred for 16hr at ambient temperature before being concentrated under reduced pressure. The resulting residue was taken up in EtOAc, washed once with H$_2$O, once with 1 M HCl, and once with brine before being dried over Na$_2$SO$_4$, and concentrated. This residue was subjected to silica gel flash chromatography eluting with 19:1 to 4:1 hex/EtOAc to yield 11.17g (84%) of the desired product (**2**) as a pale yellow solid.

^{1}HNMR (300MHz, CDCl$_3$) δ 10.27 (s, 1H), 7.88 (s, 1H), 7.55 (d, J = 8.4, 1H), 7.38 (d, J = 8.4, 1H), 2.63 (s, 1H), 1.67 (s, 6H);); ^{13}CNMR (75MHz, CDCl$_3$) δ 188.8, 157.4, 137.5, 130.9, 130.2, 122.8, 116.1, 84.7, 76.3, 74.5, 29.7; IR (NaCl, film) 3294, 1687, 1588, 1471 cm^{-1}; HRMS (+TOF) 267.0015 calcd for C$_{12}$H$_{12}$BrO$_2$ [M+H]$^+$, found: 267.0016; R$_f$ = 0.38 (9 : 1 hex./ EtOAc).

Synthesis of 6-bromo-2,2-dimethyl-2H-chromene-8-carbaldehyde (3): To an 80 mL microwave reaction vessel containing 4.00 g (14.8 mmol, 1 equiv.) 5-bromo-2-((2-methylbut-3-yn-2-yl)oxy)benzaldehyde (**2**) dissolved in 60 mL dry MeCN was added 66.0 mg (0.300 mmol, 0.02 equiv.) BHT. The reaction was heated in a microwave reactor to 180°C for 20 min before being concentrated and purified by silica gel flash chromatography eluting with 19:1 hex./EtOAc to yield 2.10 g (53%) of the desired product (**3**) as a yellow oil.

^{1}HNMR (300MHz, CDCl$_3$) δ 10.35 (s, 1H), 7.73 (d, J = 2.7, 1H), 7.27 (dd, J = 2.7, 0.3, 1H), 6.29 (d, J = 9.9, 1H), 5.75 (d, J = 9.9, 1H), 1.50 (s, 3H); ^{13}CNMR (75MHz, CDCl$_3$) δ 188.0, 155.3, 134.3, 132.8, 129.4, 125.6, 124.6, 120.8, 113.4, 78.4, 28.4; IR (NaCl, film) 2863, 1678, 1574 cm^{-1}; HRMS (+TOF) 267.0015 calcd for C$_{12}$H$_{12}$BrO$_2$ [M+H]$^+$, found: 267.0012; R$_f$ = 0.33 (9:1 hex./ EtOAc).

Synthesis of 6-(2-(9H-carbazol-9-yl)ethyl)-2,2-dimethyl-2H-chromene-8-carbaldehyde (B106): To a flame dried 10 mL round bottomed flask containing 57.0mg (0.213 mmol, 1 equiv.) 6-bromo-2,2-dimethyl-2*H*-chromene-8-carbaldehyde (**3**), 64.0mg (0.213 mmol, 1 equiv.) Molander Salt (**4**) (9-(2-(trifluoro-»^{4}-boranyl)ethyl)-9*H*-carbazole, potassium salt), 8.0 mg (0.011 mmol, 0.05 equiv.) PdCl$_2$(dppf)-CH$_2$Cl$_2$, and 208 mg (0.639 mmol, 3 equiv.) anhydrous Cs$_2$CO$_3$ was added 1.5 mL dry toluene and 0.5 mL deionized H$_2$O. The reaction was heated to 80°C for 16hr, added to brine, extracted into EtOAc, dried over Na$_2$SO$_4$, and concentrated under reduced pressure. The resulting residue was purified by silica gel flash chromatography eluting with 19 : 1 hex./EtOAc to 1 : 1 hex./EtOAc yielding 36 mg (44%) of the desired product (**B106**) as a colorless oil.

^{1}HNMR (300MHz, CDCl$_3$) δ 10.44 (s, 1H), 8.09 (d, J = 7.5, 2H), 7.56 (d, J = 2.4, 1H), 7.43 (t, J = 6.9, 2H), 7.32 (t, J = 8.4, 2H), 7.23 (t, J = 6.9, 2H), 6.73 (d, J = 2.1, 1H), 6.14

(d, J = 9.9, 1H), 5.65 (d, J = 9.6, 1H), 4.48 (t, J = 7.5, 2H), 3.03 (t, J = 7.5, 2H), 1.47 (s, 6H); ^{13}CNMR (75MHz, CDCl$_3$) δ 189.5, 155.4, 140.3, 133.0, 131.8, 131.0, 126.8, 125.9, 124.3, 123.1, 122.8, 121.5, 120.6, 119.2, 117.8, 108.8, 44.8, 34.3, 28.3; IR (NaCl, film) 2861, 1679 cm^{-1}; HRMS (+TOF) 382.1802 calcd for C$_{26}$H$_{23}$NO$_2$ [M+H]$^+$, found: 382.1799; R$_f$ = 0.25 (9:1 hex./ EtOAc).
Ref. BJE6-106

Cell culture, siRNA transfection, plasmid stable transfection & PLX4032-resistant sub cell lines. Human melanoma cell lines WM1366, WM1361A, WM852, FM28, FM6, SKMEL2 and SKMEL28, SBcl2, A375 and SKMEL5 were originally obtained from ATCC or the European Searchable Tumour Line Database (ESTDAB) and authenticated by these agencies using DNA fingerprinting quality control. Their respective RAS or BRAF mutations previously identified in the literature were verified by sequencing. SBcl2 and A375 and its derivative lines were maintained in Dulbecco's modified Eagle's medium (DMEM) supplemented with 10% fetal bovine serum. SKMEL5 was maintained in minimum essential medium (MEM) supplemented with 10% fetal bovine serum. All media were additionally supplemented with L-glutamine 2 mM, penicillin 100 units/ml and streptomycin 100 μg/ml. Primary human melanocytes were grown in medium 254 (Invitrogen).

siRNA transfection was performed by reverse transcription using Lipofectamine RNAiMax (Invitrogen) according to the product protocol, and media was changed the following day of transfection. PLX4032-resistant cell sublines were established according to the method described in [3]. Briefly, A375 and SKMEL5 cells were plated at low cell density and treated with PLX4032 at 1 μM or 0.5 μM, respectively. The concentration of PLX4032 was gradually increased up to 4μM (A375) or 2 μM (SKMEL5) over the course of a 3-4 week period, and clonal colonies were picked. Derived sublines of A375 and SKMEL5 were maintained in PLX4032-containing medium at 1-2 μM (A375) or 0.5 μM (SKMEL5).

Cell proliferation & Caspase assays. Cell proliferation assays (MTS assay) and caspase assays were performed with CellTiter 96 AQueous Non-Radioactive Cell Proliferation Assay kit and Caspase-Glo 3/7 Assay Systems (Promega) according to the manufacturers' protocols. Briefly, for the assays employing inhibitors, cells were plated in a 96-well plate (500-4000 cells per well depending on the cell lines and duration of the experiment), exposed to inhibitors 24 hr later and cultured for the durations indicated in the individual figure legends. For the assays employing siRNA, cells were plated the day of siRNA transfection, cultured for the duration indicated in the figure legends, and if indicated, treated with inhibitors or vehicle. After the indicated treatment times, assay reagent was added and cell plates were incubated for 1 hr at 37°C (MTS assay) or 30 min at RT (caspase assay). Absorbance at 490 nm (MTS assay) or luminescence (caspase assay) were measured using microplate readers for quantification. Human primary melanocytes were plated in triplicate on a 12-well plate. Test compounds at different concentrations or vehicle (DMSO) were added on the second day, and viable cells were enumerated 72 rh after addition of compounds. Cell survival was evaluated against the DMSO-treated controls.

Clonogenic colony assay. For the experiments depicted in Figure 2E, cells were treated with drugs for the time indicated in the figure, and then the same number of viable cells from each treatment was replated at low cell density and cultured in medium without inhibitors for 8 days, at which time colony formation was quantitated. Cell colonies were stained with ethidium bromide for visualization on an ImageQuant LAS 4000 (GE Healthcare) and colonies enumerated.

DNA fragmentation assays. Cells were harvested and fixed in 1 ml of a 35% ethanol/DMEM solution at 4°C for 30 min. Cells were then stained with a solution containing 25 μg/ml of propidium iodide/ml and 50 μg/ml of RNase A in PBS and incubated in the dark at 37°C for 30 min for flow cytometric analysis. The proportion of cells in the sub-G1 population, which contain a DNA content of less than 2N (fragmented DNA), was measured as an indicator of apoptosis.

Immunoblotting. Whole cell lysates were prepared in a buffer containing 20 mM Hepes (pH 7.4), 10% glycerol, 2 mM EDTA, 2 mM EGTA, 50 mM β-glycerophosphate and 1% Triton-X100, 1 mM dithiothreitol (DTT) and 1 mM sodium vanadate, supplemented with Halt Protease and Phosphatase Inhibitor Cocktail (100X) (Thermo Scientific). Lysates were subjected to SDS-PAGE and transferred to nitrocellulose membranes. Membranes were blocked at RT for 1-1.5 hr with 5% BSA or 5% non-fat dry milk in TBS-T (10 mM Tris [pH 7.5], 100 mM NaCl, 0.1% Tween 20) and probed with the appropriate primary antibodies (1:500-1:10,000) overnight. After washing, the blots were incubated with horseradish peroxidase-conjugated secondary antibodies (1:2000-1:10,000) and visualized using the ECL system (GE Healthcare) on an ImageQuant LAS 4000. As loading controls, either α-tubulin, β-actin or GAPDH was selected, depending on the molecular weight of the proteins being studied in each experiment or the acrylamide percentage of the gels. In some experiments, photographs of the same gel processed from the same experiment, are presented in two separate panels. In some cases, lanes not directly relevant to the particular panel have been deleted for clarity, and this is indicated in the respective figure legends.

Quantitative real-time PCR. RNA was extracted with RNeasy Mini kit purchased (Qiagen) according to the manufacturer's protocol. 1 μg of RNA was used to synthesize cDNA in a 20 μl reaction volume employing SuperScript III First-Strand Synthesis System (Invitrogen) or QuaniTect Reverse Transcription Kit (Qiagen) according to the product protocol. Quantitative real-time PCR was performed with SYBR Green PCR Master Mix (Applied Biosystems (now under Life Technologies)) according to the manufacturer's protocol. Briefly, cDNA was diluted to a final concentration of 25 ng per reaction, added to a primer set (5 μM) and SYBR Green PCR Master Mix to a final volume of reaction mixture of 20 μl, and run on an Applied Biosystems 7500 Fast Real-Time PCR system using the following thermal cycling protocol: 50°C for 2 min, 95°C for 10 min, and 40 cycles of 95°C for 15 sec and 60°C for 1 min. The relative amount of an mRNA of interest was calculated by normalizing the Ct value of the mRNA to the Ct of the internal control (β-actin). Primer sequences were: H2AX Forward: 5'-CAACAAGAAGACGCGAATCA-3', H2AX Reverse: 5'-CGGGCCCTCTTAGTACTCCT-3', β-actin Forward: 5'-

GCTCGTCGTCGACAACGGCTC-3', β-actin Reverse: 5'-CAAACATGATCTGGGTCATCTTCTC-3'

References

1. Molander, G. A. and Vargas, F. (2007) Beta-aminoethyltrifluoroborates: efficient aminoethylations via Suzuki-Miyaura cross-coupling, *Org. Lett. 9*, 203-206.

2. Molander, G. A., Yun, C. S., Ribagorda, M. et al. (2003) B-alkyl suzuki-miyaura cross-coupling reactions with air-stable potassium alkyltrifluoroborates, *J Org. Chem. 68*, 5534-5539.

3. Nazarian, R., Shi, H., Wang, Q. et al. (2010) Melanomas acquire resistance to B-RAF(V600E) inhibition by RTK or N-RAS upregulation, *Nature. 468*, 973-977.

BMC
Cancer

RESEARCH ARTICLE

Open Access

Protein kinase C-delta inactivation inhibits the proliferation and survival of cancer stem cells in culture and *in vivo*

Zhihong Chen[1], Lora W Forman[1], Robert M Williams[3,4] and Douglas V Faller[1,2,5,6,7,8,9*]

Abstract

Background: A subpopulation of tumor cells with distinct stem-like properties (cancer stem-like cells, CSCs) may be responsible for tumor initiation, invasive growth, and possibly dissemination to distant organ sites. CSCs exhibit a spectrum of biological, biochemical, and molecular features that are consistent with a stem-like phenotype, including growth as non-adherent spheres (clonogenic potential), ability to form a new tumor in xenograft assays, unlimited self-renewal, and the capacity for multipotency and lineage-specific differentiation. PKCδ is a novel class serine/threonine kinase of the PKC family, and functions in a number of cellular activities including cell proliferation, survival or apoptosis. PKCδ has previously been validated as a synthetic lethal target in cancer cells of multiple types with aberrant activation of Ras signaling, using both genetic (shRNA and dominant-negative PKCδ mutants) and small molecule inhibitors. In contrast, PKCδ is not required for the proliferation or survival of normal cells, suggesting the potential tumor-specificity of a PKCδ-targeted approach.

Methods: shRNA knockdown was used validate PKCδ as a target in primary cancer stem cell lines and stem-like cells derived from human tumor cell lines, including breast, pancreatic, prostate and melanoma tumor cells. Novel and potent small molecule PKCδ inhibitors were employed in assays monitoring apoptosis, proliferation and clonogenic capacity of these cancer stem-like populations. Significant differences among data sets were determined using two-tailed Student's t tests or ANOVA.

Results: We demonstrate that CSC-like populations derived from multiple types of human primary tumors, from human cancer cell lines, and from transformed human cells, require PKCδ activity and are susceptible to agents which deplete PKCδ protein or activity. Inhibition of PKCδ by specific genetic strategies (shRNA) or by novel small molecule inhibitors is growth inhibitory and cytotoxic to multiple types of human CSCs in culture. PKCδ inhibition efficiently prevents tumor sphere outgrowth from tumor cell cultures, with exposure times as short as six hours. Small-molecule PKCδ inhibitors also inhibit human CSC growth *in vivo* in a mouse xenograft model.

Conclusions: These findings suggest that the novel PKC isozyme PKCδ may represent a new molecular target for cancer stem cell populations.

Keywords: Protein Kinase C isozymes, Synthetic lethal interaction, Cancer-initiating cell, Xenograft tumor model

* Correspondence: dfaller@bu.edu
[1]Cancer Center, Boston University School of Medicine, K-712C, 72 E. Concord St., Boston, MA 02118, USA
[2]Department of Medicine, Boston University School of Medicine, K-712C, 72 E. Concord St., Boston, MA 02118, USA
Full list of author information is available at the end of the article

Background

Much recent data supports the model that a subpopulation of tumor cells with distinct stem-like properties is responsible for tumor initiation, invasive growth, and possibly dissemination to distant organ sites [1-3]. This small subpopulation of cells can divide asymmetrically, producing an identical daughter cell and a more differentiated cell, which, during their subsequent divisions, generate the vast majority of tumor bulk [4,5]. A number of names have been used to identify this subpopulation, including "cancer progenitor cells," "cancer stem cell-like cells," and "cancer-initiating cells," but the term "cancer stem cell" (CSC) has received wide acceptance [6].

The first identification of CSCs in solid tumors was made in 2003, when CSCs were identified and isolated from breast cancers using CD44 and CD24 markers [7]. Subsequently, CSCs have been identified in a variety of solid tumors, including glioblastoma [8-10], osteosarcoma [11], chondrosarcoma [12], prostate cancer [13], ovarian cancer [14-18], gastric cancer [19], lung cancer [20,21], colon cancer [22-25], pancreatic cancer [26,27], melanoma [28-30], head and neck cancer [31], and others. CSCs isolated from these different tumor types share some common characteristics including drug resistance, ability to repopulate tumors, and asymmetric division.

CSC exhibit a spectrum of biological, biochemical, and molecular features that are consistent with a stem-like phenotype, including growth as non-adherent spheres (clonogenic potential), superior ability to form a new tumor in *in vivo* xenograft assays, unlimited self-renewal, and the capacity for multipotency and lineage-specific differentiation [1,32-35]. In particular, CSCs are able to form colonies from a single cell more efficiently than their progeny [36] and to grow as spheres in non-adherent, serum-free culture conditions [37]. Sphere formation in non-adherent cultures has been used as a surrogate *in vitro* method for detecting CSCs from primary human tumors [8,20,25,38,39]. CSC populations also variably exhibit "stem cell-like" markers, such as Nanog, Sox2, aldehyde-dehydrogenase positivity, and telomerase.

Chemoresistance is also considered a hallmark of CSCs [6,40]. They characteristically survive chemo- and radiotherapeutic interventions [41] and may thus be responsible for both tumor relapse and metastasis [42]. CSCs are often innately less sensitive to treatment than are the bulk of the tumor cells that they generate [43,44]. These features support the hypothesis that CSCs are the cell subpopulation that is most likely responsible for treatment failure and cancer recurrence [32].

Aberrant activation of Ras signaling, either through mutation of the Ras genes themselves, or through constitutive upstream or downstream signaling, is very common in solid tumors. We have previously identified the protein

kinase C delta (PKCδ) isozyme as a Ras synthetic lethal interactor [45-48]. PKCδ is a serine/threonine kinase of the PKC family, a member of the novel class, and functions in a number of cellular activities including cell proliferation, survival or apoptosis [49]. However, PKCδ is not required for the proliferation of normal cells, and PKCδ-null animals develop normally and are fertile, suggesting the potential tumor-specificity of a PKCδ-targeted approach [50]. PKCδ was validated as a target in cancer cells of multiple types with aberrant activation of Ras signaling, using both genetic (siRNA and dominant-negative PKCδ) and small molecule inhibitors [45], by our group [45,47] and later by others [51,52]. "Ras-dependency" in these tumors was not required for these synthetic-lethal cytotoxic effects [45,46]. Tumors with aberrant activation of the PI₃K pathway or the Raf-MEK-ERK pathway in the setting of wild-type RAS alleles have also been shown to require PKCδ activity for proliferation or survival [47,48].

In this report, we demonstrate that CSC-like cell populations derived from multiple types of human primary tumors, from human cancer cell lines, and from transformed human cells require PKCδ activity and are susceptible to agents which deplete PKCδ protein or activity.

Methods

Cell culture

MCF10A and MCF10C breast cell lines were derived at the Barbara Ann Karmanos Cancer Institute (Detroit, MI) and maintained in DMEM-F/12 medium containing 5% heat-inactivated horse serum, 10 μg/mL insulin, 20 ng/mL epidermal growth factor, 0.1 μg/mL cholera enterotoxin, and 0.5 μg/mL hydrocortisone [53,54]. Breast cancer cell lines MCF7, Hs587T, and MDA231 were purchased from ATCC, and were propagated in 10% fetal bovine serum (Invitrogen, Grand Island, NY); Dulbecco's Modification of Earle's Media (Cellgro, Herndon, VA); 2 mM L-Glutamine (Invitrogen); 200 U Penicillin/ml; 200 μg Streptomycin/ml (Invitrogen).

Human breast cancer stem cells (BCSC: CD133+, CD44+, SSEA3/4+, Oct4+, Alkaline Phosphatase+, Aldehyde Dehydrogenase+, Telomerase+), pancreatic cancer stem cells (PCSC: CD44⁺, CD133⁺, SSEA3/4⁺, Oct4⁺, Alkaline Phosphatase⁺, Aldehyde Dehydrogenase⁺, Telomerase⁺, and Nestin⁺), and prostate cancer stem cells (PrCSC: CD44⁺, CD133⁺, SSEA3/4⁺, Oct4⁺, alkaline phosphatase⁺, aldehyde dehydrogenase⁺, and telomerase⁺) were purchased from Celprogen (San Pedro, CA), and cultured using specialized media and tissue culture plastic and matrix, to preserve their CSC phenotype, according to the manufacturer's instructions.

Reagents

Rottlerin was purchased from (EMD Biosciences, San Diego, CA). The PKCδ inhibitor KAM1 was previously

described [47]. BJE6-106 was synthesized as described elsewhere [55]. Briefly, 9-(2-(trifluoro-λ^4-boranyl)ethyl)-9*H*-carbazole, potassium salt (Molander Salt 1), 6-bromo-2,2-dimethyl-2H-chromene-8-carbaldehyde, 64.0 mg (0.213 mmol, 1 equiv.), PdCl2(dppf)-CH2Cl2, and anhydrous Cs_2CO_3 were combined to form 6-(2-(9*H*-carbazol-9-yl)ethyl)-2,2-dimethyl-2*H*-chromene-8-carbaldehyde (BJE6-106).

Tumor sphere formation

Tumor self-renewing and anchorage-independent spheroids were obtained by culturing breast cancer cells MCF7, Hs587T and MDA231; melanoma cells SBcl2 and FM6; human breast cancer stem cells and pancreatic cancer stem cells in stem cell-selective conditions according to the manufacturer's instructions (StemCell Technologies, Tukwila, WA). Briefly, cancer and cancer stem cells were propagated in 6-well ultra-low adherent plates (Corning) in Complete MammoCult Medium (Human) by adding 50 mL of MammoCult Proliferation Supplements to 450 mL of MammoCult Basal Medium (StemCell Technologies). The following were added to obtain Complete MammoCult Medium: 4 ug/mL Heparin (StemCell Technologies), 0.48 μg/mL hydrocortisone (StemCell Technologies), 200 U penicillin/ml; and 200 μg streptomycin/ml (Invitrogen).

Flow cytometry

Cell staining for CD24 or CD44: MCF7 and MCF7 spheres, Hs587T and Hs587T spheres, MDA231 and MDA231 spheres, breast cancer stem cells and breast cancer stem cell spheres were collected and stained or dual-stained with Fluorescein isothiocyanate (FITC)-anti-CD24 and (PerCP-Cy)-anti-CD44 (BD Pharmingen, San Diego, CA) monoclonal antibody (mAbs) for 30 min on ice. The stained cancer cells and sphere populations were analyzed by FACSCAN analysis.

Clonogenic assays

100,000 cells were seeded on 100 mm dishes with 10 ml media per dish [47]. On day 4, cells were treated with a PKCδ inhibitor or vehicle control for either 6, 18, 24 or 48 hours. Cells were trypsinized; counted *via* the trypan blue exclusion method in order to determine the number of live cells in the sample, and 300 live cells were seeded in triplicate onto 6-well plates. Cells were monitored for appropriate colony size and re-fed every three to four days. At Day 15, cells were stained with ethidium bromide [56] and counted using UVP LabWorks software (Waltham, MA).

Cell proliferation assays

Cell proliferation was assessed using an MTT [3-(4,5-dimethylthiazol-2-yl)-2,5-diphenyltetrazolium bromide] assay

(Roche, Mannheim, Germany). The number of viable cells growing in a single well on a 96-well microtiter plate was estimated by adding 10 μl of MTT solution (5 mg/ml in phosphate-buffered saline [PBS]). After 4 h of incubation at 37°C, the stain was diluted with 100 μl of dimethyl sulfoxide. The optical densities were quantified at a test wavelength of 570 nm and a reference wavelength of 690 nm on a multiwell spectrophotometer. In some assays, MTS was used as substrate (Promega, Madison, WI), and the absorbance of the product was monitored at 490 nm. Cell enumeration was carried out using a hemocytometer, and viable cells identified by trypan blue exclusion.

PKC kinase activity assays

Assays were carried out using recombinant PKCδ or PKCα, (Invitrogen) and the Z-lyte Kinase Assays (Invitrogen) with a "PKC-kinase-specific" peptide substrate. FRET interactions produce a change in fluorescence (ex455/ex520) upon phosphorylation. The kit was used according to the manufacturer's instructions.

Cytotoxicity assay

LDH release was assessed by spectrophotometrically measuring the oxidation of NADH in both the cells and media. Cells were seeded in 24-well plates, and exposed to PKCδ inhibitors or vehicle. After different times of exposure, cytotoxicity was quantified by a standard measurement of LDH release with the use of the LDH assay kit (Roche Molecular Biochemicals) according to the manufacturer's protocol. Briefly, total culture medium was cleared by centrifugation. For assay of released LDH, supernatants were collected. To assess total LDH in cells, Triton X-100 was added to vehicle (control) wells to release intracellular LDH. LDH assay reagent was added to lysates or supernatants and incubated for up to 30 min at room temperature in dark, the reaction was stopped, and the absorbance was measured at 490 nm. The percentage of LDH release was then calculated as the LDH in the supernatants as a fraction of the total LDH.

Immunoblot analyses

Levels of proteins were measured and quantitated in cells as we have previously reported [45]. Harvested cells were disrupted in a buffer containing 20 mM Tris (pH 7.4), 0.5% NP-40, and 250 mM NaCl with protease and phosphatase inhibitors. Total protein (40 μg) was separated on 10% SDS-polyacrylamide gels and transferred to nitrocellulose membranes or PVDF membranes. Membranes were blocked overnight and probed with affinity-purified antibodies against: PKCδ (BD Transduction Labs, San Jose, CA), or β-actin or α-tubulin (Sigma Aldrich, St. Louis, MO). Antibodies against human ERK, phospho-ERK1/2 (Thr202/Tyr204), AKT and phospho-AKT (Ser473), JNK and phospho-JNK (Thr183/Tyr185) were purchased from

Cell Signaling (Danvers, MA). After washing, the blots were incubated with horseradish peroxidase-conjugated secondary antibodies and visualized using the Amersham enhanced chemiluminescence ECL system, and quantitated by digital densitometry.

Down-regulation of PKC by shRNA and lentiviral vectors

shRNA duplexes for PKCδ (shRNAs) were obtained from Qiagen (Valencia, Ca). The shRNA sequences for targeting PKCδ and the corresponding scrambled shRNAs used as negative controls were previously described [47]. The lentiviral vectors were previously described [46]. After infection of cells with the vectors, one aliquot was utilized in proliferation assays and a parallel aliquot was subjected to immunoblotting to assay the efficiency of the knockdown.

Xenograft studies

These studies were performed with the approval of the Institutional Animal Care and Use Committee of Boston University. Breast cancer stem cells (2×10^5) grown from a metastatic tumor were suspended in human breast cancer stem cell complete growth media (Celprogen, San Pedro, CA) and injected subcutaneous into the right flank of female J:NU mice (The Jackson Laboratory, ME) under anesthesia. After palpable tumors developed, the mice were divided into two groups of animals. The control group received daily intraperitoneal injections of vehicle (DMSO) while the treatment group received daily intraperitoneal injections of a PKCδ inhibitor (rottlerin 5,000 μg/kg) for 15 days. The length and width of tumors were measured with a vernier caliper and tumor volumes were calculated. Survival was calculated as the day tumors reached the maximum size allowed by the protocol (2 cm diameter).

Statistical analysis

Experiments were carried out in triplicate for all experimental conditions. Data are shown as mean ± SD. Where applicable, a two-tailed Student's t test or ANOVA was performed on the means of two sets of sample data and considered significant if $p \le 0.05$.

Results

Inhibition of PKCδ is growth-inhibitory and cytotoxic in human prostate and pancreatic cancer stem cells

The sensitivity of human cancer stem cell cultures to inhibition of PKCδ was first examined using shRNA methodology to specifically and selectively knockdown transcripts for this PKC isozyme and thereby specifically validate PKCδ as a target in CSCs. Cell cultures derived from a primary human pancreatic adenocarcinoma (PCSC) and from a primary human prostate adenocarcinoma (PrCSC), isolated by phenotypic markers, were studied. These cells were characterized as "stem-like" by a number of criteria. The PCSC and the PrCSC cultures

were CD44^{+}, CD133^{+}, Nanog^{+}, Sox2^{+}, aldehyde dehydrogenase^{+}, and telomerase^{+}. The PCSC cultures were also Nestin^{+}. Both cell types were tumorigenic at <1000 cells in xenograft assays in SCID mice, and also formed tumor spheroids at high efficiency. Lentiviral vectors expressing PKCδ-specific shRNAs (PKCδ-shRNA), which we have previously shown to be specific for the PKCδ isozyme among all the other PKC isozymes [45-47], were used to deplete PKCδ levels in the cells. A vector containing a scrambled shRNA (sc-shRNA) served as a control. Specific knockdown of PKCδ by shRNA was growth-inhibitory in both the human prostate (PrCSC) and pancreatic (PCSC) cancer stem cells, with significant effects observed at early as 24 hr after infection, and progressing up to 72 hr (Figure 1A). The non-targeted lentiviral vector (sc-shRNA) generated modest but reproducible effects on cell growth over time, as we have observed in prior reports [45-47]. Cytotoxic effects of PKCδ depletion on the PCSC and PrCSC cultures were assessed by quantitating release of cellular LDH. Significant cytotoxicity was elicited by the PKCδ-specific shRNA as early as 24 hr after infection, with LDH release approaching the maximum possible levels by 72 hr. The effects of the scrambled shRNA on LDH release did not differ from those of the infection vehicle alone at any time point (Figure 1B). Efficient knockdown of the PKCδ isozyme was verified by immunoblotting (Figure 1C).

While the specificity of shRNA is essential for validation of a target, small-molecule enzyme inhibitors are more likely than shRNA to translate towards clinical application. We therefore next examined the effects of existing and novel small molecule inhibitors of PKCδ. Rottlerin, a natural product, has been identified as a PKCδ inhibitor for many years [47], with an *in vitro* IC_{50} of approximately 5 μM in our kinase assays (Table 1), in good agreement with the literature [57,58] (although it also exerts inhibitory effects on certain non-PKC kinases at concentrations comparable to the IC_{50} for PKCδ [59]). We and others have shown that rottlerin, at the concentrations employed herein, is not cytostatic or cytotoxic to normal primary cells or cell lines, and is well-tolerated when administered orally or intraperitoneally to mice (see also the studies on normal human breast epithelial cells and the *in vivo* studies later in this report) [45-47]. Exposure of PCSC and PrCSC cultures to rottlerin produced a significant dose-dependent inhibition of proliferation as early as 24 hr after exposure (Figure 2A). Similarly, rottlerin induced cytotoxicity in both CSC cultures in a dose-dependent fashion, as assessed by LDH release (Figure 2B). The duration of PKCδ inhibition required to irreversibly prevent CSC proliferation was next assessed. Exposure to rottlerin efficiently decreased the clonogenic capacity of PCSC. Eighteen hr of exposure to rottlerin, followed by washout,
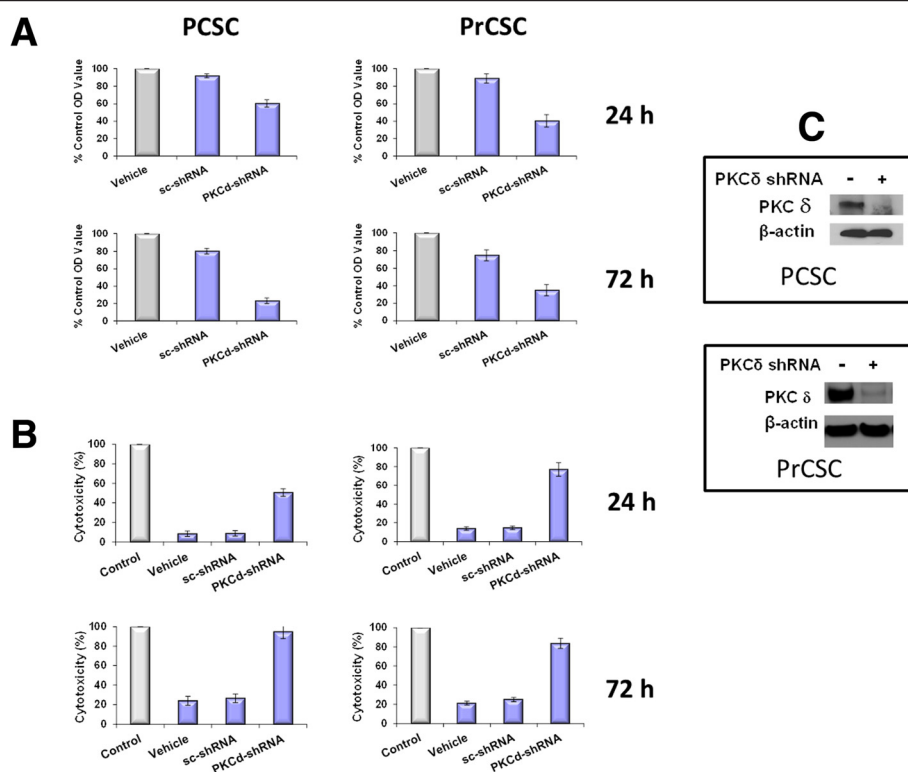
Figure 1 Effects of PKCδ knockdown by shRNA on proliferation and viability of human pancreatic (PCSC) and prostate (PrCSC) cancer stem cell cultures. (A) PCSC and PrCSC cells were grown to 50% confluence in 96-well plates and then infected with PKCδ-shRNA-expressing lentivirus vector or a lentiviral vector containing a scrambled shRNA (sc-shRNA). The corresponding equivalent volumes of diluent used for infection served as vehicle controls (Vehicle). 24 and 72 hr after transfection, cell mass was evaluated by MTS assay. Error bars represent SEM. p values for comparison between control (scrambled shRNA) and PKCδ-shRNA effects on cell number reached significance at 24 hr of exposure (p < 0.001) for all cell lines, and remained significant at the 72 hr time point. **(B)** PCSC and PrCSC cells were grown to 50% confluence in 96-well plates and then infected with PKCδ-shRNA or scrambled shRNA (sc-shRNA) expressing lentiviruses. The corresponding equivalent volumes of diluent were used as vehicle controls (Vehicle). After 24 and 72 hr of infection, cell cytotoxicity was evaluated by LDH-release assay. Total maximal LDH release was assigned the arbitrary value of 100% (Control). Error bars represent SEM. p values for comparison between effects on LDH release for cells infected with scrambled shRNA-expressing vectors compared to PKCδ-shRNA vectors reached significance at 24 hr of exposure (p < 0.01) for all cell lines, and remained significant at the 72 hr time point. **(C)** Immunoblot analysis of PKCδ protein levels in the same cell lines 72 hr after infection with PKCδ-targeting shRNA expressing lentiviral vectors (+) or scrambled shRNA (−). PKCδ-targeted shRNA vectors efficiently reduced PKCδ protein expression. Immunoblotting with a β-actin antibody after stripping the blots served as a loading control.

was sufficient to decrease the clonogenic capacity of PCSC by 40%, and increasing the duration of the exposure to 48 hr reduced the clonogenic potential by more than 90% (Figure 2C).
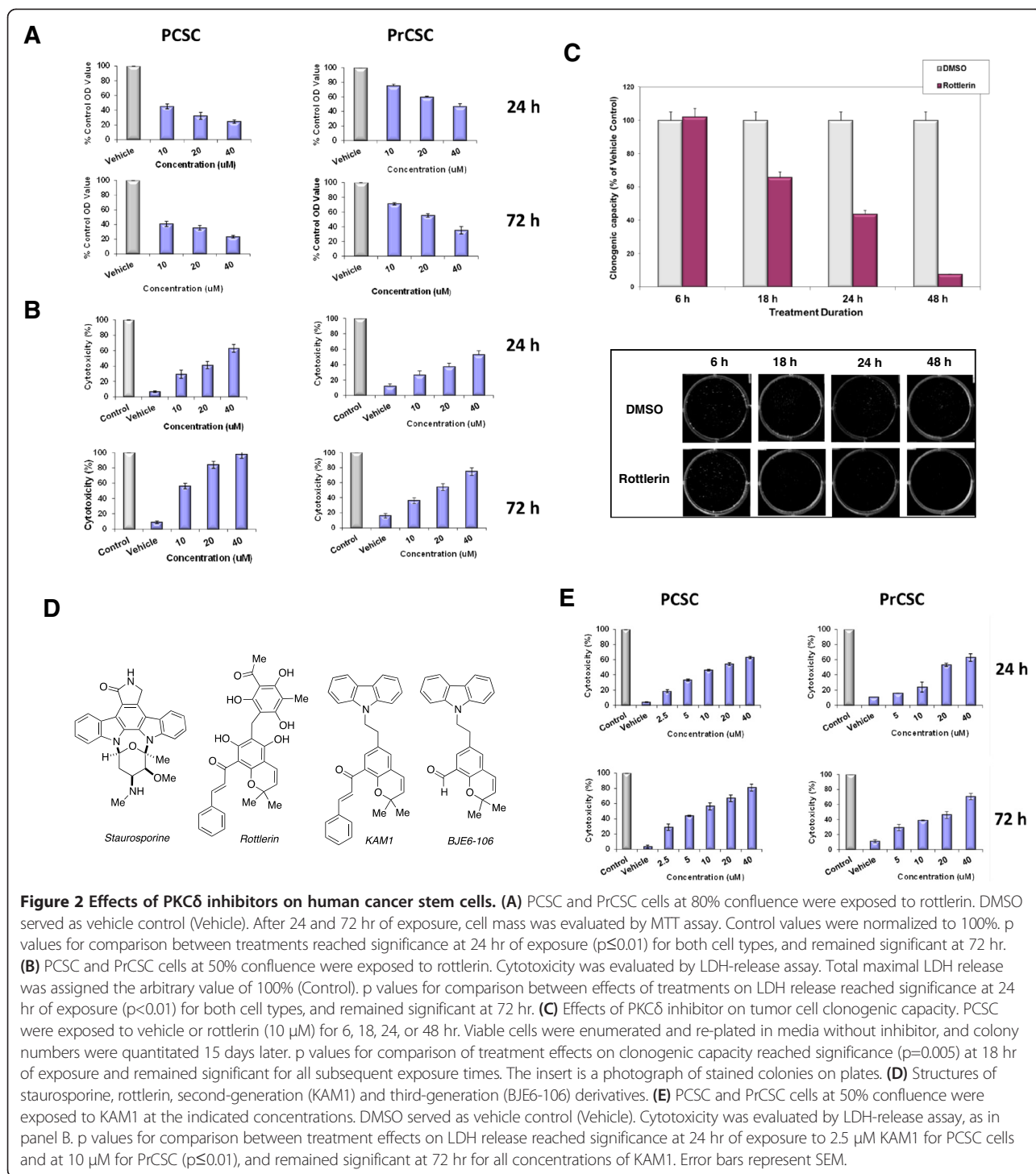
As previously reported, we have sought to develop novel PKCδ-inhibitory molecules with greater specificity for PKCδ compared to essential PKC isozymes, such as PKCα, using pharmacophore modeling and structure-

activity relationships (SAR) [47]. We designed and synthesized a set of analogs based on this strategy. In this 2nd generation of PKCδ inhibitors, the "head" group (carbazole portion) was made to resemble that of staurosporine, a potent general PKC inhibitor, and other bisindoyl maleimide kinase inhibitors, with two other domains (cinnamate side chain and benzopyran) conserved from the rottlerin scaffold to preserve isozyme specificity. The first such chimeric molecule reported, KAM1 (Figure 2D), was indeed active, like staurosporine, but was also more PKCδ-specific, and showed potent activity against Ras-mutant human cancer cells in culture and *in vivo* animal models, while not producing cytotoxicity in non-transformed cell lines [47]. KAM1 induced cytotoxicity as assessed by LDH release in a dose-dependent fashion in both PCSC and PrCSC cultures at concentrations as low as 2.5 μM (PCSC) and 5 μM (PrCSC) (Figure 2E).

Table 1 Comparison of three generations of PKCδ inhibitors

Generation	PKCδIC$_{50}$	PKCαIC$_{50}$	PKCδ/PKCα Selectivity ratio
1	3 μM	75 μM	28-fold
2	2 μM	157 μM	56-fold
3	0.05 μM	50 μM	1000-fold

Figure 2 Effects of PKCδ inhibitors on human cancer stem cells. (A) PCSC and PrCSC cells at 80% confluence were exposed to rottlerin. DMSO served as vehicle control (Vehicle). After 24 and 72 hr of exposure, cell mass was evaluated by MTT assay. Control values were normalized to 100%. p values for comparison between treatments reached significance at 24 hr of exposure (p≤0.01) for both cell types, and remained significant at 72 hr. **(B)** PCSC and PrCSC cells at 50% confluence were exposed to rottlerin. Cytotoxicity was evaluated by LDH-release assay. Total maximal LDH release was assigned the arbitrary value of 100% (Control). p values for comparison between effects of treatments on LDH release reached significance at 24 hr of exposure (p<0.01) for both cell types, and remained significant at 72 hr. **(C)** Effects of PKCδ inhibitor on tumor cell clonogenic capacity. PCSC were exposed to vehicle or rottlerin (10 μM) for 6, 18, 24, or 48 hr. Viable cells were enumerated and re-plated in media without inhibitor, and colony numbers were quantitated 15 days later. p values for comparison of treatment effects on clonogenic capacity reached significance (p=0.005) at 18 hr of exposure and remained significant for all subsequent exposure times. The insert is a photograph of stained colonies on plates. **(D)** Structures of staurosporine, rottlerin, second-generation (KAM1) and third-generation (BJE6-106) derivatives. **(E)** PCSC and PrCSC cells at 50% confluence were exposed to KAM1 at the indicated concentrations. DMSO served as vehicle control (Vehicle). Cytotoxicity was evaluated by LDH-release assay, as in panel B. p values for comparison between treatment effects on LDH release reached significance at 24 hr of exposure to 2.5 μM KAM1 for PCSC cells and at 10 μM for PrCSC (p≤0.01), and remained significant at 72 hr for all concentrations of KAM1. Error bars represent SEM.

On the basis of SAR analyses of KAM1, we then designed thirty-six new 3rd-generation analogs. The synthetic chemistry platform that was used to prepare KAM1 was modified to synthesize these additional analogs, which were then tested for biochemical and cellular activity. The PKCδ-inhibitory activity and isozyme-specificity of this 3rd generation was quantitated *in vitro*. A number of these 3rd

generation analogs demonstrated significant increases in potency and isozyme specificity over rottlerin (1st generation) and KAM1 (2nd generation). The new compound selected for study in this report, BJE6-106, is much more potent than rottlerin. BJE6-106 has an (*in vitro*) PKCδ IC_{50} in the range of 0.05 μM, compared to 3 μM for rottlerin (Table 1), is approximately 1000-fold more

inhibitory against PKCδ than PKCα *in vitro*, and produces cytotoxic activity against cells with aberrant Ras signaling at nM concentrations [55].

The activity of the 3rd generation PKCδ inhibitor BJE6-106 on the growth of PCSC cells in culture was compared to rottlerin. BJE6-106 inhibited the growth of PCSC cultures at concentrations as low as 0.1 μM, and had an (in culture) IC$_{50}$ of approximately 0.5 μM at 48 hr (Figure 3). In contrast, rottlerin produced no significant inhibitory activity at 0.5 μM, and displayed an IC$_{50}$ at 48 hr of approximately 3 μM. LDH release assays also showed greater than 10-fold increases in potency for BJE6-106 compared to rottlerin (data not shown).

Inhibition of PKCδ prevents tumor sphere formation

Sphere formation assays, which have been commonly used to identify and purify normal and malignant stem cells, were used to select a "CSC-like population" from established human breast cancer cell lines Hs578T, MDA231 and MCF7. A subpopulation of these cell lines could grow as non-adherent spheres and be continuously propagated in a defined serum-free medium *in vitro*. Flow cytometry and immunofluorescence analysis indicated that sphere-derived cells from cell lines contained a much larger proportion of cells expressing CD44, a candidate surface marker of breast cancer stem cells, and/or a smaller proportion of cells expressing the non-stem cell marker CD24, compared with adherent cells (Figure 4A). The frequency of spheroid formation relative to input cell number was low for the tumor cell lines (≤2-3%), as expected. In contrast, spheroid formation from the cultures of primary PCSC or primary breast cancer stem cells (BCSC) was much more efficient (45% and 53%, respectively). As expected, the CD24/CD44 profiles of cells in the spheres derived from the primary PCSC and BCSC did not differ from the adherent cells (not shown).

Addition of rottlerin or BJE6-106 to the culture medium very efficiently inhibited the formation of spheroids from all of these cell types (Figure 4B), demonstrating cytostatic or cytotoxic activity on tumor cells having a CSC-like phenotype. Interestingly, the actions of these compounds appeared to be even more potent on the CSC subpopulation in the MCF7 cell line than on the adherent "parental" cells (although different assays are being compared). When the MCF7 adherent population, containing predominantly non-CSC, was exposed
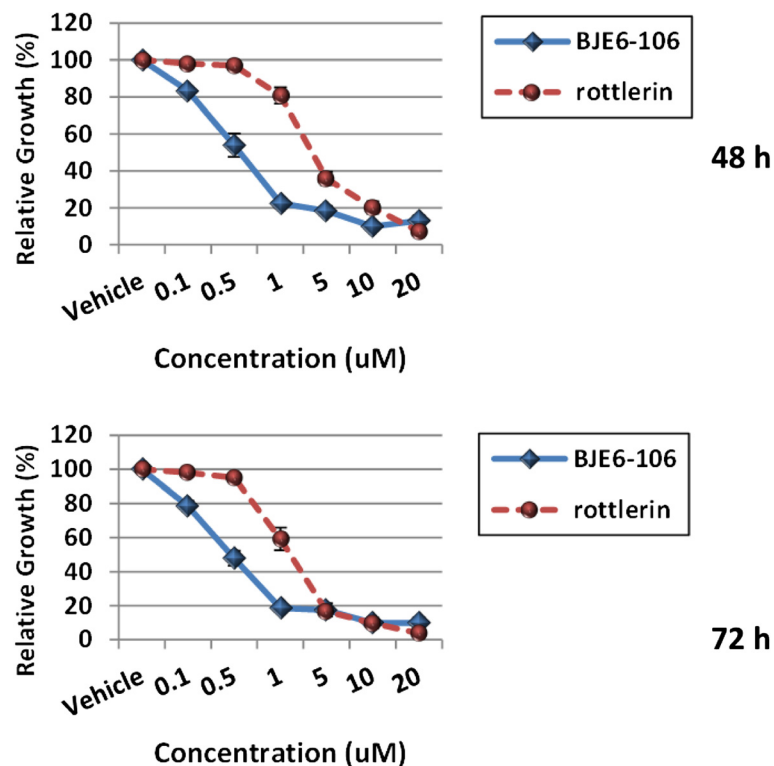
Figure 3 Effects of a 3rd generation small molecule PKCδ inhibitor on human pancreatic cancer stem cell cultures. PCSC cells were grown to 80% confluence in 96-well plates and then exposed to BJE6-106 at concentrations ranging from 0.1 to 20 μM, or to rottlerin at concentrations ranging from 1 to 20 μM. The corresponding equivalent volume of solvent (DMSO) was used as a vehicle control (Vehicle). After 48 and 72 hr of exposure, cell mass was evaluated by MTT assay. Control values were normalized to 100%. Error bars represent SEM. p values for comparison between vehicle and rottlerin effects on cell number at 48 hr reached significance at 1 μM, and for BJE6-106 at 0.1 μM (p ≤ 0.02), and remained significant at the 72 hr time point.

Figure 4 (See legend on next page.)
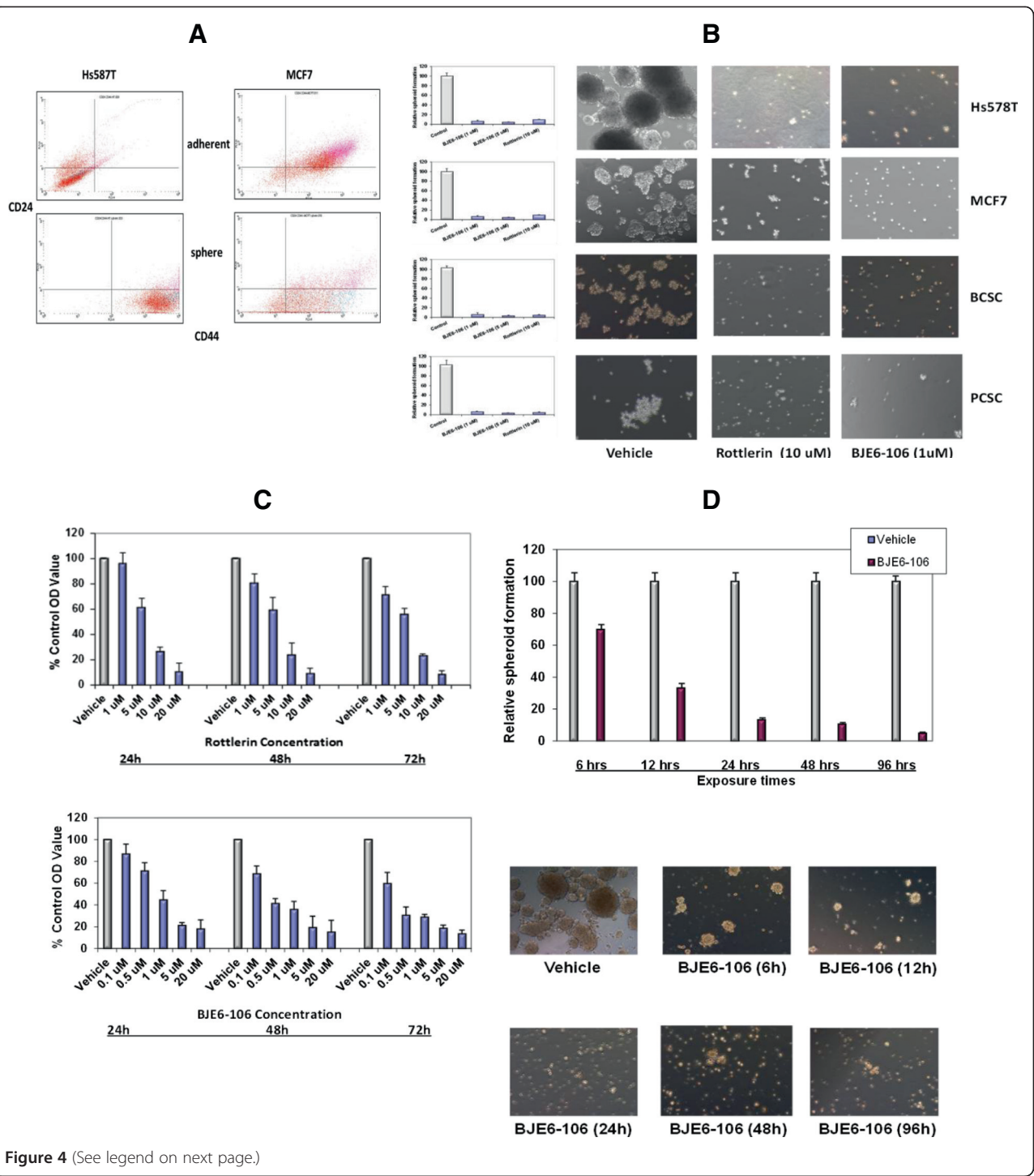
(See figure on previous page.)

Figure 4 Effects of PKCδ inhibitors on human tumor cell spheroid formation. (A) Hs578T and MCF7 were plated under adherent or non-adherent conditions. Tumor spheroids and adherent cells were collected at 96 hr, stained for CD24 and CD44, and analyzed by flow cytometry. **(B)** Hs578T, MCF7, breast cancer stem cells (BCSC) and pancreatic cancer stem cells (PCSC) were plated in tumor spheroid media, in the presence of rottlerin, BJE6-106, or DMSO (Control). Tumor spheroids were enumerated at 96 hr, and normalized to the number of spheroids in the control cultures (assigned an arbitrary value of 100%). p values for comparison between vehicle and rottlerin or BJE6-106 effects were significant (p≤0.001). Photographs are of representative areas of the culture plates. **(C)** MCF7 cells were exposed BJE6-106 or to rottlerin at the indicated concentrations. The corresponding equivalent volume of solvent (DMSO) was used as a vehicle control (Vehicle). After 24, 48 and 72 hr of exposure, cell mass was evaluated by MTT assay. Control values were normalized to 100%. p values for comparison between vehicle and rottlerin effects on cell number at 24 hr reached significance at 5 μM, and for BJE6-106 at 0.5 μM (p ≤ 0.02), and were significant for all concentrations tested at 48 and 72 hr time points. **(D)** Hs578T cells were exposed to vehicle or BJE6-106 (1 μM) for 6, 12, 24, 48 or 96 hr. Viable cells were enumerated and re-plated in media without BJE6-206, and spheroid numbers were quantitated 96 hr later. p values for comparison between vehicle and BJE6-106 effects on spheroid number were significant after 6 hr of exposure (p≤0.02), and remained significant at all time points thereafter. Error bars represent SEM.

to rottlerin or BJE6-106, concentrations in excess of 10 μM and 1 μM, respectively, were required to repress growth by more than 80% (Figure 4C). In contrast, growth of MCF7 spheroids was inhibited greater than 90% by rottlerin at 10 μM and BJE6-106 at 1 μM. Wash-out studies using spheroid formation demonstrated that as little as 6 hr of exposure to BJE6-106 at 1 μM significantly repressed spheroid formation of Hs578T cells, with near maximum inhibition achieved by 24 hr of exposure (Figure 4D).

In parallel studies, BJE6-106 at 0.5-1.0 μM and rottlerin at 10 μM also efficiently inhibited the growth of tumor spheroids generated from two human melanoma cell lines (SBcl2, >99.5% inhibition, p < 0.001; FN5, >99.5% inhibition, p < 0.001), two human pancreatic cancer cell lines (MiaPaCa2, >97% inhibition, p < 0.001; Panc1, >99% inhibition, p < 0.001); and two prostate cancer cell lines (DU145, >98% inhibition, p < 0.001; PC3, >96% inhibition, p < 0.001).

A CSC-like phenotype can be induced during epithelial-mesenchymal transition (EMT) in transformed cell lines. Transformation of the "normal" human mammary epithelial cell line MCF 10A and selection for a tumorigenic, metastatic phenotype *in vivo* produced the derivative line MCF 10C [53,54], which exhibits an EMT phenotype [60]. Cells of this malignant derivative also became ALDH + [61]. Transformation of these cells rendered them sensitive to rottlerin (Figure 5A) and to BJE6-106 (Figure 5B), compared to the parental MCF 10A line. The IC$_{50}$ of rottlerin and BJE6-106 for the MCF 10C derivative was approximately 1 μM and 0.1 μM, respectively, at 72 hr, whereas the IC$_{50}$ for the parental MCF 10A cells were >20 μM.

The MCF 10C derivative also acquired the ability to efficiently form non-adherent spheroids (Figure 5C), in contrast to the parental MCF 10A cells. Growth of these spheroids was efficiently inhibited by exposure to rottlerin at 10 μM or to BJE6-106 at 1 μM (Figure 5D and E).

The relative lack of toxicity of PKCδ inhibition on the non-transformed, "normal" breast epithelial MCF 10A cells is noteworthy, and further supports the established

non-essential role of this isozyme in normal cells and tissues. In other work, we have demonstrated that normal mouse embryo fibroblasts and human primary fibroblasts and epithelial cells and microvascular endothelial cells and primary melanocytes survive and proliferate in the setting of PKCδ knockdown or in concentrations of PKCδ inhibitors which are lethal to tumor cell lines with aberrant Ras signaling ([45-47,55]; Trojanowska et al., in preparation).

Inhibition of PKCδ inhibits CSC tumor xenograft growth

Another property of CSCs is their high tumorigenic potential. We therefore next sought to determine if PKCδ inhibition would inhibit the growth of CSCs *in vivo*. While the 3rd generation PKCδ inhibitory compounds such as BJE6-106 are more potent and more cytotoxic to tumor cells and CSCs than previous generations, they have not been optimized for drug-like properties and are highly hydrophobic and poorly bioavailable, making efficient delivery of this generation of compounds *in vivo* unreliable. We therefore tested a prior-generation PKCδ inhibitor, rottlerin, which is readily bioavailable, in a tumor model. The human breast cancer stem cell (BCSC) cultures efficiently formed tumors as xenografts in nude mice. In comparison to vehicle control, rottlerin delivered intraperitoneally 5 days out of 7 effectively inhibited the growth of the xenografts, even producing tumor regression (Figure 6A). Survival was calculated on the day when tumor size reached the predetermined limit volume in the animals. The survival of the treated cohort extended long beyond the treatment interval, with some animals remaining tumor-free even at day 300 (Figure 6B).

We have previously demonstrated that depletion of PKCδ is selectively toxic for cells with aberrant activation of Ras or Ras signaling pathways. Of the cell lines and CSC studied in this report, only a minority bore activating mutations of Ras itself (the pancreatic cancer cells are K-Ras mutant, and the melanoma cells are N-Ras mutant). MCF7 and the primary prostate and breast cancer stem cells, for example, had normal Ras
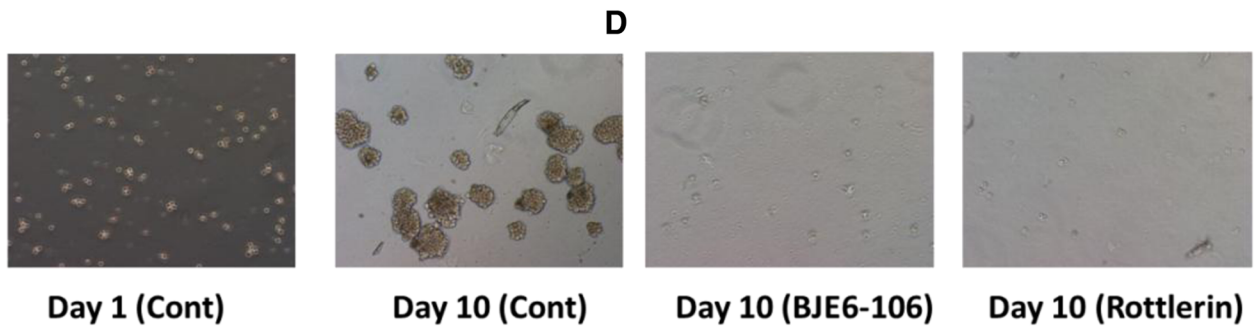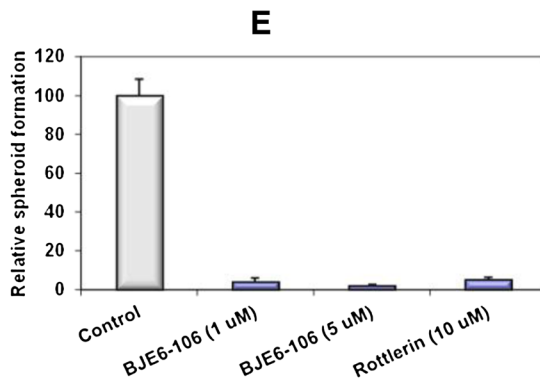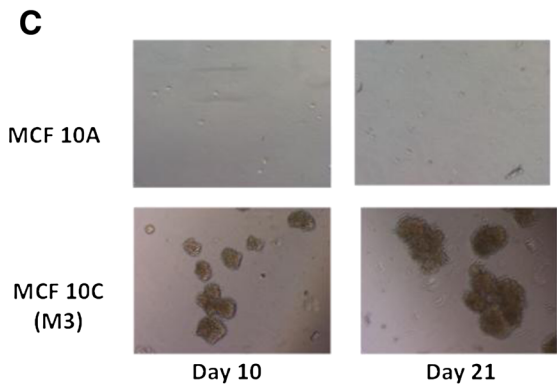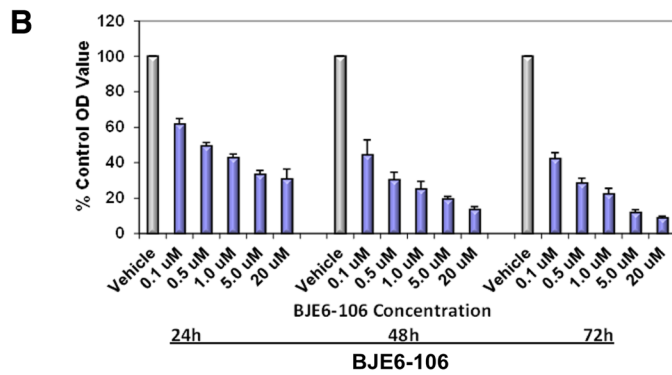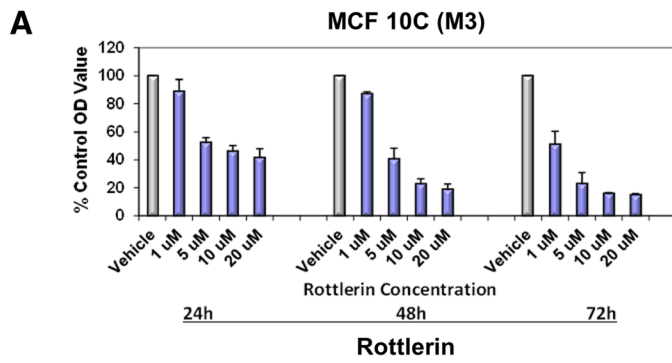
Figure 5 (See legend on next page.)

(See figure on previous page.)

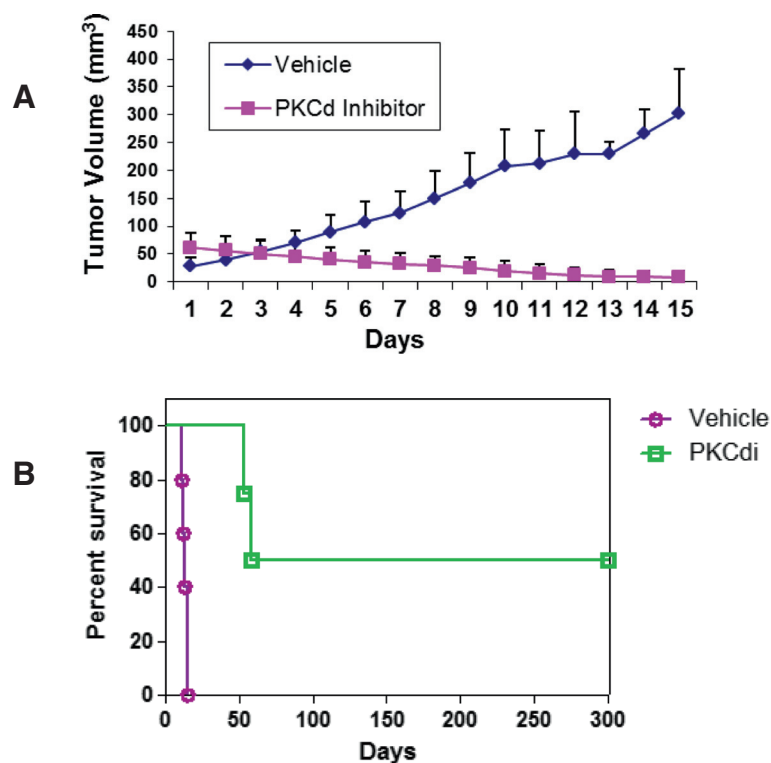**Figure 5 Effects of PKCδ inhibitors on growth and spheroid formation in non-transformed and transformed human breast epithelial cells.** MCF 10A cells and cells from the derived tumorigenic line MCF 10C (also called M3), were grown to 80% confluence in 96-well plates and then exposed to rottlerin at concentrations ranging from 1 to 20 μM **(A)** or to BJE6-106 at concentrations ranging from 0.1 to 20 μM **(B)**. The corresponding equivalent volume of solvent (DMSO) was used as a vehicle control (Vehicle). After 24, 48 and 72 hr of exposure, cell mass was evaluated by MTT assay. Control (vehicle) values were normalized to 100%. Error bars represent SEM. p values for comparison between vehicle and PKCδ inhibitors on MCF 10A cell number only reached significance (p < 0.05) at 48 hr at 20 μM for rottlerin, and at 1 μM for BJE6-106. In contrast, significant effects of the inhibitors on the MCF 10C cells were observed as early as 24 hr for rottlerin (at 5 μM) and for BJE6-106 (at 0.1 μM). **(C)** MCF 10A and MCF 10C cells were plated at 10,000 cells per well in tumor spheroid media, and spheroid formation was assessed at days 10 and 21. Representative photographs are shown. **(D)** MCF 10C cells were plated at 10,000 cells per well in tumor spheroid media, in the presence of rottlerin (5 μM), or BJE6-106 (1 μM or 5 μM), or DMSO vehicle (Control). Tumor spheroids were enumerated at 10 days. Representative photographs are shown. **(E)** Spheroid numbers were normalized to the number of spheroids in the control cultures (assigned an arbitrary value of 100%) and plotted. Error bars represent SEM. p values for comparison between vehicle and rottlerin or BJE6-106 effects on spheroid number were significant (p < 0.001).

alleles. Analysis of Ras signaling pathways of cells derived from the CSCs, however, showed relative increases of pERK or pAKT, compared to the respective parental (adherent, non-spheroid) cells (Figure 7). These findings indicate relative activation of the MEK/ERK pathway in BCSC, MCF7 and Hs578T CSCs, and relative activation of the PI$_3$K-AKT pathway in MDA231 CSCs.

## Discussion

Small populations of cancer cells within multiple types of solid tumors have been identified based on cell surface marker expression and other phenotypic and functional characteristics. These subpopulations of tumor cells have often demonstrated a >100-fold increase in tumorigenic potential, compared to the remainder of the cells in the tumor. Furthermore, tumors that form from these cancer stem cells are indistinguishable from the human tumors in which they originate, indicating that the tumor-initiating cells are stem cell-like in their ability to self-renew and give rise to a heterogeneous cell population. Much recent data suggests that elimination of these cancer stem cells, which are typically resistant to conventional

Figure 6 Effects of PKCδ inhibitor on tumor growth and survival in a xenograft human breast cancer stem cell model. Breast cancer stem cell xenografts were established and animals were treated with vehicle or rottlerin for 15 days, as described in Methods. **(A)** Tumor volumes plotted over time, until tumors in all the control animals reached the maximum volume allowed by the protocol (approximately 15 days). **(B)** Kaplan-Meier plot of survival of vehicle control or rottlerin (PKCδi)-treated animals, with monitoring continuing after cessation of treatment at day 15.
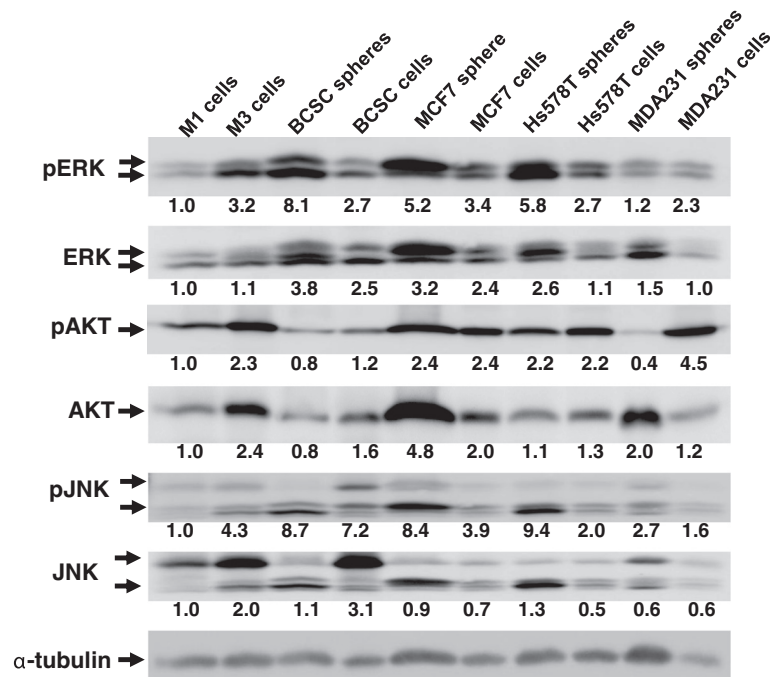
Figure 7 Immunoblot analysis of Ras-signaling pathways in tumor cells, cell lines, or spheres. Hs578T, MCF7, MDA231 and breast cancer stem cells (BCSC) were plated in tumor spheroid media under adherent or non-adherent conditions. Tumor spheroids and adherent cells were collected at 96 hr, and lysed. MCF 10A (M1) and MCF 10C (M3) lysates were also prepared. The lysates were separated by electrophoresis and immunoblotted with antibodies against ERK, pEKR, AKT, pAKT, JNK, pJNK. Immunoblotting of α-tubulin serves as a loading control. For quantitation, the digital intensity of the bands was first normalized to α-tubulin in each lane, and then expressed relative to the signal for the MCF 10A (M1) cell line. Values are shown under each band.

therapies, represents the most formidable barrier to curing solid tumors [1,4,5,32,33,35]. CSCs, or subclones thereof, are the most likely perpetrators of invasion and metastasis [6,62].

Recent findings have shown the existence of activated and quiescent repertoires of stem cells in established tumor cell lines as well as primary tumor cell isolates, and their ability to interchange between these conditions [37]. Sphere-forming assays (SFA) are believed to evaluate the differentiation and self-renewal capabilities of a tumor cell population by assessing the potential of a tumor cell to behave like a stem cell, and are widely used in stem cell studies [37]. Sphere-forming assays have been commonly used to retrospectively identify normal and cancer stem cells, and measure stem cell/early progenitor activity in multiple types of solid cancers [38,63,64]. Increased expression of "stemness-related genes" [65] was observed when comparing solid tumor cell lines grown as 3D spheroids to monolayers.

Our identification of PKCδ as a critical mediator of survival in multiple types of solid tumors, including prostate, breast, lung, pancreatic, neuroendocrine and melanomas [45-48] raised the possibility that CSC populations might be similarly dependent upon the activity of

this enzyme. The effects of PKCδ inhibition on CSCs, however, had not been previously explored.

We first validated PKCδ as a target in diverse CSCs by demonstrating here that specific and selective downregulation of PKCδ by shRNA was sufficient to prevent the growth of human breast, pancreatic and prostate cancer stem-like cell cultures, and to induce cytotoxicity.

Potential therapeutic translation of this synthetic lethal approach required the development of small molecule probes. As no PKCδ-selective inhibitors had been developed to date, we initially used pharmacophore modeling and docking of rottlerin, a well-established but not highly-specific inhibitor of PKCδ, into the crystal structure of PKCθ, to identify regions of the molecule important for PKCδ-selectivity. The initial new molecule showing activity against PKCδ (KAM1) was formed by combining structural elements of the broad spectrum protein kinase inhibitor staurosporine and rottlerin. The chromene portion of rottlerin was combined with the carbazole portion of staurosporine to produce KAM1 [47]. KAM1 was further modified to develop 36 new analogs, including BJE6-106, which inhibits PKCδ with an IC_{50} value of 50 nM and is approximately 1000-fold selective versus PKCα. Specificity for PKCδ over "classical" PKC isoforms, like

PKCα, is important, as inhibition of PKCα is generally toxic to all cells, normal and malignant, and would render these inhibitors non-"tumor-targeted". We have shown that B106 exerts potent cytotoxic activity against N-Ras-mutant human melanomas and B-Raf-mutant melanoma lines that have developed resistance to B-Raf inhibitors by aberrant activation of alternative Ras signaling pathways [48,55].

We demonstrate here that first, second and third generation PKCδ inhibitors (exemplified by rottlerin, KAM1 and BJE6-106, respectively), inhibit the growth of human cancer stem-like cell cultures isolated from tumors, as well as CSC-like cells derived from cell lines by spheroid formation on non-adherent surfaces. Our prior studies would have predicted that the CSC isolates or spheroids derived from cell lines that contained activating mutations of N-Ras or K-Ras would likely be susceptible to PKCδ suppression (*e.g.*, the K-Ras mutant pancreatic carcinomas and the N-Ras mutant melanomas). The reason for the susceptibility of the stem-like tumor cells containing wt-Ras alleles, however, was not immediately apparent. One reason for their susceptibility is likely to be upregulation of Ras effector pathways (MEK-ERK or PI$_3$K/AKT signaling) in CSC spheres derived from cell lines, compared to the non-CSC parental cultures. We have reported previously that isolated activation of the MEK-ERK effector pathway or the PI$_3$K/AKT effector pathway was sufficient to make cells dependent upon PKCδ for survival [45-47]. The finding of higher levels of Ras effector pathway activation in the CSC sphere subpopulation compared to the parental cells may also explain why in at least one instance (MCF7) the sphere-forming CSC cells were substantially more susceptible to PKCδ inhibition than non-CSC cells population. Interestingly, a recent report has identified a requirement for PKCδ in erbB2-driven proliferation of breast cancer cells [66], and erbB2 drives aberrant Ras pathway signaling. Furthermore, activation of MAPK pathways in basal-like breast cancers has been reported to promote a cancer stem cell-like phenotype [67], and activation of Ras/MAPK signaling was reported to protect breast cancer stem cells from certain stem-cell targeted drugs [68]. Collectively, these reports, together with our findings, suggest that a PKCδ-targeted approach to breast cancer stem cell populations, which exploits a synthetic lethal interaction with aberrant Ras signaling, may be particularly effective.

Inhibitory effects of PKCδ suppression on the IL6-Stat3 axis, which is critical for CSC genesis or maintenance in a number of tumor cells types [69-71], may also contribute to the actions of PKCδ inhibition on CSC growth and survival, and will be reported separately.

Epithelial-to-mesenchymal transition (EMT), induced either by paracrine signaling from cancer-associated fibroblasts (CAFs) or neighboring tumor cells, has been associated with the acquisition of a stem cell phenotype [72]. In culture, when immortalized normal or transformed human mammary epithelial cells (HMECs) are stimulated to undergo an epithelial-to-mesenchymal transition (EMT), the transition confers stem-like cell properties upon normal or transformed epithelial cells in culture, partly because the cells acquire a CD44+/CD24 (low) phenotype, similar to breast cancer stem cells.

The idea that cancer cells might reversibly transition between epigenetically-defined tumorigenic and non-tumorigenic states is of interest in part because mechanisms that generate reversible heterogeneity can confer resistance to therapies [73,74]. We took advantage of a previously-established cell line model system for breast cancer EMT, which consists of a parental spontaneously-immortalized mammary epithelial cell line, MCF 10A (M1), and one of its derivatives, MCF 10C (M3), derived from a xenograft in nude mice that progressed to carcinoma [53,54]. These cell lines were previously reported to exhibit distinct tumorigenic properties when re-implanted in nude mice; MCF 10A is non-tumorigenic, while MCF 10C forms low-grade, well-differentiated carcinomas [53,54,60]. Furthermore, MCF 10C has acquired phenotypic changes consistent with mesenchymal morphology and gene and protein expression patterns characteristic of EMT, including expression of mesenchymal markers (fibronectin, vimentin, and N-cadherin) with concomitant downregulation of E-cadherin, β-catenin, and γ-catenin. MCF 10C also expresses high levels of Nanog, and Sox4, which are markers of cancer stem cells [61]. We found that the mesenchymal, CSC-like MCF 10C subline was much more sensitive to PKCδ inhibitors than the epithelial-like "normal" MCF 10A cells from which they were derived. Furthermore, the MCF 10C line acquired the capacity to efficiently form spheroids when grown in non-adherent conditions, and this tumor spheroid formation was inhibited by inhibition of PKCδ activity.

Conclusions

Collectively, these findings suggest that human cancer stem-like cells isolated from diverse sources and tumor types require PKCδ activity for their growth or maintenance *in vitro* and *in vivo*, making this isozyme a novel tumor-specific target. Taken together with the previous demonstration by our group and others of the cytotoxic effects of PKCδ inhibition on the non-CSC population of many tumor cell types, PKCδ inhibitors hold the promise of eliminating both the majority non-CSC population and the latent and resistant CSC population comprising human tumors.

Abbreviations
BCSC: Primary human breast adenocarcinoma stem cells; CSC: Cancer stem-like cell; MAPK: MAP kinase; PCSC: Primary human pancreatic adenocarcinoma stem

cells; PKCδ: Protein kinase C delta; PKCα: Protein kinase C alpha; PrCSC: Primary human prostate adenocarcinoma stem cells; shRNA: Short hairpin RNA.

Authors' contributions

ZC and LWF carried out the molecular and biochemical studies, and participated in the preparation of the manuscript. RMW and DVF designed the novel inhibitory compounds. RMW synthesized the compounds and participated in the preparation of the manuscript. DVF conceived the study, and participated in its design and coordination and drafted the manuscript. All authors read and approved the final manuscript.

Author details

[1]Cancer Center, Boston University School of Medicine, K-712C, 72 E. Concord St., Boston, MA 02118, USA. [2]Department of Medicine, Boston University School of Medicine, K-712C, 72 E. Concord St., Boston, MA 02118, USA. [3]Department of Chemistry, Colorado State University, 1301 Centre Ave, Fort Collins, CO 80523, USA. [4]University of Colorado Cancer Center, Aurora, CO 80045, USA. [5]Department of Pediatrics, Boston University School of Medicine, K-712C, 72 E. Concord St., Boston, MA 02118, USA. [6]Department of Biochemistry, Boston University School of Medicine, K-712C, 72 E. Concord St., Boston, MA 02118, USA. [7]Department of Microbiology, Boston University School of Medicine, K-712C, 72 E. Concord St., Boston, MA 02118, USA. [8]Department of Pathology, Boston University School of Medicine, K-712C, 72 E. Concord St., Boston, MA 02118, USA. [9]Department of Laboratory Medicine, Boston University School of Medicine, K-712C, 72 E. Concord St., Boston, MA 02118, USA.

References

1. Reya T, Morrison SJ, Clarke MF, Weissman IL: **Stem cells, cancer, and cancer stem cells.** *Nature* 2001, **414**:105–111.
2. Lapidot T, Sirard C, Vormoor J, Murdoch B, Hoang T, Caceres-Cortes J, *et al*: **A cell initiating human acute myeloid leukaemia after transplantation into SCID mice.** *Nature* 1994, **367**:645–648.
3. Tirino V, Desiderio V, Paino F, De RA, Papaccio F, La NM, *et al*: **Cancer stem cells in solid tumors: an overview and new approaches for their isolation and characterization.** *FASEB J* 2012.
4. Clevers H: **Stem cells, asymmetric division and cancer.** *Nat Genet* 2005, **37**:1027–1028.
5. Trumpp A, Wiestler OD: **Mechanisms of Disease: cancer stem cells– targeting the evil twin.** *Nat Clin Pract Oncol* 2008, **5**:337–347.
6. Baccelli I, Trumpp A: **The evolving concept of cancer and metastasis stem cells.** *J Cell Biol* 2012, **198**:281–293.
7. Al-Hajj M, Wicha MS, Benito-Hernandez A, Morrison SJ, Clarke MF: **Prospective identification of tumorigenic breast cancer cells.** *Proc Natl Acad Sci USA* 2003, **100**:3983–3988.
8. Singh SK, Clarke ID, Terasaki M, Bonn VE, Hawkins C, Squire J, *et al*: **Identification of a cancer stem cell in human brain tumors.** *Cancer Res* 2003, **63**:5821–5828.
9. Bao S, Wu Q, McLendon RE, Hao Y, Shi Q, Hjelmeland AB, *et al*: **Glioma stem cells promote radioresistance by preferential activation of the DNA damage response.** *Nature* 2006, **444**:756–760.
10. Piccirillo SG, Reynolds BA, Zanetti N, Lamorte G, Binda E, Broggi G, *et al*: **Bone morphogenetic proteins inhibit the tumorigenic potential of human brain tumour-initiating cells.** *Nature* 2006, **444**:761–765.
11. Tirino V, Desiderio V, D'Aquino R, De FF, Pirozzi G, Graziano A, *et al*: **Detection and characterization of CD133+ cancer stem cells in human solid tumours.** *PLoS One* 2008, **3**:e3469.
12. Tirino V, Desiderio V, Paino F, De RA, Papaccio F, Fazioli F, *et al*: **Human primary bone sarcomas contain CD133+ cancer stem cells displaying high tumorigenicity in vivo.** *FASEB J* 2011, **25**:2022–2030.
13. Collins AT, Berry PA, Hyde C, Stower MJ, Maitland NJ: **Prospective identification of tumorigenic prostate cancer stem cells.** *Cancer Res* 2005, **65**:10946–10951.
14. Bapat SA, Mali AM, Koppikar CB, Kurrey NK: **Stem and progenitor-like cells contribute to the aggressive behavior of human epithelial ovarian cancer.** *Cancer Res* 2005, **65**:3025–3029.
15. Alvero AB, Chen R, Fu HH, Montagna M, Schwartz PE, Rutherford T, *et al*: **Molecular phenotyping of human ovarian cancer stem cells unravels the mechanisms for repair and chemoresistance.** *Cell Cycle* 2009, **8**:158–166.
16. Curley MD, Therrien VA, Cummings CL, Sergent PA, Koulouris CR, Friel AM, *et al*: **CD133 expression defines a tumor initiating cell population in primary human ovarian cancer.** *Stem Cells* 2009, **27**:2875–2883.
17. Stewart JM, Shaw PA, Gedye C, Bernardini MQ, Neel BG, Ailles LE: **Phenotypic heterogeneity and instability of human ovarian tumor- initiating cells.** *Proc Natl Acad Sci U S A* 2011, **108**:6468–6473.
18. Zhang S, Balch C, Chan MW, Lai HC, Matei D, Schilder JM, *et al*: **Identification and characterization of ovarian cancer-initiating cells from primary human tumors.** *Cancer Res* 2008, **68**:4311–4320.
19. Takaishi S, Okumura T, Tu S, Wang SS, Shibata W, Vigneshwaran R, *et al*: **Identification of gastric cancer stem cells using the cell surface marker CD44.** *Stem Cells* 2009, **27**:1006–1020.
20. Eramo A, Lotti F, Sette G, Pilozzi E, Biffoni M, Di VA, *et al*: **Identification and expansion of the tumorigenic lung cancer stem cell population.** *Cell Death Differ* 2008, **15**:504–514.
21. Tirino V, Camerlingo R, Franco R, Malanga D, La RA, Viglietto G, *et al*: **The role of CD133 in the identification and characterisation of tumour- initiating cells in non-small-cell lung cancer.** *Eur J Cardiothorac Surg* 2009, **36**:446–453.
22. Dalerba P, Dylla SJ, Park IK, Liu R, Wang X, Cho RW, *et al*: **Phenotypic characterization of human colorectal cancer stem cells.** *Proc Natl Acad Sci USA* 2007, **104**:10158–10163.
23. O'Brien CA, Pollett A, Gallinger S, Dick JE: **A human colon cancer cell capable of initiating tumour growth in immunodeficient mice.** *Nature* 2007, **445**:106–110.
24. Huang EH, Hynes MJ, Zhang T, Ginestier C, Dontu G, Appelman H, *et al*: **Aldehyde dehydrogenase 1 is a marker for normal and malignant human colonic stem cells (SC) and tracks SC overpopulation during colon tumorigenesis.** *Cancer Res* 2009, **69**:3382–3389.
25. Ricci-Vitiani L, Lombardi DG, Pilozzi E, Biffoni M, Todaro M, Peschle C, *et al*: **Identification and expansion of human colon-cancer-initiating cells.** *Nature* 2007, **445**:111–115.
26. Hermann PC, Huber SL, Herrler T, Aicher A, Ellwart JW, Guba M, *et al*: **Distinct populations of cancer stem cells determine tumor growth and metastatic activity in human pancreatic cancer.** *Cell Stem Cell* 2007, **1**:313–323.
27. Li C, Heidt DG, Dalerba P, Burant CF, Zhang L, Adsay V, *et al*: **Identification of pancreatic cancer stem cells.** *Cancer Res* 2007, **67**:1030–1037.
28. Schatton T, Murphy GF, Frank NY, Yamaura K, Waaga-Gasser AM, Gasser M, *et al*: **Identification of cells initiating human melanomas.** *Nature* 2008, **451**:345–349.
29. Boiko AD, Razorenova OV, van de Rijn M, Swetter SM, Johnson DL, Ly DP, *et al*: **Human melanoma-initiating cells express neural crest nerve growth factor receptor CD271.** *Nature* 2010, **466**:133–137.
30. Fang D, Nguyen TK, Leishear K, Finko R, Kulp AN, Hotz S, *et al*: **A tumorigenic subpopulation with stem cell properties in melanomas.** *Cancer Res* 2005, **65**:9328–9337.
31. Prince ME, Sivanandan R, Kaczorowski A, Wolf GT, Kaplan MJ, Dalerba P, *et al*: **Identification of a subpopulation of cells with cancer stem cell properties in head and neck squamous cell carcinoma.** *Proc Natl Acad Sci USA* 2007, **104**:973–978.
32. Li Y, Laterra J: **Cancer stem cells: distinct entities or dynamically regulated phenotypes?** *Cancer Res* 2012, **72**:576–580.
33. Dick JE: **Stem cell concepts renew cancer research.** *Blood* 2008, **112**:4793–4807.

34. Clevers H: **The cancer stem cell: premises, promises and challenges.** *Nat Med* 2011, **17**:313–319.
35. Nguyen LV, Vanner R, Dirks P, Eaves CJ: **Cancer stem cells: an evolving concept.** *Nat Rev Cancer* 2012, **12**:133–143.
36. Franken NA, Rodermond HM, Stap J, Haveman J, Van BC: **Clonogenic assay of cells in vitro.** *Nat Protoc* 2006, **1**:2315–2319.
37. Pastrana E, Silva-Vargas V, Doetsch F: **Eyes wide open: a critical review of sphere-formation as an assay for stem cells.** *Cell Stem Cell* 2011, **8**:486–498.
38. Ponti D, Costa A, Zaffaroni N, Pratesi G, Petrangolini G, Coradini D, et al: **Isolation and in vitro propagation of tumorigenic breast cancer cells with stem/progenitor cell properties.** *Cancer Res* 2005, **65**:5506–5511.
39. Han ME, Jeon TY, Hwang SH, Lee YS, Kim HJ, Shim HE, et al: **Cancer spheres from gastric cancer patients provide an ideal model system for cancer stem cell research.** *Cell Mol Life Sci* 2011, **68**:3589–3605.
40. Dean M, Fojo T, Bates S: **Tumour stem cells and drug resistance.** *Nat Rev Cancer* 2005, **5**:275–284.
41. Gomez-Casal R, Bhattacharya C, Ganesh N, Bailey L, Basse P, Gibson M, et al: **Non-small cell lung cancer cells survived ionizing radiation treatment display cancer stem cell and epithelial-mesenchymal transition phenotypes.** *Mol Cancer* 2013, **12**:94.
42. Fabian A, Barok M, Vereb G, Szollosi J: **Die hard: are cancer stem cells the Bruce Willises of tumor biology?** *Cytometry A* 2009, **75**:67–74.
43. Valent P, Bonnet D, De MR, Lapidot T, Copland M, Melo JV, et al: **Cancer stem cell definitions and terminology: the devil is in the details.** *Nat Rev Cancer* 2012, **12**:767–775.
44. Li X, Lewis MT, Huang J, Gutierrez C, Osborne CK, Wu MF, et al: **Intrinsic resistance of tumorigenic breast cancer cells to chemotherapy.** *J Natl Cancer Inst* 2008, **100**:672–679.
45. Xia S, Forman LW, Faller DV: **Protein Kinase C{delta} is required for survival of cells expressing activated p21RAS.** *J Biol Chem* 2007, **282**:13199–13210.
46. Xia S, Chen Z, Forman LW, Faller DV: **PKCdelta survival signaling in cells containing an activated p21Ras protein requires PDK1.** *Cell Signal* 2009, **21**:502–508.
47. Chen Z, Forman LW, Miller KA, English B, Takashima A, Bohacek RA, et al: **The proliferation and survival of human neuroendocrine tumors is dependent upon protein kinase C-delta.** *Endocr Relat Cancer* 2011, **18**:759–771.
48. Takashima A, Faller DV: **Targeting the RAS oncogene.** *Expert Opin Ther Targets* 2013.
49. Basu A, Pal D: **Two faces of protein kinase Cdelta: the contrasting roles of PKCdelta in cell survival and cell death.** *ScientificWorldJournal* 2010, **10**:2272–2284.
50. Leitges M, Mayr M, Braun U, Mayr U, Li C, Pfister G, et al: **Exacerbated vein graft arteriosclerosis in protein kinase Cdelta-null mice.** *J Clin Invest* 2001, **108**:1505–1512.
51. Zhu T, Chen L, Du W, Tsuji T, Chen C: **Synthetic Lethality Induced by Loss of PKC delta and Mutated Ras.** *Genes Cancer* 2010, **1**:142–151.
52. Symonds JM, Ohm AM, Carter CJ, Heasley LE, Boyle TA, Franklin WA, et al: **Protein kinase C delta is a downstream effector of oncogenic K-ras in lung tumors.** *Cancer Res* 2011, **71**:2087–2097.
53. Strickland LB, Dawson PJ, Santner SJ, Miller FR: **Progression of premalignant MCF10AT generates heterogeneous malignant variants with characteristic histologic types and immunohistochemical markers.** *Breast Cancer Res Treat* 2000, **64**:235–240.
54. Santner SJ, Dawson PJ, Tait L, Soule HD, Eliason J, Mohamed AN, et al: **Malignant MCF10CA1 cell lines derived from premalignant human breast epithelial MCF10AT cells.** *Breast Cancer Res Treat* 2001, **65**:101–110.
55. Takashima A, English B, Chen Z, Cao J, Cui R, Williams RM, et al: **Protein Kinase C delta is a therapeutic target in malignant melanoma with NRAS mutation.** *ACS Chem Biol.* in press.
56. Guda K, Natale L, Markowitz SD: **An improved method for staining cell colonies in clonogenic assays.** *Cytotechnology* 2007, **54**:85–88.
57. Gschwendt M, Muller HJ, Kielbassa K, Zang R, Kittstein W, Rincke G, et al: **Rottlerin, a novel protein kinase inhibitor.** *Biochem Biophys Res Commun* 1994, **199**:93–98.
58. Susarla BT, Robinson MB: **Rottlerin, an inhibitor of protein kinase Cdelta (PKCdelta), inhibits astrocytic glutamate transport activity and reduces GLAST immunoreactivity by a mechanism that appears to be PKCdelta-independent.** *J Neurochem* 2003, **86**:635–645.
59. Davies SP, Reddy H, Caivano M, Cohen P: **Specificity and mechanism of action of some commonly used protein kinase inhibitors.** *Biochem J* 2000, **351**:95–105.
60. Pan H, Gao F, Papageorgis P, Abdolmaleky HM, Faller DV, Thiagalingam S: **Aberrant activation of gamma-catenin promotes genomic instability and oncogenic effects during tumor progression.** *Cancer Biol Ther* 2007, **6**:1638–1643.
61. Papageorgis P, Lambert AW, Ozturk S, Gao F, Pan H, Manne U, et al: **Smad signaling is required to maintain epigenetic silencing during breast cancer progression.** *Cancer Res* 2010, **70**:968–978.
62. Chaffer CL, Weinberg RA: **A perspective on cancer cell metastasis.** *Science* 2011, **331**:1559–1564.
63. Wang L, Mezencev R, Bowen NJ, Matyunina LV, McDonald JF: **Isolation and characterization of stem-like cells from a human ovarian cancer cell line.** *Mol Cell Biochem* 2012, **363**:257–268.
64. Dontu G, Al-Hajj M, Abdallah WM, Clarke MF, Wicha MS: **Stem cells in normal breast development and breast cancer.** *Cell Prolif* 2003, **36**(Suppl 1):59–72.
65. Busse A, Letsch A, Fusi A, Nonnenmacher A, Stather D, Ochsenreither S, et al: **Characterization of small spheres derived from various solid tumor cell lines: are they suitable targets for T cells?** *Clin Exp Metastasis* 2013, **30**:781–789.
66. Allen-Petersen BL, Carter CJ, Ohm AM, Reyland ME: **Protein kinase Cdelta is required for ErbB2-driven mammary gland tumorigenesis and negatively correlates with prognosis in human breast cancer.** *Oncogene* 2013, **10**:32–1.
67. Balko JM, Schwarz LJ, Bhola NE, Kurupi R, Owens P, Miller TW, et al: **Activation of MAPK pathways due to DUSP4 loss promotes cancer stem cell-like phenotypes in basal-like breast cancer.** *Cancer Res* 2013, **73**:6346–6358.
68. Bhat-Nakshatri P, Goswami CP, Badve S, Sledge GW Jr, Nakshatri H: **Identification of FDA-approved Drugs Targeting Breast Cancer Stem Cells Along With Biomarkers of Sensitivity.** *Sci Rep* 2013, **3**:2530.
69. Iliopoulos D, Hirsch HA, Wang G, Struhl K: **Inducible formation of breast cancer stem cells and their dynamic equilibrium with non-stem cancer cells via IL6 secretion.** *Proc Natl Acad Sci U S A* 2011, **108**:1397–1402.
70. Wang H, Lathia JD, Wu Q, Wang J, Li Z, Heddleston JM, et al: **Targeting interleukin 6 signaling suppresses glioma stem cell survival and tumor growth.** *Stem Cells* 2009, **27**:2393–2404.
71. Lin L, Liu A, Peng Z, Lin HJ, Li PK, Li C, et al: **STAT3 is necessary for proliferation and survival in colon cancer-initiating cells.** *Cancer Res* 2011, **71**:7226–7237.
72. Alison MR, Lin WR, Lim SM, Nicholson LJ: **Cancer stem cells: in the line of fire.** *Cancer Treat Rev* 2012, **38**:589–598.
73. Roesch A, Fukunaga-Kalabis M, Schmidt EC, Zabierowski SE, Brafford PA, Vultur A, et al: **A temporarily distinct subpopulation of slow-cycling melanoma cells is required for continuous tumor growth.** *Cell* 2010, **141**:583–594.
74. Sharma SV, Lee DY, Li B, Quinlan MP, Takahashi F, Maheswaran S, et al: **A chromatin-mediated reversible drug-tolerant state in cancer cell subpopulations.** *Cell* 2010, **141**:69–80.